THE UNIVERSITY OF MANITOBA

DECENTRALIZED CONTROLLER DESIGN FOR THE DYNAMIC LOAD-FREQUENCY CONTROL OF AN INTERCONNECTED POWER SYSTEM

by

JAGDISH CHAND

A Thesis

Submitted to the Faculty of Graduate Studies

in Partial Fulfilment of the Requirements for the Degree

of Doctor of Philosophy

DEPARTMENT OF ELECTRICAL ENGINEERING

WINNIPEG, MANITOBA, R3T 2N2

May, 1980

DECENTRALIZED CONTROLLER DESIGN FOR THE DYNAMIC LOAD-FREQUENCY CONTROL OF AN INTERCONNECTED POWER SYSTEM

BY

JAGDISH CHAND

A thesis submitted to the Faculty of Graduate Studies of the University of Manitoba in partial fulfillment of the requirements of the degree of

DOCTOR OF PHILOSOPHY

DECENTRALIZED CONTROLLER DESIGN FOR THE DYNAMIC LOAD-FREQUENCY CONTROL OF AN INTERCONNECTED POWER SYSTEM

by

JAGDISH CHAND

ABSTRACT

This thesis provides a detailed analysis of the dynamic load-frequency control of an interconnected power system and suggests a new design, a Proportional - Integral - Derivative (PID) controller, to replace conventional design of an Integral-Only controller.

First a root-locus technique and the time domain solution are used to evaluate the steady-state and dynamic interactions of interconnected areas. These methods show that the conventional Integral-Only controller does not satisfy present dynamic control requirements.

An iterative pole-placement technique and the output feedback are then used to design decentralized, dynamic load-frequency controllers for an interconnected two-area power system. As shown in Chapter3, a simple PID controller is adequate for this purpose in contrast to an unrealizable optimal controller suggested in the past. Next system simplification and on-line identification techniques are used

to determine the external system model when a large number of areas are interconnected or when the model of the external system is unknown. Then a local PID controller is designed.

In Chapter 4, the z-domain eigenvalue technique, which is especially well-suited for large-scale sampled data systems, is used to analyze the effects of sampling period and controller gains on the digital realization of the conventional and the proposed PID controllers. The choice of the sampling period is found critical for the PID controller. Above a certain period, the system with the PID controller becomes unstable, whereas the system with conventional controller remains stable for a wider range of sampling periods. The controller gains determined for the continuous system also remain optimal for the discrete system.

Finally the effects of a d.c. link within an area on the design of the dynamic load-frequency controller is studied. A d.c. link model is derived. It is shown that a d.c. link acting in parallel with a slow governing system influences the magnitudes of the PID controller gains and that higher participation by the d.c. link improves the dynamic performance of the entire system. Further, a d. c. link as an interconnecting tie is shown to be detrimental to the operating requirements of an interconnected power system. The d.c. link is then modified to avoid these defects. At this stage the decentralized PID controller is shown to be superior to the conventional controller.

ACKNOWLEDGEMENTS

The author wishes to express his sincere appreciation and deep gratitude to Dr. Glen W. Swift for his guidance and encouragement not only during the preparation of this thesis, but throughout his entire graduate program.

The financial support of the National Research Council, University of Manitoba and Manitoba Hydro are gratefully acknowledged.

TABLE OF CONTENTS

LIST OF FIGURES

LIST OF TABLES

CHAPTER 1

INTRODUCTION

The interconnection of power systems creates, in effect, a single larger system with greater economies, reliability, flexibility and overall regulation than any of the separate smaller systems individually implies. To provide these advantages for itself, any single member system would have to provide greater generation reserves.

Still the simple joining of the member systems by tie-lines does not, in itself, realize the advantages associated with a larger system. Regulation of tie-line flows is mandatory both for normal operating conditions and for disturbances in any one of the member systems of the interconnection. Also, the the members must comply with the commandment of interconnection: while participating in the benefits of parallel operation each area must likewise contribute to the regulation of the interconnected system. This relationship implies that each member shall absorb its own load changes and contribute its share to the frequency regulation of the combined system.

The above rules are very desirable, but because the various governors throughout the interconnection cannot

discriminate whether or not a load change has occurred in their own area, they cause undesirable and unscheduled power flows over the tie-lines in carrying out their functions of matching generation to load demand.

Manual control of the governor settings could never effectively supply the corrective measures necessary to maintain tie-line schedules and system frequency, especially because each member area will continually be issuing instructions from its own dispatch centre. This situation would be chaotic and unworkable. Thus, automatic control equipment, supplementary to the unit governors, has been developed to provide the necessary added intelligence to the governor action and to reduce the deviations in tie-line load and system frequency to zero. Such a supplementary unit is called Load-Frequency Controller (LFC).[1-3]

This load-frequency controller maintains the scheduled system frequency and tie-line interchange between areas during steady-state normal operating conditions only. During dynamic operating conditions, system frequency and tie-line power usually experience oscillations. Unless these oscillations are damped, danger of separation between areas exists, especially at high power transfer levels. In such circumstances, the tie-line interchange schedule would have to be lowered to prevent tie-line trips.

Since the load-frequency controller resides at the

highest level in the pyramidal control structure of an area, improving its design can be used to minimize dynamic oscillations both in its own area and between interconnected areas. Power transfer capabilities of the interconnecting tie-lines can thus be increased, and the danger of area separation at high power transfer levels can be decreased.

In the past, attempts were made to minimize dynamic oscillations by optimizing the frequency bias setting and the integral gain of the existing analog load-frequency controller.[4-6] These attempts provided only marginal improvement in the dynamic system behaviour.[7] More recently, controller synthesis has focused on applying optimal control techniques.[8-14] These controllers, however, still exhibit a number of disadvantages:

(i) They use a cost criterion to minimize area frequency and tie-line schedule deviations to zero. When an area cannot meet its load demand, these controllers will deny assistance from other areas resulting in further lowering of the frequency in the troubled area and ultimately in separating the area from the rest of the system. These controllers thus act against the basic principle of interconnection to provide power assistance between areas.

(ii) These controllers use the states of all interconnected areas to generate the control signal.

Measurement and communication of all states in an interconnected multi-area power system is physically impossible. So these controllers cannot be physically realized.

(iii) These controllers can cause unstable system behaviour in the absence of a signal or a component failure.

(iv) These controllers generate optimal control signals only when the system is operating at a particular load level and only when small perturbations occur around this level. But because in real life a system is never at a particular load-level and disturbances are both small and large, the dynamic behaviour of the system with these controllers will be unpredictable.

Because of these four main disadvantages, optimal load-frequency controllers have received little attention in the field.

The purpose of this thesis is therefore to design a practical analog or digital load-frequency controller which minimizes dynamic oscillations for a wide range of operating conditions, fulfills the steady-state performances required of the existing load-frequency controller and does not require additional signal measurement, communication and processing.

In this thesis a two area interconnected power system

is used to design a practical load-frequency controller. In Chapter 2, a model for the two-area power system with an a.c. tie is developed. The effects of an a.c. interconnection on the steady-state and dynamic performances of the interconnected system are then examined with and without the conventional (existing) load-frequency controllers.

In Chapter 3, a realizable controller design technique is presented. Since the load-frequency controller resides at each area control centre, a decentralized, multivariable control principle is applied in the controller design. A simple "Proportional - Integral - Derivative (PID)" load-frequency controller is selected for each area. An iterative pole-placement technique is then applied to determine the optimum set of PID gains and to place the characteristic roots (eigenvalues) of the system in a desired sector of the s-plane. This sector is selected to provide an acceptable minimum damping and maximum frequency of oscillations for all possible conditions of system operation. A two-area interconnected power system is used to examine the feasibility of the controller design. A time domain solution is carried out to confirm the Laplace domain analysis. Finally, dynamic behaviour of the system is evaluated for the large disturbance to examine the effects of system nonlinearity.

Once the design has been completed, a system order reduction technique is used to simplify the model of the

external system when an area is interconnected with a large number of areas. The effect of such simplification on the controller design and the dynamic performance of the local area is examined in a two-area interconnected power system. When the model of the external system is unknown or known only partially, a simplified model of the external system is assumed. A recursive least-square identification technique is then used to determine the parameters of the simplified model. The effects of changes in the operating level on this design of the local controller is evaluated.

In Chapter 4, the digital realizations of the conventional and PID controllers are examined. Analysis is carried out in both the z-domain and the time-domain to examine the effects of the sampling period and the controller gains on the steady-state and dynamic performance of the interconnected two-area system.

During the last two decades, a number of electrical utilities all over the world have acquired HVDC links to bring power from remote areas to their load centres or to transfer power between two areas operating at different frequencies.[15,16] Because of the fast control action, the HVDC link in an area has also been used to damp oscillations in adjoining a.c. systems.[17-21] No research has yet been reported, however, using HVDC links as a viable source for the load-frequency control. But because of the fast controlling action, HVDC

link seems a promising alternative to the present scheme of governor control. In Chapter 5, effect of parralel operation of the HVDC link and governor controls in an area on the area controller design is examined. The effect of the HVDC link as a tie between areas on the load-frequency control is also analysed.

Chapter 6 provides the concluding remarks.

CHAPTER 2

MODELLING AND ANALYSIS OF THE CONVENTIONAL SYSTEM

2.1 Introduction

The design of a control system[22] is usually divided into two steps: (i) determining a mathematical model and (ii) planning a control strategy. Any inherent lack or complication in the initial modelling will later be reflected in poor system analysis and controller synthesis.

Process models can be obtained (i) from basic physical laws, (ii) from pure input-output experiments or (iii) from a combination of the above two methods. Models derived from basic physical laws are complex, whereas the models derived from input-output relations by a black-box approach are usually simple and linear. The first method leads to a complex controller which is therefore difficult to realize, whereas the second method provides a simple controller which does not take into account effects of nonlinearity and operation at other than normal operating conditions. Any controller design based on either method will, therefore, be unrealistic. But a controller design based on both physical laws and the input-output relations will ensure a realistic controller.

The combined method is used in this thesis to model each area of an interconnected power system[2,7] for the load-frequency control. In this method the term area[1] identifies that part of an interconnected system which is to absorb its own load changes during normal operating conditions. An area may be a single company responding to its own load changes that occur in only a given part of the company's network or it may be a whole group of companies pooled together to absorb the load-changes that occur anywhere within their collective boundaries.

An interconnected power system can be viewed as a pyramidal structure as depicted in Figure 2.1. Division of power systems according to areas (see Figure 2.1) is based on a geographical concept of system structure. Each area of an interconnected power system consists of a number of power plants. Within an area a power plant usually consists of a number of generators which are equipped with governors to control their speed.

Because of the slow response of an area to any load changes, an area can be represented by an equivalent governor-turbine-generator (inertial model) combination for the load-frequency control purposes.[2] Even for a large load change, the frequency deviation within an area is usually small, and therefore a small signal model based on input-output relations[2,7] can be assumed.

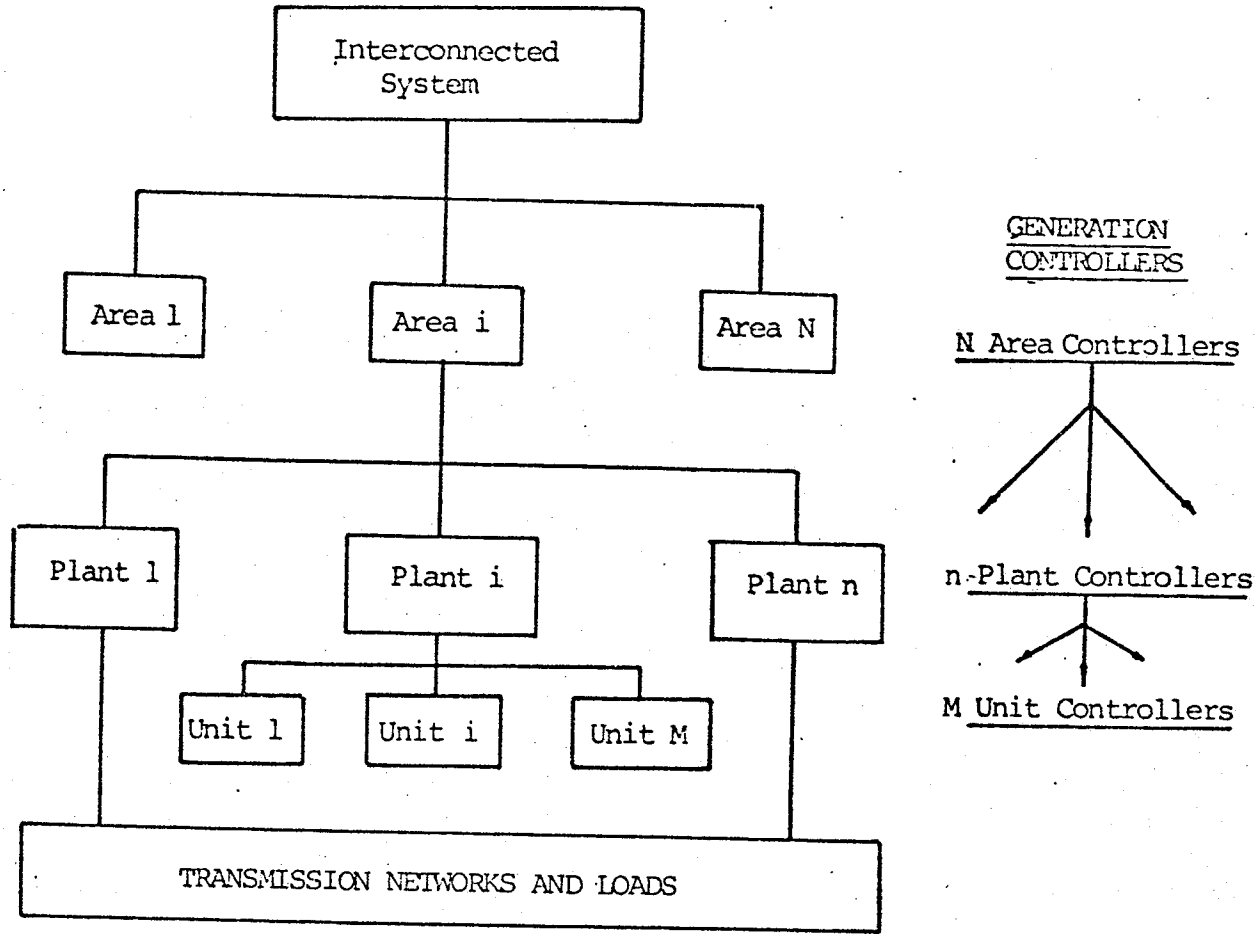

Figure 2.1 'PYRAMIDAL' STRUCTURE OF AN INTERCONNECTED POWER SYSTEM AND CONTROL ALLOCATIONS AT THE INDICATED LEVELS.

2.2 System Representation

An interconnected two-area power system, as shown in Figure 2.2, is considered for the purpose of dynamic load-frequency control. Each area is assumed to have a large thermal source of generation and to be interconnected by an a.c. tie-line.

The block-diagram of an area is shown in Figure 2.3. It consists of models for the governor, turbine and generator; and it also shows the connection between these elements. Even though there are complex models for each of these devices, their simple representations as shown in Figure 2.3 are assumed adequate for the purpose of dynamic load-frequency control problems.[2,7]

The block-diagram of an interconnected two-area system[7] is shown in Figure 2.4. It includes models of each area and an a.c. tie-line which interconnects the two areas.

To investigate the effects of coupling introduced by the a.c. tie-line and the roles played by the load-frequency controllers, dynamic models of the following system configurations are derived:

(i) The isolated operation of an area.

(ii) The interconnected operation of the two-area system without load-frequency controllers.

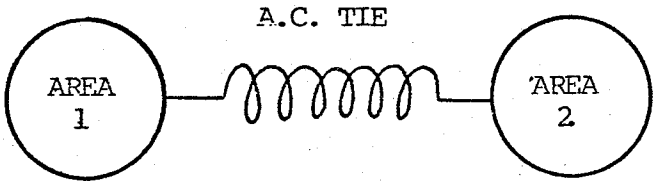

FIG. 2.2 An interconnected two-area power system

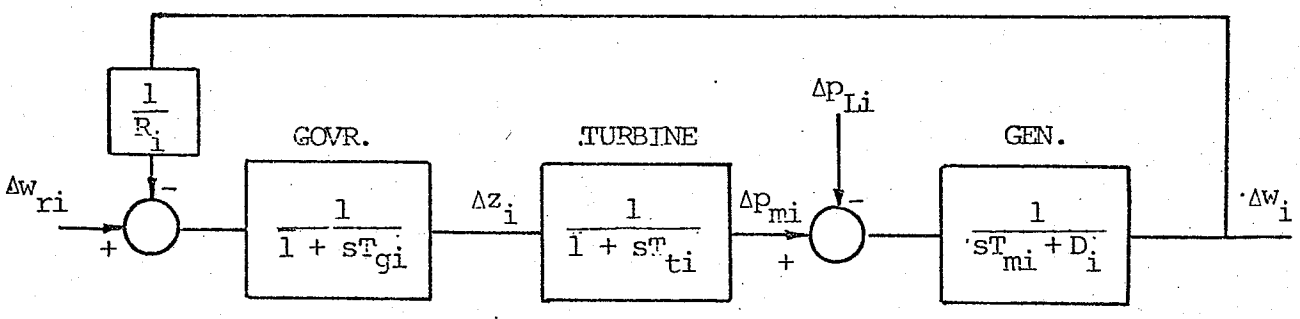

FIG. 2.3 Linear model of an isolated steam area system

NOTE: Symbols used here are defined in Appendix V.

(iii) The interconnected operation of the two-area system with conventional load-frequency controllers.

Dynamic models of the two-area system with PID load-frequency controllers and the d.c. link as an element in an area or as an interconnecting tie between areas are derived in Chapters 3 and 5.

2.3 State-Space Equations

In the state-space form, the system dynamic equations are represented by a set of first order differential equations. Since most numerical and digital computer programs are suited to this form of system representation, state equations describing the dynamics of elements and of the system configurations (given in section 2.2 above) are now derived from the transfer functions as shown in Figures 2.3 and 2.4. The list of the symbols and their meanings are given in Appendix V.

2.3.1 The Isolated Operation of an Area (Figure 2.3)

State equations for each of the elements in Figure 2.3 are first derived from their transfer functions and then combined to describe the dynamics of an area in the isolated mode of operation. Equations 2.1, 2.2 and 2.3 below represent the state equations for the governor, turbine and generator of the ith area.

Governor:

$$\frac{\Delta z_i}{\Delta w_{ri} - \frac{1}{R_i}\Delta w_i} = \frac{1}{1 + sT_{gi}}$$

$$\Delta \dot{z}_i = -\frac{1}{T_{gi}}\Delta z_i - \frac{1}{R_i T_{gi}}\Delta w_i + \frac{1}{T_{gi}}\Delta w_{ri} \qquad 2.1$$

Turbine:

$$\frac{\Delta p_{mi}}{\Delta z_i} = \frac{1}{1 + sT_{ti}}$$

$$\Delta \dot{p}_{mi} = -\frac{1}{T_{ti}}\Delta p_{mi} + \frac{1}{T_{ti}}\Delta z_i \qquad 2.2$$

Generator:

$$\frac{\Delta w_i}{\Delta p_{mi} - \Delta p_{Li}} = \frac{1}{sT_{mi} + D_i}$$

$$\Delta \dot{w}_i = -\frac{D_i}{T_{mi}}\Delta w_i + \frac{1}{T_{mi}}\Delta p_{mi} - \frac{1}{T_{mi}}\Delta p_{Li} \qquad 2.3$$

The foregoing set of equations for this area in matrix form can be written as:

$$\begin{bmatrix} \Delta \dot{w}_i \\ \Delta \dot{z}_i \\ \Delta \dot{p}_{mi} \end{bmatrix} = \begin{bmatrix} -\frac{D_i}{T_{mi}} & 0 & \frac{1}{T_{mi}} \\ -\frac{1}{R_i T_{gi}} & -\frac{1}{T_{gi}} & 0 \\ 0 & \frac{1}{T_{ti}} & -\frac{1}{T_{ti}} \end{bmatrix} \begin{bmatrix} \Delta w_i \\ \Delta z_i \\ \Delta p_{mi} \end{bmatrix} + \begin{bmatrix} 0 \\ \frac{1}{T_{gi}} \\ 0 \end{bmatrix} \begin{bmatrix} \Delta w_{ri} \end{bmatrix} + \begin{bmatrix} -\frac{1}{T_{mi}} \\ 0 \\ 0 \end{bmatrix} \begin{bmatrix} \Delta p_{Li} \end{bmatrix} \qquad 2.4$$

and the output, Δw_i can be written as

$$\Delta w_i = [1 \quad o \quad o] \, [\Delta w_i \; \Delta z_i \; \Delta p_{mi}]^T \qquad 2.5$$

Equations 2.4 and 2.5 are of the standard state-space form:

$$\dot{x}_i = A_i x_i + B_i u_i + S_i v_i \qquad 2.6$$

$$y_i = C_i x_i \qquad 2.7$$

where $x_i = (\Delta w_i , \Delta z_i , \Delta p_{mi})^T$ is the state vector,

$u_i = (\Delta w_{ri})$ is the control vector,

$v_i = (\Delta p_{Li})$ is the disturbance vector,

$y_i = (\Delta w_i)$ is the output vector

A_i , B_i , S_i and C_i are the matrices associated with the state, control, disturbance and output vectors respectively.

2.3.2 The Interconnected Operation of the Two-Area System without Load-Frequency Controllers (Figure 2.4)

The dynamic model of an interconnected two area system is shown in Figure 2.4. An a.c. tie is assumed to interconnect two areas.

Since equations for a general ith area have already been developed in section 2.3.1, the equation for the a.c. tie line will be developed in this section.

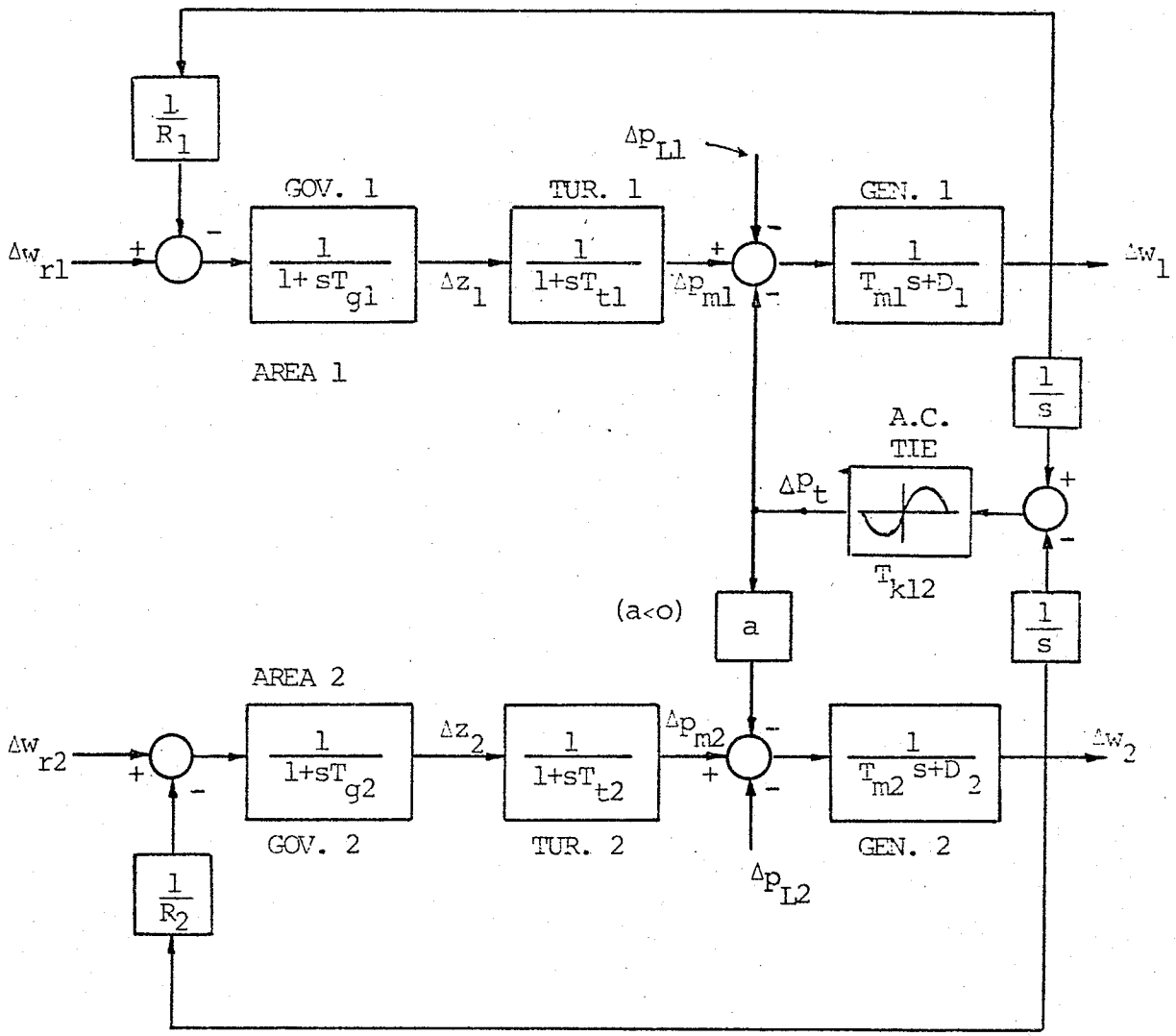

FIG. 2.4 An interconnected two-area system without load frequency controllers.

An a.c. tie-line can be represented by the following non-linear equation

$$p_t = \frac{v_1 v_2}{x_{12}} \sin (\delta_1 - \delta_2) \qquad 2.8$$

where p_t is the per unit power transfer from area 1 to area 2.

v_1 , v_2 are the per unit voltages of areas 1 and 2,

x_{12} is the per unit reactance of the tie-line

and δ_1 , δ_2 are the phase angles of areas 1 and 2 at the point of interconnection.

For the small signal analysis, equation 2.8 is linearised about an operating point. Hence the tie-line power deviation is

$$\Delta p_t = \frac{v_1 v_2}{x_{12}} \cos \delta_{120} \ (\Delta\delta_1 - \Delta\delta_2) \qquad 2.9$$

where Δ denotes the small deviation

and $\delta_{120} = (\delta_{10} - \delta_{20})$ is the initial phase angle difference between area 1 and area 2.

Since the per unit phase angle δ is the integral of the per unit frequency w, equation 2.9 can be written as

$$\Delta p_t = \frac{T_{k12}}{s} (\Delta w_1 - \Delta w_2) \qquad 2.10$$

where $T_{k12} = \frac{377 \ v_1 \ v_2}{x_{12}} \cos \delta_{120}$ is the synchronising torque coefficient

and Δw_1 and Δw_2 are the frequency deviations of area 1 and area 2 respectively.

In the state-space form, equation 2.10 can be written as

$$\Delta \dot{p}_t = T_{k12}\ \Delta w_1 - T_{k12}\ \Delta w_2 \qquad 2.11$$

Thus as shown by the state equation 2.11, an a.c. interconnection introduces an additional state Δp_t.

Since the state Δp_t is a linear function of the frequency deviations Δw_1 and Δw_2 of the interconnected areas, it couples areas dynamically and appears as a dynamic load to an area generator (as shown in Figure 2.4). The magnitudes of this load, seen by the interconnected areas, are:

$$\Delta p_{t1} = \Delta p_t \qquad 2.12$$

$$\Delta p_{t2} = a\ \Delta p_t$$

$$\text{where}\quad a = -\frac{\text{MW capability of area 1, } P_{R1}}{\text{MW capability of area 2, } P_{R2}} \qquad (7)$$

Since an a.c. tie-line introduces an additional input to each interconnected area generator, the equation 2.3 for the i th area generator is modified to (See Figure 2.4)

$$\frac{\Delta w_i}{\Delta p_{mi} - \Delta p_{Li} - \Delta p_{ti}} = \frac{1}{sT_{mi} + D_i}$$

$$\Delta \dot{w}_i = -\frac{D_i}{T_{mi}}\Delta w_i + \frac{1}{T_{mi}}\Delta p_{mi} - \frac{1}{T_{mi}}\Delta p_{Li} - \frac{1}{T_{mi}}\Delta p_{ti} \qquad 2.14$$

Because an a.c. interconnection does not influence the inputs to an area governor or turbine directly, equations 2.1 and 2.2 remain the same for an area even in the interconnected mode of operation.

A dynamic set of equations for an area in an interconnected two-area system can thus be written as:

$$\begin{bmatrix} \Delta\dot{w}_i \\ \Delta\dot{z}_i \\ \Delta\dot{p}_{mi} \\ \Delta\dot{p}_{ti} \end{bmatrix} = \begin{bmatrix} -\frac{D_i}{T_{mi}} & o & \frac{1}{T_{mi}} & -\frac{1}{T_{mi}} \\ -\frac{1}{R_i T_{gi}} & -\frac{1}{T_{gi}} & o & o \\ o & \frac{1}{T_{ti}} & -\frac{1}{T_{ti}} & o \\ T_{kij} & o & o & o \end{bmatrix} \begin{bmatrix} \Delta w_i \\ \Delta z_i \\ \Delta p_{mi} \\ \Delta p_{ti} \end{bmatrix} + \begin{bmatrix} o \\ o \\ o \\ -T_{kij} \end{bmatrix} \begin{bmatrix} \Delta w_j \end{bmatrix} + \begin{bmatrix} o \\ \frac{1}{T_{gi}} \\ o \\ o \end{bmatrix} \begin{bmatrix} \Delta w_{ri} \end{bmatrix} + \begin{bmatrix} -\frac{1}{T_{mi}} \\ o \\ o \\ o \end{bmatrix} \begin{bmatrix} \Delta p_{Li} \end{bmatrix} \qquad 2.15$$

and the outputs Δw_i and Δp_{ti} can be written as

$$\begin{bmatrix} \Delta w_i \\ \Delta p_{ti} \end{bmatrix} = \begin{bmatrix} 1 & o & o & o \\ o & o & o & 1 \end{bmatrix} \begin{bmatrix} \Delta w_i & \Delta z_i & \Delta p_{mi} & \Delta p_{ti} \end{bmatrix}^T \qquad 2.16$$

Equations 2.15 and 2.16 can be written in the simplified state-space form as:

$$\dot{x}_i = A_i x_i + A_{ij} x_j + B_i u_i + S_i v_i \qquad 2.17$$

$$y_i = C_i x_i \qquad 2.18$$

The tie-line introduces an additional state Δp_{ti} to the area

dynamics and couples areas dynamically through Δw_j (See Equation 2.15).

The complete set of equations for an interconnected two-area system can now be written as

$$\dot{x} = Ax + Bu + Sv \qquad 2.19$$

$$y = Cx \qquad 2.20$$

where

$$x = (x_1, x_2)^T$$

$$= \left[(\Delta w_1, \Delta z_1 \Delta p_{m1}, \Delta p_{t1}), (\Delta w_2, \Delta z_2 \Delta p_{m2}, \Delta p_{t2})\right]^T$$

$$u = (u_1, u_2)^T$$

$$= (\Delta w_{r1}, \Delta w_{r2})^T$$

$$v = (v_1, v_2)^T$$

$$= (\Delta p_{L1}, \Delta p_{L2})^T$$

$$A = \begin{bmatrix} A_1 & A_{12} \\ A_{21} & A_2 \end{bmatrix}, \quad B = \begin{bmatrix} B_1 & o \\ o & B_2 \end{bmatrix}, \quad S = \begin{bmatrix} S_1 & o \\ o & S_2 \end{bmatrix}$$

$$C = \begin{bmatrix} C_1 & o \\ o & C_2 \end{bmatrix}$$

Subscripts 1 and 2 denote area 1 and area 2 variables, and subscripts 12 and 21 denote the effects of coupling between area 1 and area 2.

2.3.3 The Interconnected Operation of the Two-Area System with the Conventional Load-Frequency Controllers

The dynamic model of an interconnected two-area system with the conventional load-frequency controllers is shown in Figure 2.5. This model is similar to the model shown in Figure 2.4 except that a conventional load-frequency controller for each area now generates a control signal Δw_{ri} according to the equation

$$\Delta w_{ri} = -\left(\Delta p_{ti} + b_{si}\ \Delta w_i\right)\ \frac{k_{si}}{s}$$

$$\text{or}\quad \Delta \dot{w}_{ri} = -\ k_{si}\ \Delta p_{ti} - k_{si}\ b_{si}\ \Delta w_i \qquad 2.21$$

where b_{si} is the tie-line bias,

k_{si} is the integral gain,

and $(\Delta p_{ti} + b_{si}\ \Delta w_i)$ is the area control error.

The conventional load-frequency controller of an area thus generates a state-vector Δw_{ri} and a state-equation 2.21. This additional state increases the dynamic order of an area by one. In this case the dynamic set of equations for an area is now given by

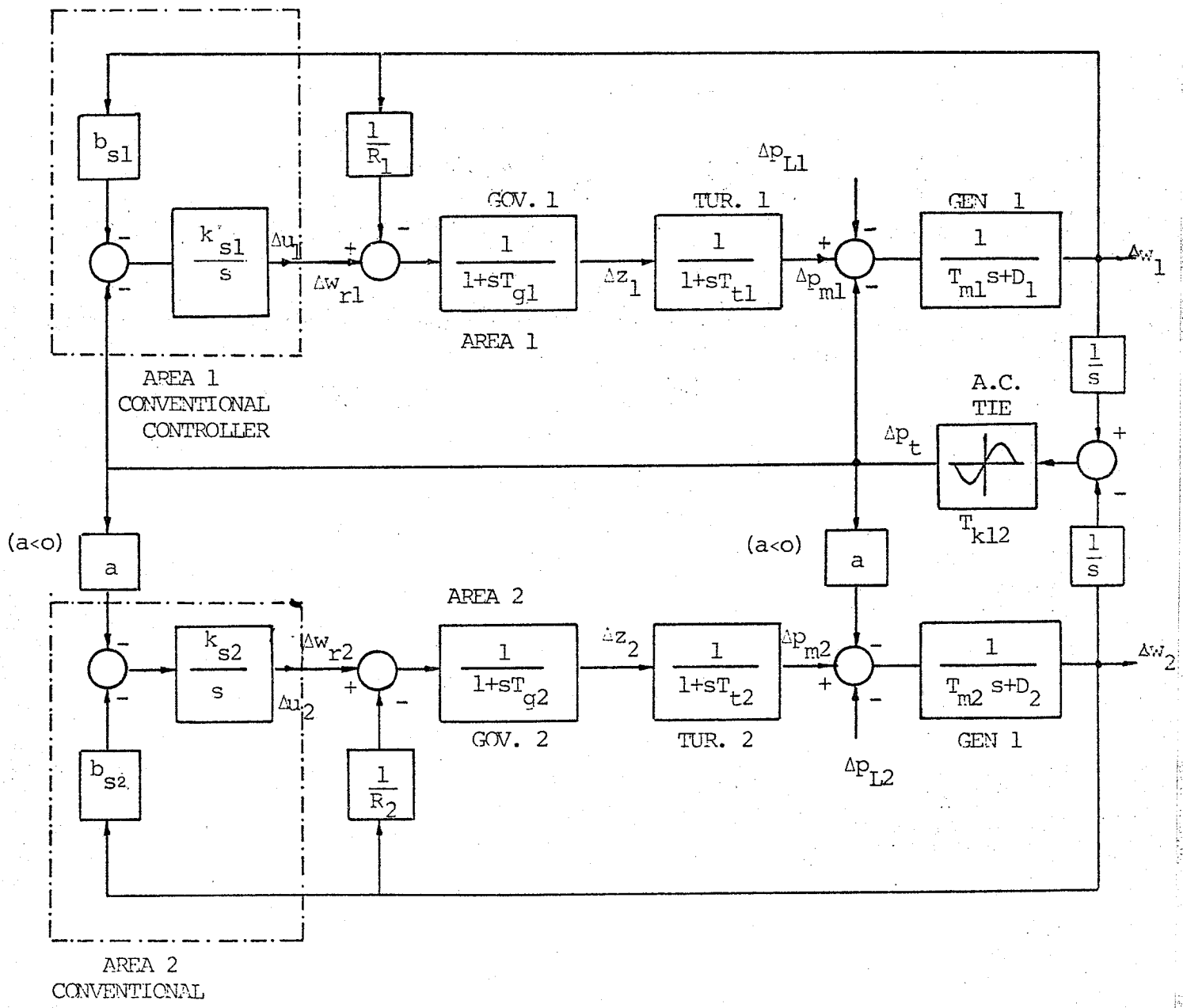

FIG. 2.5 An interconnected two-area system with Conventional load-frequency controllers.

$$\begin{bmatrix} \Delta\dot{w}_i \\ \Delta\dot{z}_i \\ \Delta\dot{p}_{mi} \\ \Delta\dot{p}_{ti} \\ \Delta\dot{w}_{ri} \end{bmatrix} = \begin{bmatrix} -\frac{D_i}{T_{mi}} & 0 & \frac{1}{T_{mi}} & -\frac{1}{T_{mi}} & 0 \\ -\frac{1}{R_i T_{gi}} & -\frac{1}{T_{gi}} & 0 & 0 & \frac{1}{T_{gi}} \\ 0 & \frac{1}{T_{ti}} & -\frac{1}{T_{ti}} & 0 & 0 \\ T_{kij} & 0 & 0 & 0 & 0 \\ -k_{si} b_{si} & 0 & 0 & -K_{si} & 0 \end{bmatrix} \begin{bmatrix} \Delta w_i \\ \Delta z_i \\ \Delta p_{mi} \\ \Delta p_{ti} \\ \Delta w_{ri} \end{bmatrix} + \begin{bmatrix} 0 \\ 0 \\ 0 \\ -T_{kij} \\ 0 \end{bmatrix} \begin{bmatrix} \Delta w_j \end{bmatrix} + \begin{bmatrix} -\frac{1}{T_{mi}} \\ 0 \\ 0 \\ 0 \\ 0 \end{bmatrix} \begin{bmatrix} \Delta p_{Li} \end{bmatrix} \qquad 2.22$$

and the outputs Δw_i and Δp_{ti} are given by

$$\begin{bmatrix} \Delta w_i \\ \Delta p_{ti} \end{bmatrix} = \begin{bmatrix} 1 & 0 & 0 & 0 & 0 \\ 0 & 0 & 0 & 1 & 0 \end{bmatrix} [\Delta w_i \ \Delta z_i \ \Delta p_{mi} \ \Delta p_{ti} \ \Delta w_{ri}]^T \qquad 2.23$$

Equations 2.22 and 2.23 can be written in the simplified form as:

$$\dot{x}_i = A_i x_i + A_{ij} x_j + S_i v_i \qquad 2.24$$

$$y_i = C_i x_i \qquad 2.25$$

The complete set of state and output equations for an interconnected two-area system with the conventional load-frequency controllers can now be written as:

$$\dot{x}_o = A_o x_o + S_o v_o \qquad 2.26$$

$$y_o = C_o x_o \qquad 2.27$$

where $x_o = (x_1, x_2)^T$

$$= \Big[(\Delta w_1, \Delta z_1, \Delta p_{m1}, \Delta p_{t1}, \Delta w_{r1}) ,$$

$$(\Delta w_2, \Delta z_2, \Delta p_{m2}, \Delta p_{t2}, \Delta w_{r2}) \Big]^T$$

$$v_o = (v_1, v_2)^T$$

$$= (\Delta p_{L1}, \Delta p_{L2})^T$$

$$y_o = (y_1, y_2)^T$$

$$\Big((\Delta w_1, \Delta p_{t1}) , (\Delta w_2, \Delta p_{t2}) \Big)^T$$

$$A_o = \begin{bmatrix} A_1 & A_{12} \\ A_{21} & A_2 \end{bmatrix}, \quad S_o = \begin{bmatrix} S_1 & o \\ o & S_2 \end{bmatrix}, \quad C_o = \begin{bmatrix} C_1 & o \\ o & C_2 \end{bmatrix}$$

2.4 Analysis of the Conventional System

2.4.1 The Isolated Operation of an Area

State equations 2.4 describe the dynamics of an isolated area system. Table 2.1 provides the constants (also used by Elgerd and Fosha[7]) for the system. The eigenvalues for this system with these constants are:

$$\lambda_1 = -13.29$$

$$\lambda_{2,3} = -1.296 \pm j\, 2.512$$

These eigenvalues indicate that the isolated area system is stable but that the dynamic behaviour is oscillatory with poor damping. Figure 2.6 shows the time domain response to a 5 percent step load increase. A dynamic behaviour of this nature

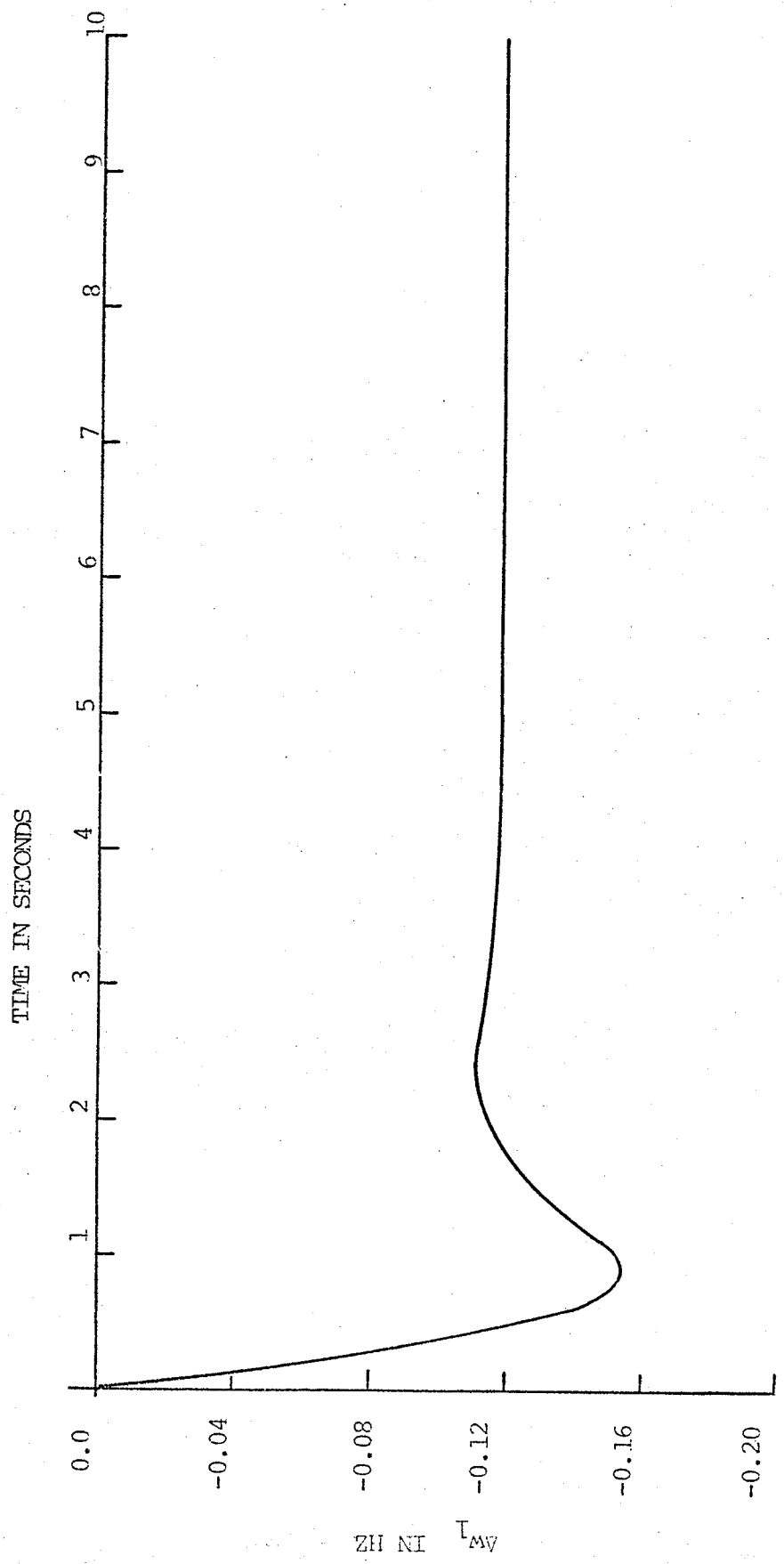

FIG. 2.6 Time-domain response of an isolated area to a 5% step load increase.

TABLE 2.1

Parameters of an interconnected two-area system

Parameters	Area 1	Area 2
T_g sec	0.08	0.08
T_t sec	0.3	0.3
R	0.04	0.04
T_m sec	10.0	10.0
v_{pu}	1.0	1.0
P_R MW	2000	16000
b_s	25.0	25.0
D	0.5	0.5

Tie Line

$x_{12} = 10.0$

$\delta_{120} = 30^{o}$

$T_{k12} = 32.5$

$$a = -\frac{P_{R1}}{P_{R2}} = -0.125$$

can be expected when an area becomes separated from the rest of the power system.

2.4.2 The Interconnected Operation of Areas without Load-Frequency Controllers

State equations 2.15 now describe the dynamics of an area in an interconnected two-area system. An examination of the state coefficient matrix A_i for the i th area indicates that an a.c. interconnection introduces an additional state and provides coupling between the states of interconnected areas.

The effect of an interconnection on the dynamic behaviour of an area can be analysed by examining the changes in the eigenvalues of the interconnected areas. Table 2.2 provides a comparison of dominant eigenvalues of an area for the isolated and for the interconnected modes of operation. This comparison shows that an interconnection decreases damping but increases the frequency of oscillation of the dominant system mode. The time domain solution for a 5 percent load increase in area 1 (See Figure 2.7) confirms the eigenvalue analysis.

An interconnection also influences the steady-state performance of an area. Table 2.2 compares the steady-state frequency and tie-line power deviations from schedule for a step load change in area 1. Table 2.2 shows that the area

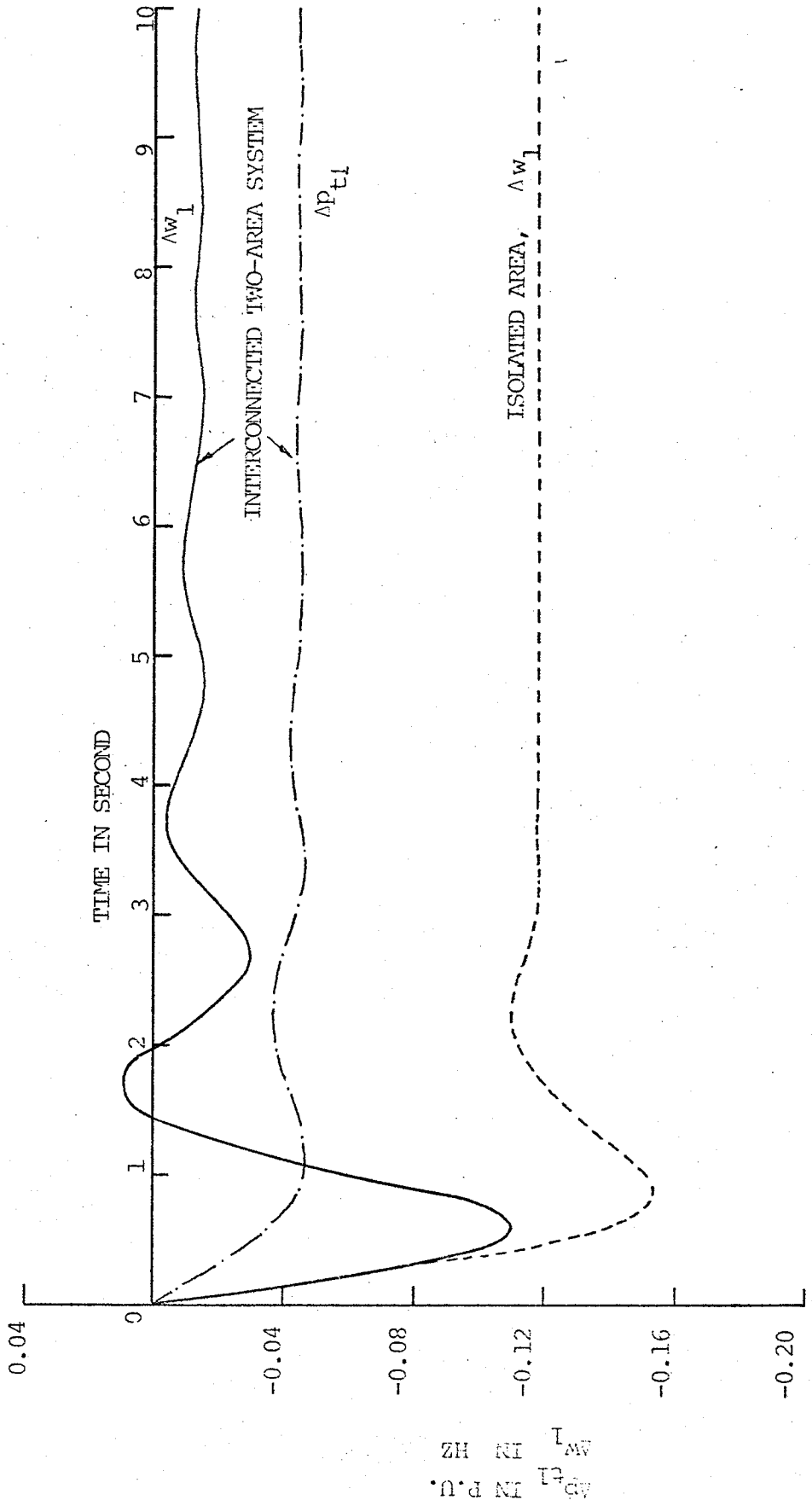

FIG. 2.7 Time-domain response of an interconnected two-area system to a 5% step load increase in Area 1.

frequency error is reduced as a result of interconnection but the tie-line power deviation is increased.

TABLE 2.2 Comparison of performance: isolated vs. interconnected modes of system operation

Performance Index	Isolated mode	Interconnected mode
Dominant eigenvalues	$-1.296 \pm j\ 2.512$	$-0.717 \pm j\ 3.053$
Steady-state error		
(i) Frequency error, Δw_1	$-\frac{\Delta P_{L1}}{D_1 + \frac{1}{R_1}} = -\frac{\Delta P_{L1}}{25.5}$	$\frac{a\,\Delta P_{L1}}{(D_2 + \frac{1}{R_2}) - a(D_1 + \frac{1}{R_1})} = -\frac{1}{9} \cdot \frac{\Delta P_{L1}}{25.5}$
(ii) Tie line deviation, ΔP_{t1}	Not Applicable	$\frac{-(D_2 + \frac{1}{R_2})\ \Delta P_{L1}}{(D_2 + \frac{1}{R_2}) - a(D_1 + \frac{1}{R_1})} = -\frac{8}{9}\Delta P_{L1}$

2.4.3 The Interconnected Operation of Areas with Conventional Load-Frequency Controllers

As seen in the previous section, an interconnection does reduce the steady-state frequency deviation of an area by the generation change in the other areas. But this behaviour of interconnection fails to meet the specification that other areas should not change their generations unless an area cannot meet its own load demand. The conventional load-frequency

controller at each area level is therefore designed to meet this specification. Figure 2.5 shows the block diagram of a conventional integral controller which uses the area control error as its input. The main function of the integral term is to reset the area control error to zero. It maintains a specified system frequency and tie-line power transfer when an area can meet its own load demand. The bias constant b_s is set equal to the area regulating coefficient R to minimize necessary hunting and interaction.[2] The integral gain k_s is the only adjustable parameter of the conventional controller to influence the dynamic behaviour of the interconnected power system. The effect of this gain on the dynamic behaviour is next examined by the eigenvalue and time-domain analyses.

Eigenvalues of the system matrix A_o (see equation 2.26) are calculated for different values of k_s at the nominal tie-line loading ($\delta_{12} = 30^o$). The root-locus plot (Figure 2.8) shows the movement of the dominant eigenvalue. For these variations in k_s the system is stable, but the damping is poor; k_s provides a small improvement in the damping of the dominant system mode.

Since the dominant eigenvalue cannot indicate the dynamic behaviour of the system fully, a time-domain solution of the system equations is carried out to verify the conclusions of the eigenvalue analysis. Figure 2.9 shows the system behaviour for a 5 percent load increase in area 1 and for differ-

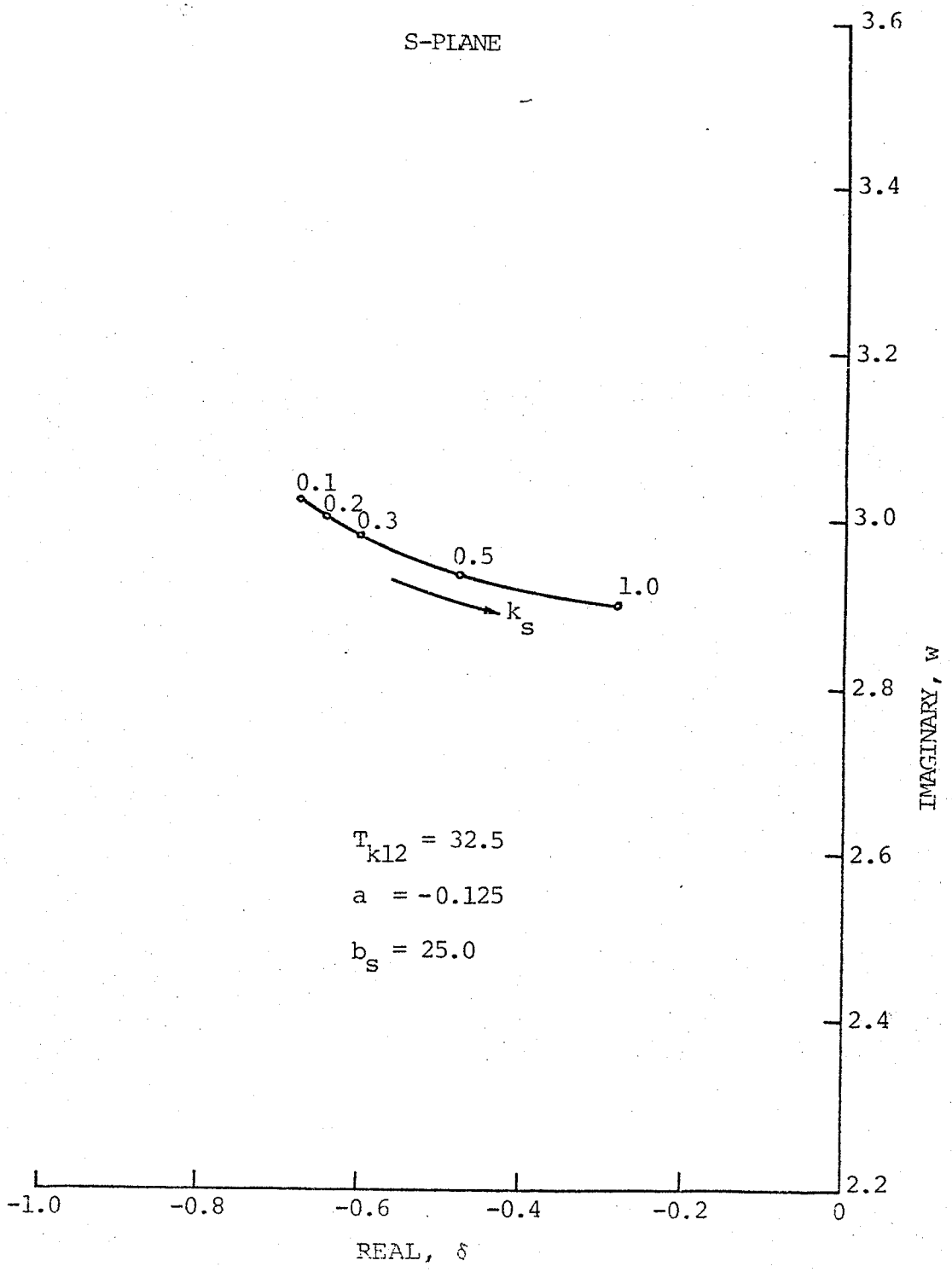

FIG. 2.8 Root-locus plot of an interconnected two-area system with the conventional load-frequency controller: Effect of k_s

ent values of k_s. The lower values of k_s (less than 0.2) improve the damping of dynamic oscillations only marginally, but they increase the settling time considerably. A value of k_s equal to 0.2 is therefore selected to minimize the steady state error without considerable decrease in damping.

Table 2.3 compares the dynamic and steady-state behaviours of an interconnected two-area system with and without the conventional load-frequency controllers. It shows that the conventional load-frequency controller mainly influences the steady-state behaviour and does not control the dynamic behaviour.

TABLE 2.3 Comparison of performance: Interconnected system with and without Conventional load-frequency controllers

Performance Index	Without LFC	With LFC
Dominant Eigenvalues	$-0.717 \pm j\,3.053$	$-0.642 \pm j\,3.008$
Steady-state error		
(i) Δw_1	$\dfrac{a\,\Delta p_{L1}}{D_2 + \frac{1}{R_2} - (\frac{1}{R_1} + D_1)\,a} = \dfrac{-\Delta p_{L1}}{9 \times 25.5}$	0.0
(ii) Δp_{t1}	$\dfrac{\Delta p_{L1}\,(D_2 + \frac{1}{R_2})}{D_2 + \frac{1}{R_2} - (\frac{1}{R_1} + D_1)\,a} = \dfrac{-8}{9}\,\Delta p_{L1}$	0.0
Dynamic Performance First peak, Δw_1	0.11	0.108

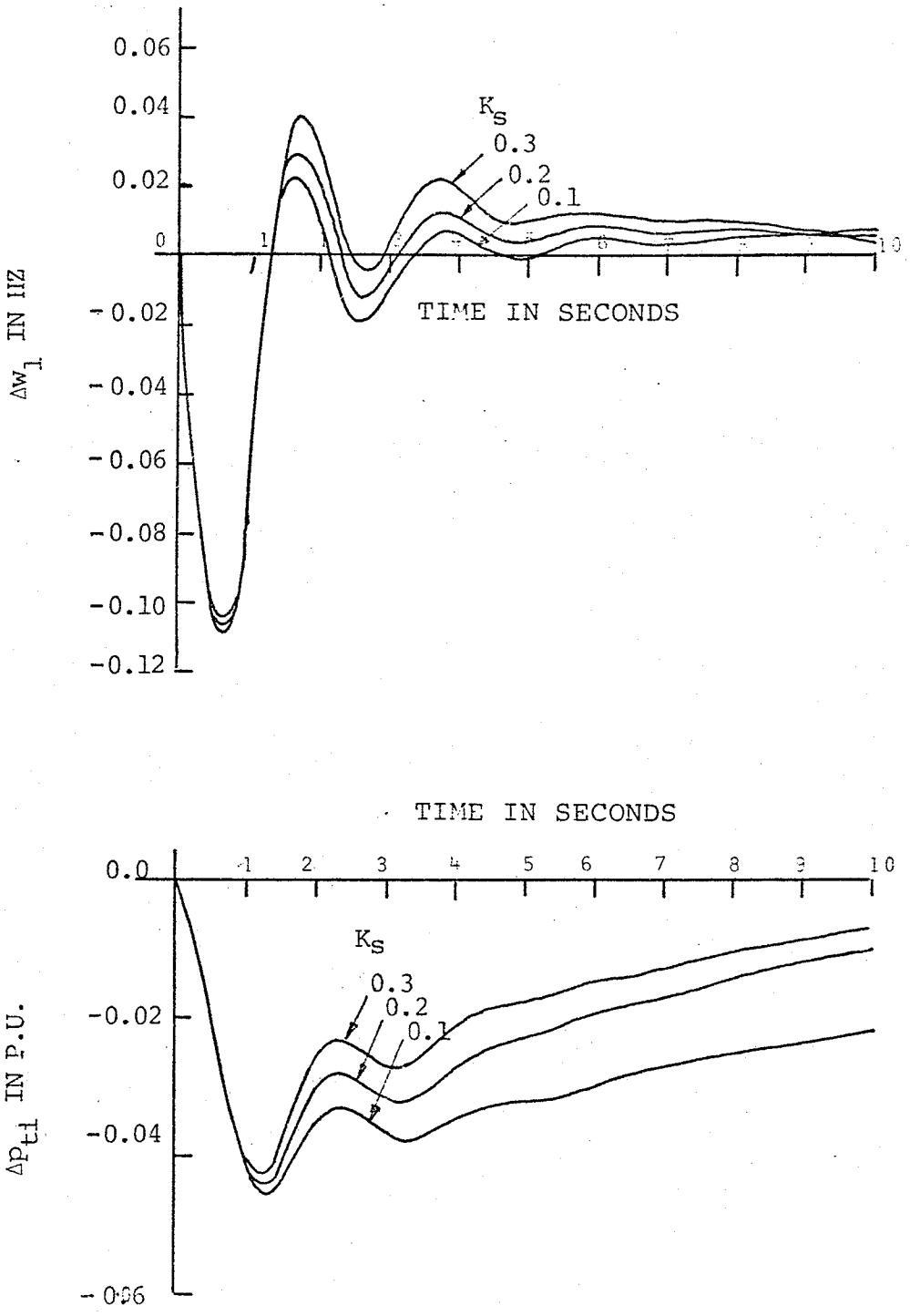

FIG. 2.9 Transient response to a 5% step load increase in Area 1 with Conventional load frequency controller, effects of K_S.

2.5 Conclusion

An a.c. interconnection improves the steady-state frequency regulation but causes unscheduled steady-state power transfer over the tie-lines. It also causes unnecessary generation changes in all areas for a load change anywhere in the interconnected system. Given these conditions, the conventional load-frequency controller maintains tie-line flow and frequency at set values by controlling generation only from the area where the load change has occurred. Only when an area cannot meet its load demand does the controller allow assistance from other areas. Thus this controller prevents normal steady-state interaction.

Additionally, an a.c. interconnection degrades the dynamic performance of each individual area. The conventional load-frequency controller has failed to improve this dynamic performance. Conversely, optimal controllers have been suggested in the past to improve the dynamic performance but all of these have failed to meet the steady-state load-frequency control requirements.[8] So neither the conventional nor previously proposed controllers have simultaneously met both the steady-state and dynamic requirements.

To solve this dilemma, Chapter 3 proposes a load-frequency controller which is easy to realize and fulfills both the steady-state and dynamic performance requirements.

CHAPTER 3

DECENTRALIZED MULTIVARIABLE CONTROLLER DESIGN

3.1 Introduction

An interconnected power system requires a load-frequency controller at each area control center to fulfill the steady-state system frequency and tie-line power schedules. As shown in Chapter 2, the conventional controller does not provide adequate damping to the system dynamic oscillations. Nevertheless, damping these oscillations is necessary to maintain stability and to avoid area separation at high power transfer levels.[2,7]

Inability of the conventional load-frequency controller to damp these oscillations led researchers[8-14] to search for other forms of controllers. Optimal control techniques have been proposed for designing a load-frequency controller. Such proposed controllers, however, have denied assistance from adjoining areas to an area which cannot meet its demand; thus the system collapses. Further, the optimal controllers require measurement or identification of states of all interconnected areas, yet provide optimal dynamic response only for a single operating condition.[23-24] Because of these problems, the suggested optimal load-frequency controllers have

received no application in the field.

As a practical alternative, this chapter proposes a decentralized dynamic controller design[25-28] which uses local output signals only.[29-47] The dynamic structure of this controller is selected not only to provide a desired degree of relative system stability but also to fulfill the steady-state requirements of the existing load-frequency controller.

An iterative pole-placement technique[40] is used to determine the parameters of this controller. The effect of operation at other than the normal operating condition is evaluated by the root-locus analysis. The effect of system nonlinearity is examined by solving the nonlinear dynamic equations in time-domain. An interconnected two-area system is used to show the feasibility of this design.

3.2 Theoretical Considerations

As shown in Chapter 2, the state and output equations for an interconnected two-area power system without load-frequency controllers can be written as:

$$\dot{x} = Ax + Bu + Sv$$

$$y = Cx$$

where $x = (x_1, x_2)^T$

$u = (u_1, u_2)^T$

$$v = (v_1, v_2)^T$$

$$A = \begin{bmatrix} A_1 & A_{12} \\ A_{21} & A_2 \end{bmatrix} \quad B = \begin{bmatrix} B_1 & o \\ o & B_2 \end{bmatrix} \quad S = \begin{bmatrix} S_1 & o \\ o & S_2 \end{bmatrix}$$

$$C = \begin{bmatrix} C_1 & o \\ o & C_2 \end{bmatrix}$$

where subscripts 1 and 2 denote area 1 and area 2 and subscripts 12 and 21 denote cross coupling between areas.

In general for the s-area interconnected power system, the state and output equations can then be written as:

$$\dot{x} = Ax + Bu + Sv \qquad 3.1$$

$$y = Cx$$

where $x = (x_1, x_2, \cdots x_s)^T$

$u = (u_1, u_2, \cdots u_s)^T$

$v = (v_1, v_2, \cdots v_s)^T$

$y = (y_1, y_2, \cdots y_s)^T$

$$A = \begin{bmatrix} A_1 & A_{12} & \cdots & A_{1s} \\ A_{21} & A_2 & \cdots & A_{2s} \\ A_{s1} & A_{s2} & \cdots & A_s \end{bmatrix}$$

$B = \text{block diag.}\ (B_1, B_2, \cdots B_s)$

$S = \text{block diag.}\ (S_1, S_2, \cdots S_s)$

$C = \text{block diag.}\ (C_1, C_2, \cdots C_s)$

The next step is to find a controller capable of generating for each area a control signal u_i based only on the local measurements y_i. This signal can be generated by a general output feedback dynamic controller of the following form:

$$\dot{z}_i = F_i z_i + G_i y_i \qquad 3.2$$
$$u_i = H_i z_i + K_i y_i$$

where z_i is the state vector of i th dynamic feedback controller and

F_i, G_i, H_i and K_i are real constant matrices.

Equation 3.2 for the whole system can now be written as:

$$\dot{z} = F z + G y \qquad 3.3$$
$$u = H z + K y$$

where F = block diag.$(F_1, F_2, \ldots F_s)$

G = block diag.$(G_1, G_2, \ldots G_s)$

H = block diag.$(H_1, H_2, \ldots H_s)$

K = block diag.$(K_1, K_2, \ldots K_s)$

With the controller defined by equation 3.3, the system dynamic equation 3.1 can be written as:

$$\begin{bmatrix} \dot{x} \\ \dot{z} \end{bmatrix} = \begin{bmatrix} A+BKC & BH \\ GC & F \end{bmatrix} \begin{bmatrix} x \\ z \end{bmatrix} + \begin{bmatrix} S \\ o \end{bmatrix} \begin{bmatrix} v \end{bmatrix} \qquad 3.4$$

$$\text{or} \quad \dot{x}_o = A_o x_o + S_o v_o \qquad 3.5$$

$$\text{where } [x_o]^T = [x \; z]$$

At this point F, G, H and K (constant matrices for the dynamic compensator) need to be determined to satisfy a specified criterion of dynamic stability for the interconnected system. This specified criterion can be satisfied by placing the eigenvalues of matrix A_o in a specified region R of the complex plane.

In this thesis this criterion of dynamic stability has been selected for the following reasons:

(i) The order of the dynamic compensator can be smaller than that required for the optimal control or for the exact pole positioning in s-plane.

(ii) A limit on the minimum settling time and the maximum damping can be specified as shown in Figure 3.1.

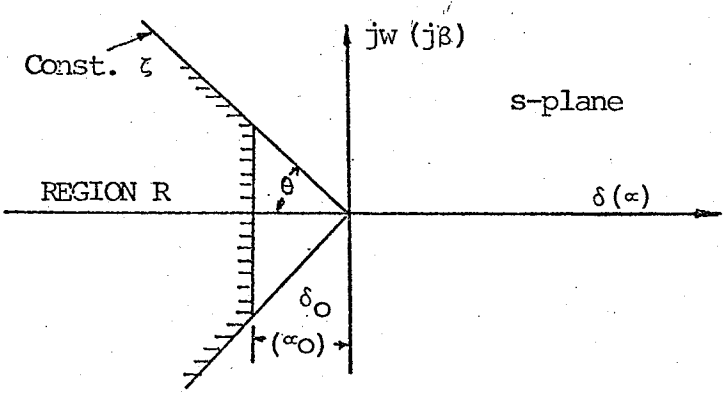

Figure 3.1 The desired sector for roots of an interconnected power system

An iterative pole-placement solution technique is described in the following section to determine F, G, H and K matrices of a dynamic compensator.

3.3 An Iterative Pole-Placement Solution Technique[40]

First a set of trial values for F, G, H and K are selected and the eigenvalues of matrix A_o

$$\lambda_i = \alpha_i \pm j\beta_i \ , \quad i = 1, 2, \ldots\ldots, n$$

are determined. Some of these eigenvalues may be outside the specified region R of the complex s-plane given by

$$h_1(\alpha, \beta) = \alpha + \alpha_o \lesssim o$$

$$h_2(\alpha, \beta) = \alpha + M_1 |\beta| \lesssim o \qquad 3.6$$

Where $M_1 = \cot\theta$, $\theta = \cos^{-1}\zeta$

Thus the next step is to modify the controller constants until all of the undesirable eigenvalues have moved into the correct region. Since complex eigenvalues occur in conjugate pairs, only those q undesirable eigenvalues that satisfy

$$\beta_i \gtrsim o \ , \quad i = 1, 2, \ldots\ldots q \qquad 3.7$$

i.e., only those eigenvalues that lie above or on the real axis need to be considered. The aim of the design is to make q = o.

For convenience, the set of controller constants can be defined by the vector M. When only first order terms are considered, the increment δM in the constants can be written

$$h\ (\alpha_i, \beta_i) + \left[\frac{\partial h\ (\alpha_i, \beta_i)}{\partial M}\right]^T \delta M = 0\ ,\ i = 1, 2, \ldots q \qquad 3.8$$

where δM and $\frac{\partial h}{\partial M}$ are stored as column vectors. Equation 3.8 can be written as

$$H + N \cdot \delta M = 0 \qquad 3.9$$

where

$$H = \text{col}\ [\ h(\alpha_1, \beta_1),\ \ h\ (\alpha_2, \beta_2), \ \ldots, \ h\ (\alpha_q, \beta_q)\ ]$$

$$N = \left[\frac{\partial h\ (\alpha_1, \beta_1)}{\partial M}\ ,\ \frac{\partial h\ (\alpha_2, \beta_2)}{\partial M}, \ \ldots, \ \frac{\partial h\ (\alpha_q, \beta_q)}{\partial M}\right]^T$$

Since N is, in general, a rectangular matrix and may not have the full rank, the solution of 3.9 will be

$$\delta M = -N^{\dagger} H \qquad 3.10$$

where $N^{\dagger}$ is the pseudoinverse[41] of N.

Solution 3.10 satisfies equation 3.9 exaclty only when the rank of N = q. When rank (N) < q, equation 3.10 satisfies 3.9 only in a minimum square sense.

Occasionally, the increment of equation 3.10 may be too large for the first order expansion in equation 3.8 to be valid. This may lead to computational instability. Hence provision is made in the logarithm for repeatedly halving δM until a favourable δM is obtained.

For the purpose of computation, the elements of N can be determined as follows:

$$\frac{\partial h\ (\alpha_i,\ \beta_i)}{\partial M} = \frac{\partial h\ (\alpha_i,\ \beta_i)}{\partial \alpha_i} \cdot \frac{\partial \alpha_i}{\partial M} + \frac{\partial h\ (\alpha_i,\ \beta_i)}{\partial \beta_i} \cdot \frac{\partial \beta_i}{\partial M} \qquad 3.11$$

where $\frac{\partial \alpha_i}{\partial M}$ and $\frac{\partial \beta_i}{\partial M}$ are the real and imaginary parts of $\frac{\partial \lambda_i}{\partial M}$ which is given by [41]

$$\frac{\partial \lambda_i}{\partial M} = \frac{V_i^T \left[\frac{\partial A_o}{\partial M}\right] W_i}{V_i^T W_i} \qquad i = 1,\ 2,\ \ldots.\ q \qquad 3.12$$

where V_i and W_i are the eigenvectors of A_o^T and A_o corresponding to λ_i.

To monitor the progress, a cost function

$$J = \sum_{i=1}^{q} [\, h\,(\alpha_i, \beta_i)\,]^2 = H^T H \qquad 3.13$$

is used at each iteration. During the iteration process any undesirable eigenvalue that may appear is automatically included in the cost function, J. So long as the new value of J is less than its previous lowest value, the solution of equation 3.10 is carried out in the normal iteratative manner. Otherwise δM is halved. A flow chart of the digital computer program is given in Appendix IV.

This solution technique attempts to move all the undesirable eigenvalues towards the R region simultaneously. The movement is brought about by changes in the controller parameters based on the eigenvalue sensitivity calculations.

3.4 Controller Design for an Interconnected Two-Area System

As indicated in section 3.2, the system eigenvalues can be moved to a desired sector in s-plane by a dynamic compensator of a smaller order than that required by an optimal controller or by a controller which places eigenvalues in specified positions.

A proportional - integral - derivative (PID) controller, at each area level, is selected to place the eigenvalues in the

desired sector because it provides the following advantages:

(i) It is a simple dynamic controller that can be realized in either the analog or the digital form.

(ii) It can remember and anticipate local area signals because this controller uses integral and derivative terms.

(iii) It can eliminate steady-state error and can increase the stability of the system because this controller uses integral and derivative terms.

(iv) It can provide the identical steady-state control as a conventional load-frequency controller because this controller uses integral term.

(v) As shown in the block diagram of Figure 3.2, this controller operates on the area control error (ACE) in a similar way to the conventional load-frequency controller; therefore it cannot prevent an area receiving assistance from another area.

(vi) When PID gains are suitably adjusted, this controller can provide the dynamic control similar to an optimal linear regulator.[43]

For these reasons the PID controller is not only feasible but also is superior to both conventional and optimal load-frequency controllers.

Based on the block diagram of Figure 3.2, the equation for this proposed PID load-frequency controller can be written as:

$$u_i = \Delta w_{ri} = - (\Delta p_{ti} + b_{si} \cdot \Delta w_i) \left(B_{pi} + \frac{B_{ii}}{s} + B_{di}\, s \right) \quad 3.14$$

where $(\Delta p_{ti} + b_{si}\ \Delta w_i) = ACE_i$

= i th area control error

Figure 3.3 shows the block diagram model of an interconnected two-area system equipped with the PID load-frequency controllers. The state equations for this system are:

$$\Delta \dot{w}_1 = - \frac{D_1}{T_{m1}}\ \Delta w_1 + \frac{1}{T_{m1}}\ \Delta p_{m1} - \frac{1}{T_{m1}}\ \Delta p_t - \frac{1}{T_{m1}}\ \Delta p_{L1}$$

$$\Delta \dot{z}_1 = - \frac{1}{T_{g1}} \left(\frac{1}{R_1} + b_{s1}\ B_{p1} - \frac{b_{s1}\ B_{d1}\ D_1}{T_{m1}} + B_{d1}\ T_{k12} \right) \Delta w_1$$

$$- \frac{1}{T_{g1}}\ \Delta z_1 - \frac{B_{d1}\ b_{s1}}{T_{m1}\ T_{g1}}\ \Delta p_{m1} + \frac{B_{d1}\ T_{k12}}{T_{g1}}\ \Delta w_2$$

$$- \left(\frac{B_{p1}}{T_{g1}} - \frac{b_{s1}\ B_{d1}}{T_{m1}\ T_{g1}} \right) \Delta p_t + \frac{1}{T_{g1}}\ \Delta u_{I1}$$

$$\Delta \dot{p}_{m1} = \frac{1}{T_{t1}}\ \Delta z_1 - \frac{1}{T_{t1}}\ \Delta p_{m1} \quad 3.15$$

$$\Delta \dot{w}_2 = - \frac{D_2}{T_{m2}}\ \Delta w_2 + \frac{1}{T_{m2}}\ \Delta p_{m2} - \frac{a}{T_{m2}}\ \Delta p_t - \frac{1}{T_{m2}}\ \Delta p_{L2}$$

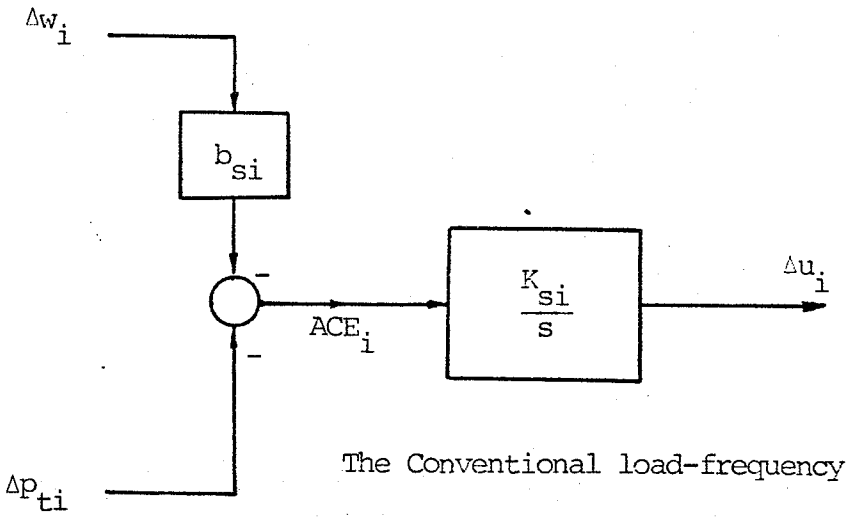

The Conventional load-frequency controller

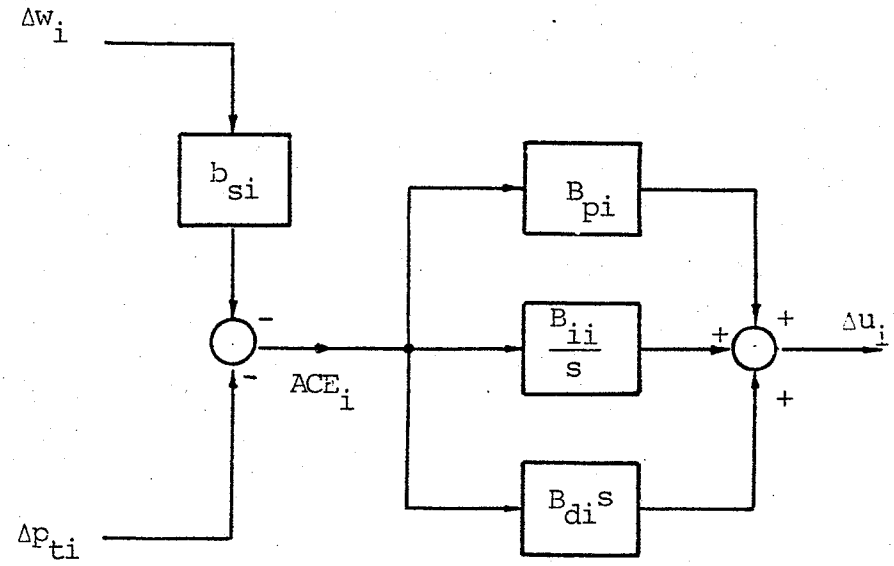

The PID load-frequency controller

FIG. 3.2 Block diagrams of the Conventional and PID load-frequency Controllers

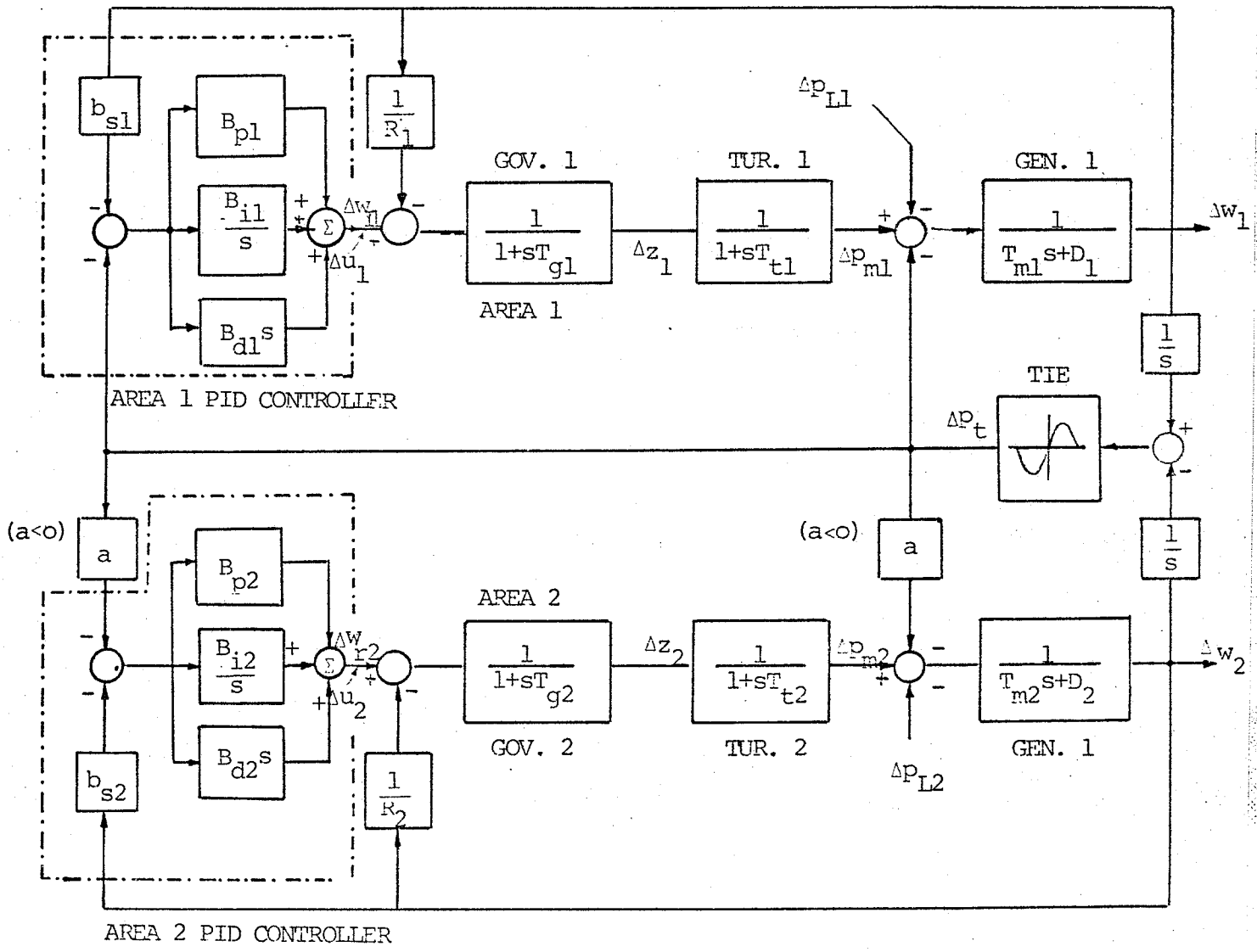

FIG. 3.3 Block diagram model of an interconnected two-area system with the PID controllers.

$$\Delta\dot{z}_2 = -\frac{1}{T_{g2}}\left(\frac{1}{R_2} + b_{s2}\,B_{p2} - \frac{D_2\,b_{s2}\,B_{d2}}{T_{m2}} - a\,B_{d2}\,T_{k12}\right)\Delta w_2$$

$$-\frac{1}{T_{g2}}\,\Delta z_2 - \frac{b_{s2}\,B_{d2}}{T_{m2}\,T_{g2}}\,\Delta\dot{p}_{m2} - \left(\frac{a\,B_{p2}}{T_{g2}} - \frac{a\,b_{s2}\,B_{d2}}{T_{m2}\,T_{g2}}\right)\Delta p_t$$

$$-\frac{a\,B_{d2}\,T_{k12}}{T_{g2}}\,\Delta w_1 + \frac{1}{T_{g2}}\,\Delta u_{I2}$$

$$\Delta\dot{p}_{m2} = \frac{1}{T_{t2}}\,\Delta z_2 - \frac{1}{T_{t2}}\,\Delta p_{m2}$$

$$\Delta\dot{p}_t = T_{k12}\,\Delta w_1 - T_{k12}\,\Delta w_2$$

$$\Delta\dot{u}_{I1} = -b_{s1}\,B_{i1}\,\Delta w_1 - B_{i1}\,\Delta p_t$$

$$\Delta\dot{u}_{I2} = -b_{s2}\,B_{i2}\,\Delta w_2 - a\,B_{i2}\,\Delta p_t$$

$$\Delta\dot{p}_{t1} = T_{k12}\,\Delta w_1 - T_{k12}\,\Delta w_2$$

$$\Delta\dot{p}_{t2} = a\,T_{k12}\,\Delta w_1 - a\,T_{k12}\,\Delta w_2$$

Equation 3.15 can be written in the simplified matrix form as:

$$\dot{x}_o = A_o x_o + s_o v_o \qquad 3.16$$

This equation is similar to equation 3.4. The unknown elements of the matrix A_o are the proportional, integral and derivative gains.

The iterative design technique described in section 3.3 is next used to determine the controller gains for the typical known parameters of an interconnected two-area system given in Table 3.1

A damping ratio greater than 0.707 and the real part less than -0.4 is selected arbitrarily to define a desired sector in s-plane for the system eigenvalues. In this case the system eigenvalues must satisfy the following two constraints:

$$h_1(\alpha_i, \beta_i) = \alpha_i + 0.4 \leq 0 \qquad 3.17$$

$$h_2(\alpha_i, \beta_i) = \alpha_i + \beta_i \leq 0$$

Hence

$$\frac{\partial h_1}{\partial \alpha_i} = 1$$

$$\frac{\partial h_1}{\partial \beta_i} = 0 \qquad 3.18$$

$$\frac{\partial h_2}{\partial \alpha_i} = 1$$

$$\frac{\partial h_2}{\partial \beta_i} = 1$$

TABLE 3.1

Parameters of the interconnected two-area system

Area Parameters	Area 1	Area 2
T_g sec	0.08	0.08
T_t sec	0.3	0.3
R	0.04	0.04
T_m sec	10.0	10.0
V, pu	1.0	1.0
P_R , MW	2000.	16000.
b_s	25.0	25.0
D	0.5	0.5

Tie Line:

$$X_{12} = 10.0$$

$$\delta_{120} = 30^{o}$$

$$T_{k12} = 32.5$$

$$a = -0.125$$

The vector of controller parameters is given by

$$[M] = [B_{p1} \quad B_{i1} \quad B_{d1} \quad B_{p2} \quad B_{i2} \quad B_{d2}]^T \qquad 3.19$$

For an i th undesirable eigenvalue, equation 3.8 can be written as

$$h_{1i}(\alpha_i, \beta_i) + \frac{\partial h_{1i}}{\partial B_{p1}} \cdot \delta B_{p1} + \frac{\partial h_{1i}}{\partial B_{i1}} \cdot \delta B_{i1} + \frac{\partial h_{1i}}{\partial B_{d1}} \cdot \delta B_{d1}$$

$$+ \frac{\partial h_{1i}}{\partial B_{p2}} \cdot \delta B_{p2} + \frac{\partial h_{1i}}{\partial B_{i2}} \cdot \delta B_{i2} + \frac{\partial h_{1i}}{\partial B_{d2}} \cdot \delta B_{d2} = 0$$

$$h_{2i}(\alpha_i, \beta_i) + \frac{\partial h_{2i}}{\partial B_{p1}} \cdot \delta B_{p1} + \frac{\partial h_{2i}}{\partial B_{i1}} \cdot \delta B_{i1} + \frac{\partial h_{2i}}{\partial B_{d1}} \cdot \delta B_{d1}$$

$$+ \frac{\partial h_{2i}}{\partial B_{p2}} \cdot \delta B_{p2} + \frac{\partial h_{2i}}{\partial B_{i2}} \cdot \delta B_{i2} + \frac{\partial h_{2i}}{\partial B_{d2}} \cdot \delta B_{d2} = 0$$

where

$$\frac{\partial h}{\partial K} = \frac{\partial h}{\partial \alpha} \quad \frac{\partial h}{\partial K} + \frac{\partial h}{\partial \beta} \quad \frac{\partial \beta}{\partial K}$$

and where K is a controller parameter

$\frac{\partial h}{\partial \alpha}$ and $\frac{\partial h}{\partial \beta}$ are given by equation 3.18;

$\frac{\partial \alpha}{\partial K}$ and $\frac{\partial \beta}{\partial K}$ are the real and imaginary parts of $\frac{\partial \lambda}{\partial K}$.

The solution of $\frac{\partial \lambda}{\partial K}$ requires the evaluation of $\frac{\partial A_o}{\partial K}$.

The initial value of parameter vector [M] is assumed to be zero, the final design is

$$[M] = \begin{bmatrix} B_{p1} \\ B_{i1} \\ B_{d1} \\ B_{p2} \\ B_{i2} \\ B_{d2} \end{bmatrix} = \begin{bmatrix} 0.8 \\ 0.6 \\ 0.7 \\ 0.8 \\ 0.6 \\ 0.7 \end{bmatrix}$$

with closed-loop poles:

$$\lambda_{1,2} = -5.5164 \pm j\ 5.4149$$
$$\lambda_{3,4} = -6.8951 \pm j\ 6.1837$$
$$\lambda_5 = -3.8251$$
$$\lambda_6 = -1.6517$$
$$\lambda_7 = -0.9590$$
$$\lambda_8 = -0.4659$$
$$\lambda_9 = -0.4411$$

Figure 3.4 shows the movement of the dominant eigenvalue λ_1 for different initial tie-line loadings. Very small movement of the eigenvalues for small to large initial tie-line loading indicates that the controller provides damped response for a wide range of operating conditions.

3.5 Dynamic and Steady-state Performances

As stated earlier, the main purpose of the new controller is to provide damped response to tie-line oscillations without sacrificing the steady state performance of the conventional controller. Small and large step load disturbances are therefore applied in one of the areas of the interconnected system to check the dynamic and steady-state behaviour of the composite nonlinear system.

3.5.1 Small Signal Analysis

First a step increase of 5 percent is applied in area 1 loading. Continuous Scientific Modelling Program (CSMP) is used to solve the nonlinear differential equations for the interconnected two-area system (shown in Figure 3.3). This system has the Load-Frequency controllers identical to those described in section 3.4. Figure 3.5 shows the time-domain response for the controlled system. As expected from the eigenvalue analysis, the dynamic response of the interconnected system is damped.

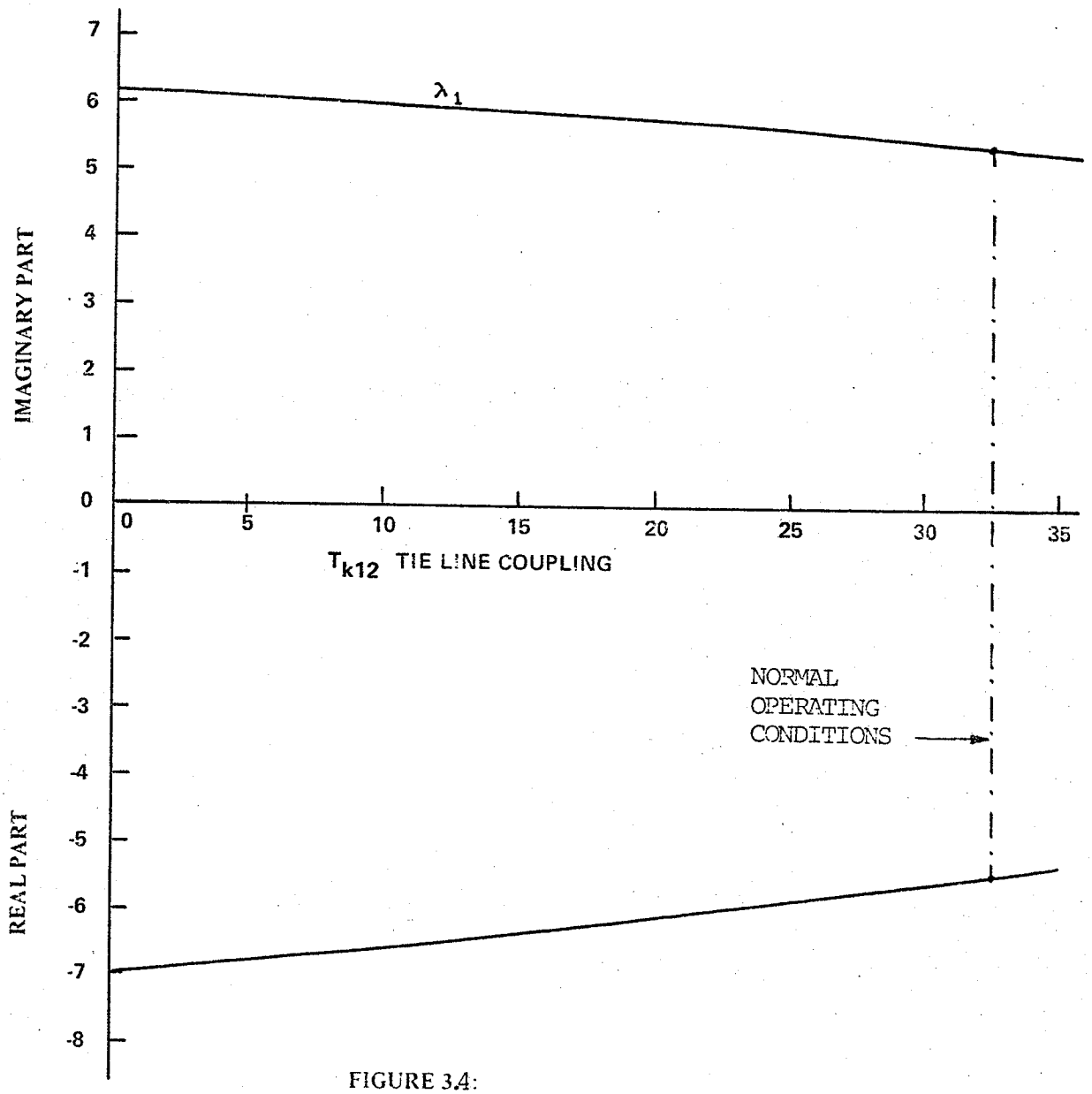

FIGURE 3.4:
EFFECT OF TIE-LINE LOADING ON THE DOMINANT EIGENVALUE OF THE CONTROLLED SYSTEM

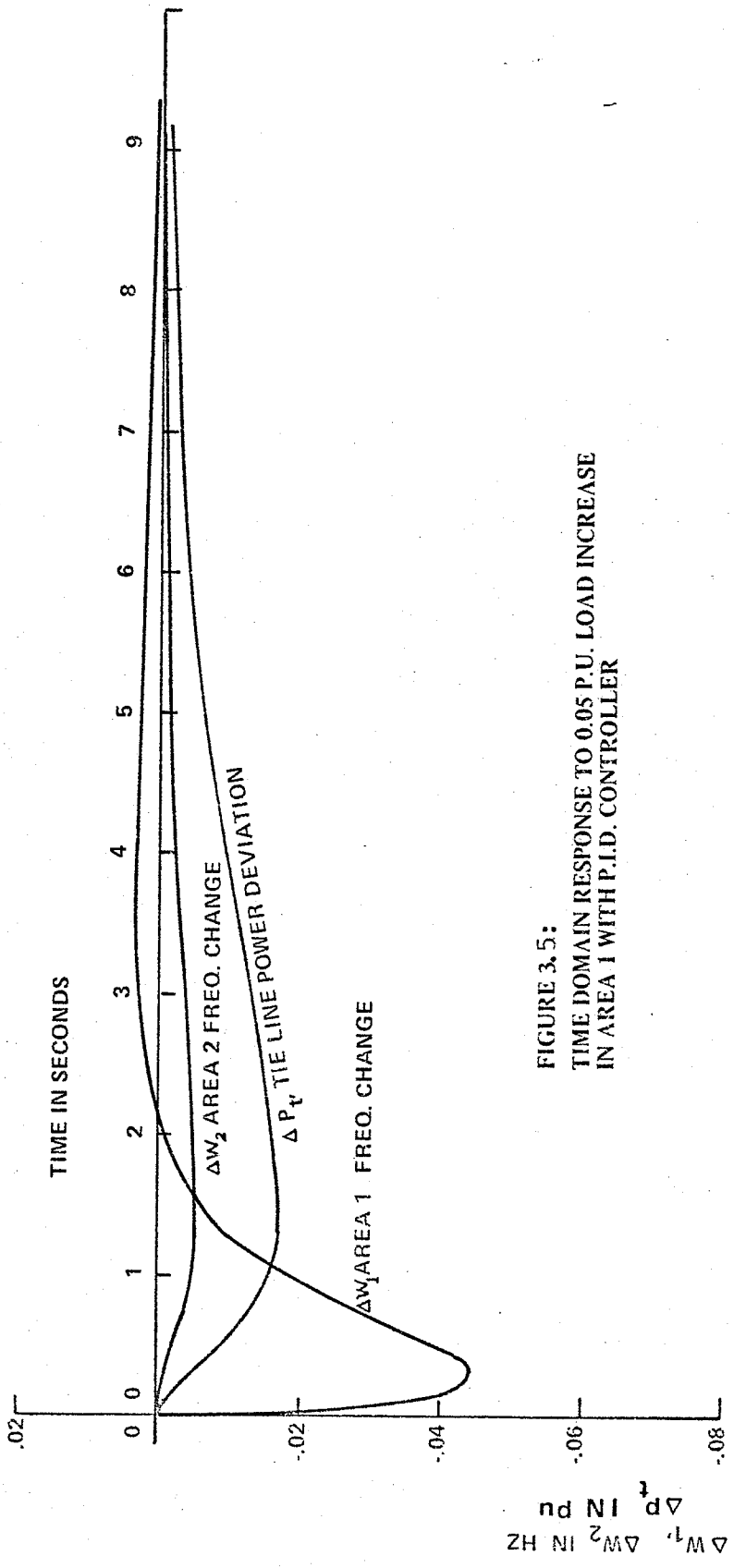

FIGURE 3.5:
TIME DOMAIN RESPONSE TO 0.05 P.U. LOAD INCREASE IN AREA 1 WITH P.I.D. CONTROLLER

3.5.2 Large Signal Analysis

Since the controller has been designed using a linear control technique, it is important that the behaviour of the system which includes nonlinearity must be examined for the large disturbance condition. Two cases are considered to evaluate the interconnected system behaviour:

1. When an area can absorb its own load changes.
2. When an area cannot meet its own demand.

The first case is expected to indicate the effects of tie-line nonlinearity on the dynamic performance. The second case on the other hand is expected to show whether a PID controller permits an area in need of power to receive that extra power from the other area.

For case 1, area one is assumed to have a 30 percent reserve capacity when its load is suddenly increased by 25 percent. Yet as shown in Figure 3.6, the system remains stable, and the response is suitably damped.

For case 2, the load in area 1 is suddenly increased by 50 percent. With a reserve of only 30 percent, area 1 is required to supply 20 percent more power than it is capable of providing on its own. As shown in Figure 3.7, the dynamic response is damped and the system frequency settles at 60 hz when area 1 receives 20 percent assistance from area 2.

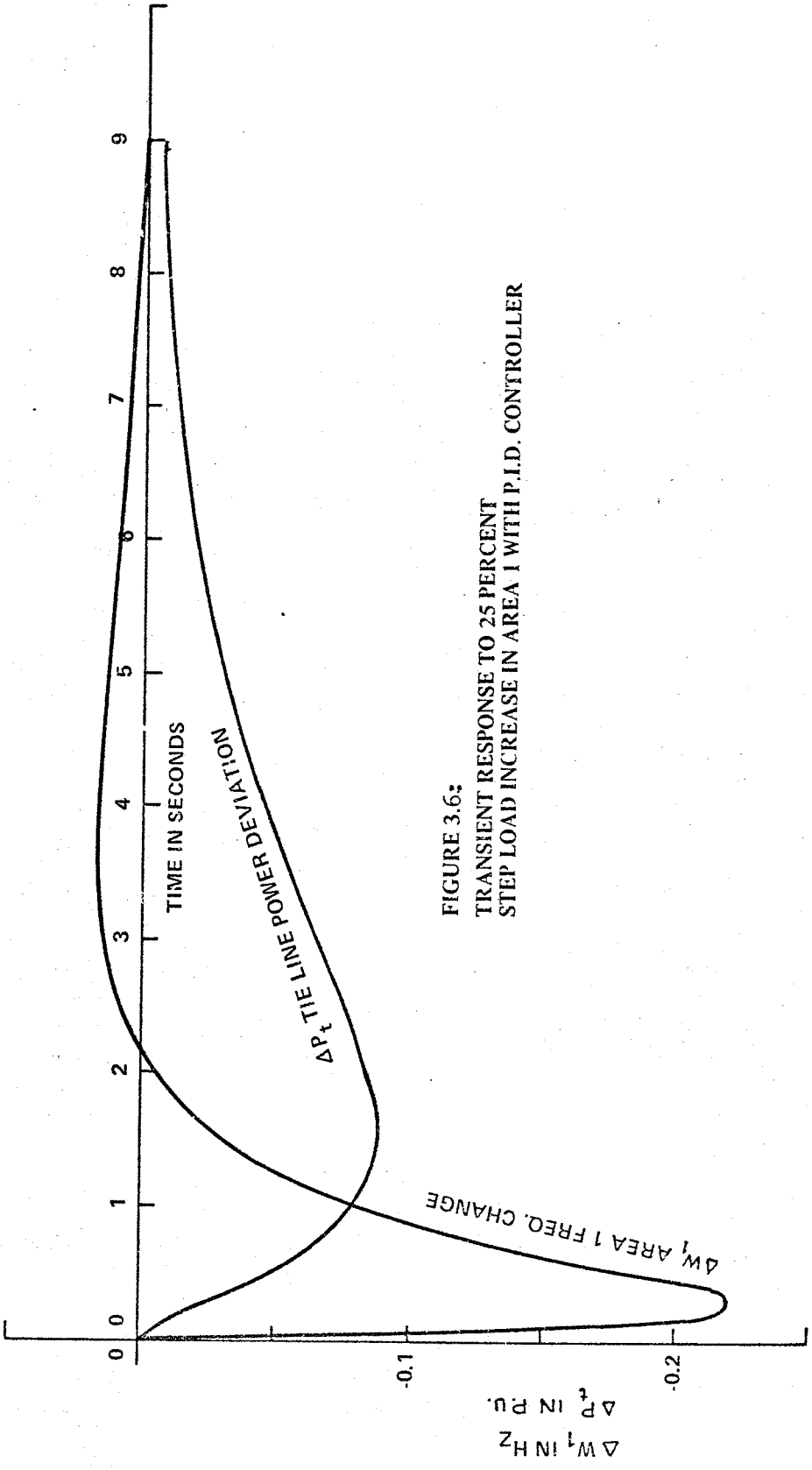

FIGURE 3.6:
TRANSIENT RESPONSE TO 25 PERCENT
STEP LOAD INCREASE IN AREA 1 WITH P.I.D. CONTROLLER

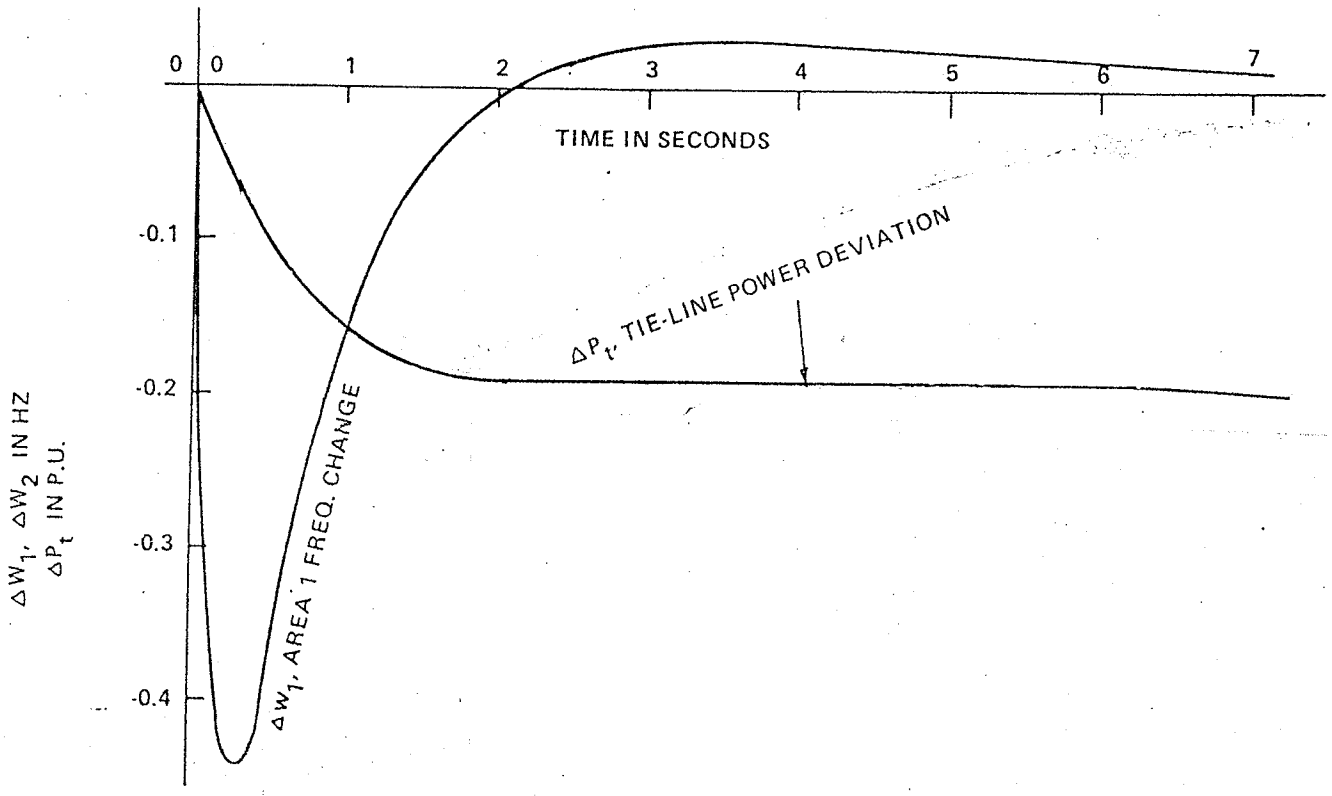

FIGURE 3.7:
TRANSIENT RESPONSE TO 50% STEP
LOAD INCREASE IN AREA 1 WITH UNLIMITED
RESERVE IN AREA 2

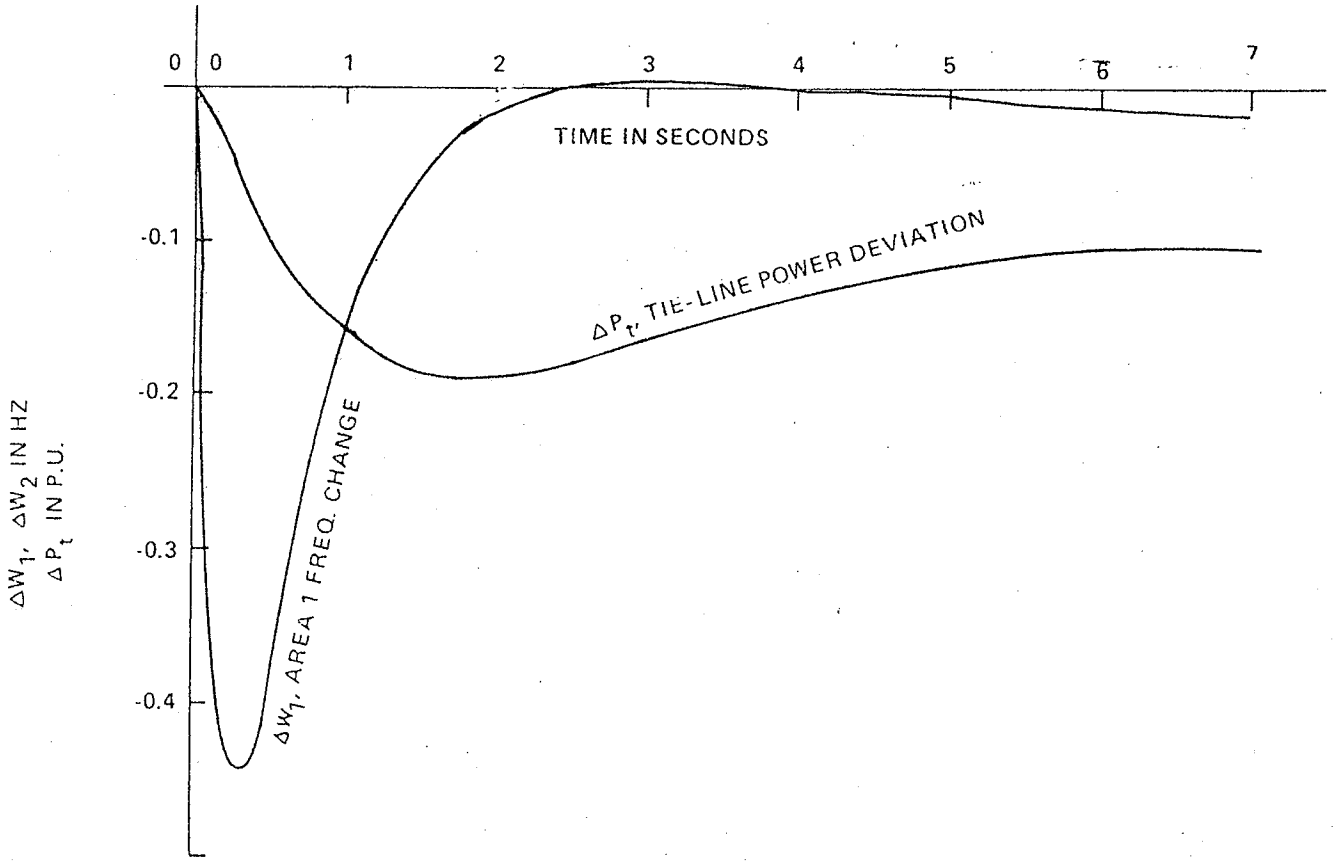

FIGURE 3.8

TRANSIENT RESPONSE TO 50% STEP
LOAD INCREASE IN AREA 1
RESERVE IN AREA 1: 30%
RESERVE IN AREA 2: 10%

Figure 3.8 shows the system response when area 2 provides only 10 percent of the area 1 demand. Because the reserve capacity of the interconnected system is only 40 percent in this case, the system frequency settles at less than 60 hz. Thus as demonstrated by Figures 3.7 and 3.8, PID controllers at each area level provide damped system responses while allowing an area in need to receive assistance from another area.

3.6 Comparison of System Performance – Conventional vs. PID Controllers

In order to compare the dynamic and steady-state performance of an interconnected power system, a two-area system is again considered.

Figure 3.9 shows the location of the dominant eigenvalues of an interconnected two-area system equipped (i) with the conventional and (ii) with the PID controllers for different loadings on the tie-line. Eigenvalues of the system equipped with the conventional controllers never enter the desired sector, whereas the eigenvalues of the system equipped with the PID controllers never leave the desired sector for a wide range of T_{k12}. For the system with the PID controllers an increase in T_{k12} decreases both damping and the frequency of oscillation, whereas for a system with the conventional controllers it decreases only the damping and increases the frequency of oscillation.

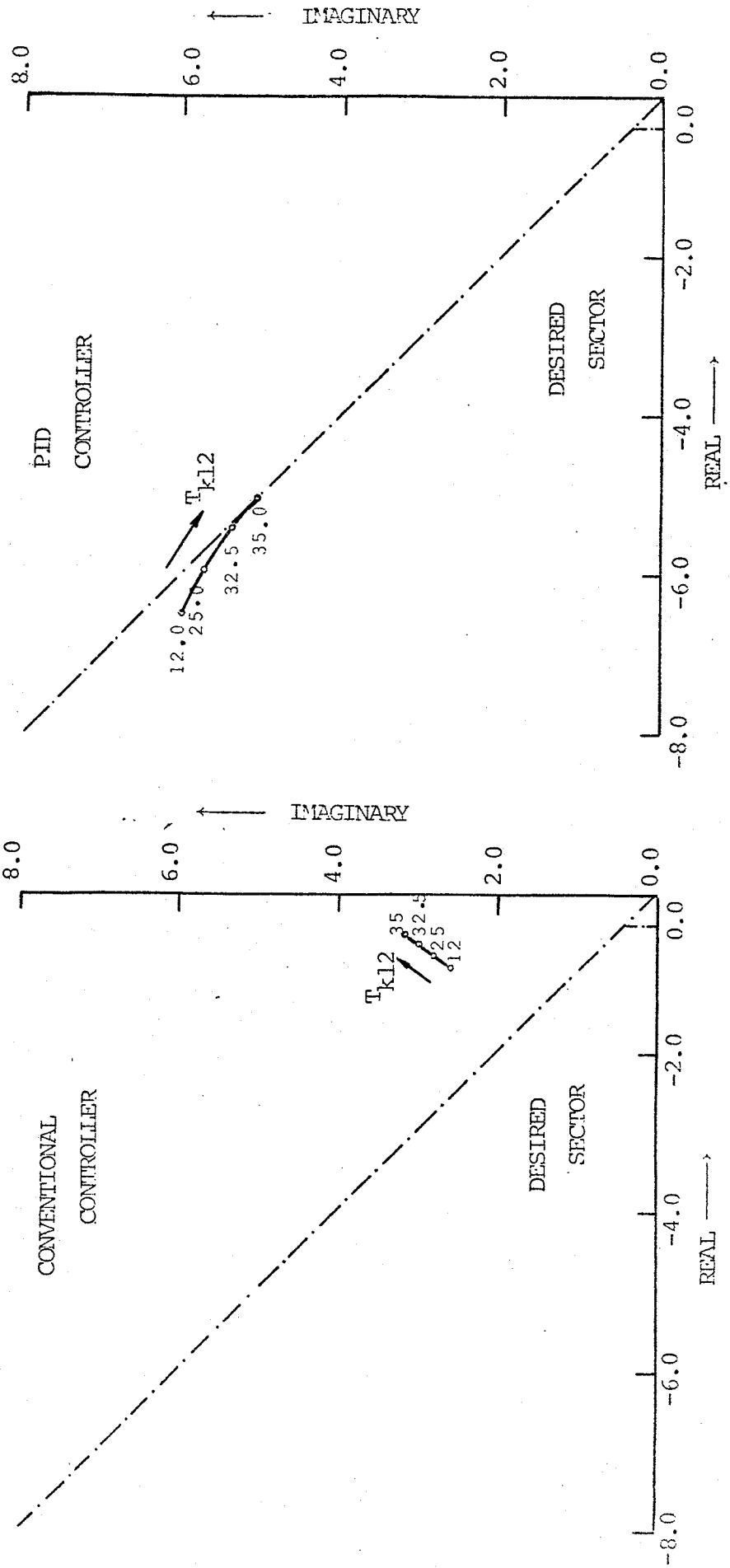

FIG. 3.9 Effect of tie-line loading T_{k12} on the dominant eigenvalue, λ_1 of the controlled system: Conventional vs PID controllers.

3.6.1 Small Signal Analysis

A step disturbance of 5 percent load increase in area 1 is applied for the same two-area system equipped first with the conventional and then with the PID controllers. When changes in frequency of each area and the tie-line power are compared, the conventional controller has poorer damping characteristics and a longer settling time (see Figure 3.10).

3.6.2 Large Signal Analysis

The evaluation of conventional and of PID controllers is carried out by solving the dynamic system equations for the following system conditions:

(i) When each area is capable of meeting its load demand.

(ii) When one of the areas is unable to meet its load demand.

With an assumed reserve of 30 percent for area 1, step load increases of 25 percent and 50 percent are applied in area 1. Since optimal controllers have been criticized for denying assistance to other areas in the system, the 50 percent increase will determine whether or not the proposed PID controller can provide at least equal services as conventional controllers.

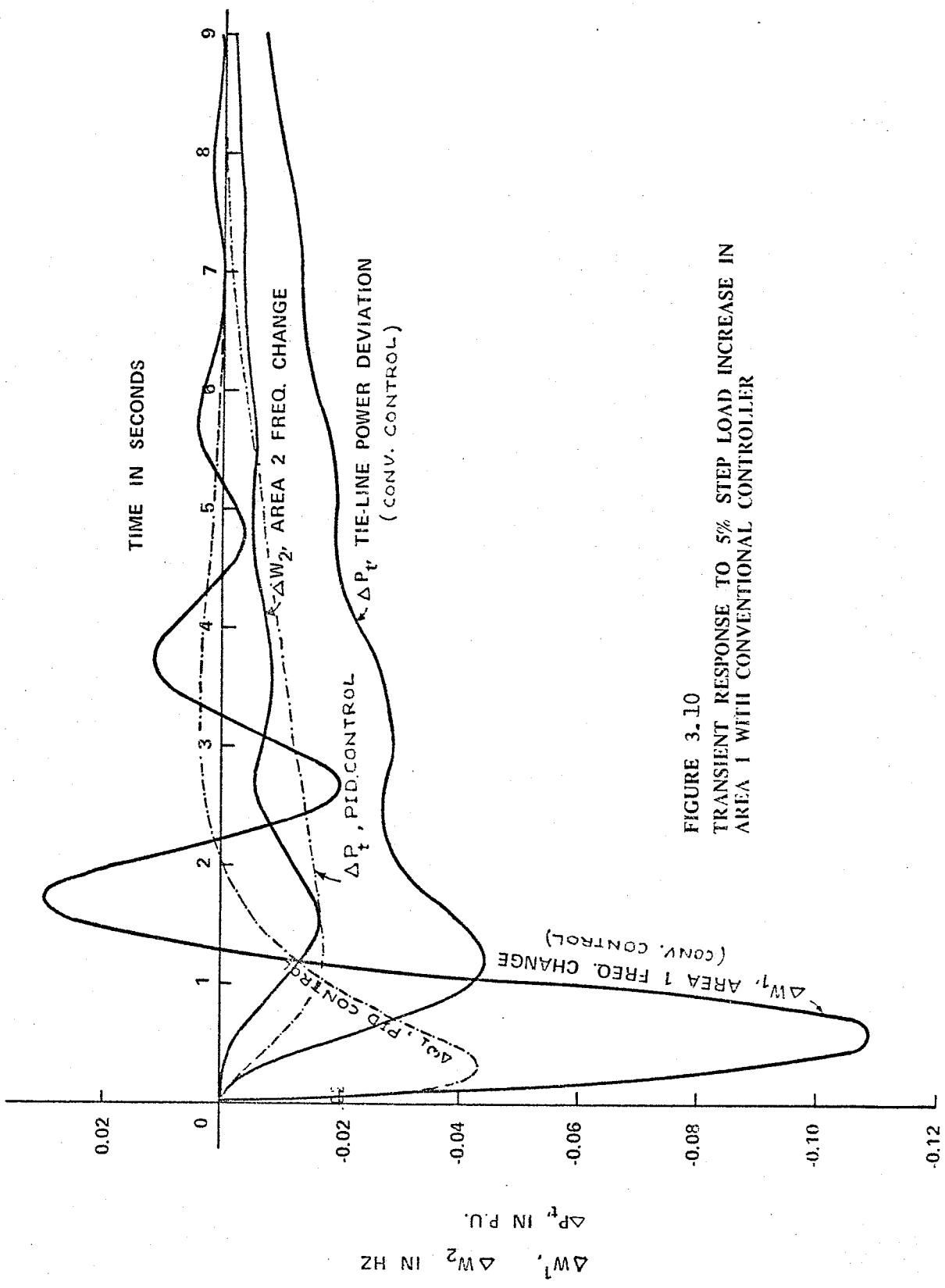

FIGURE 3.10
TRANSIENT RESPONSE TO 5% STEP LOAD INCREASE IN AREA 1 WITH CONVENTIONAL CONTROLLER

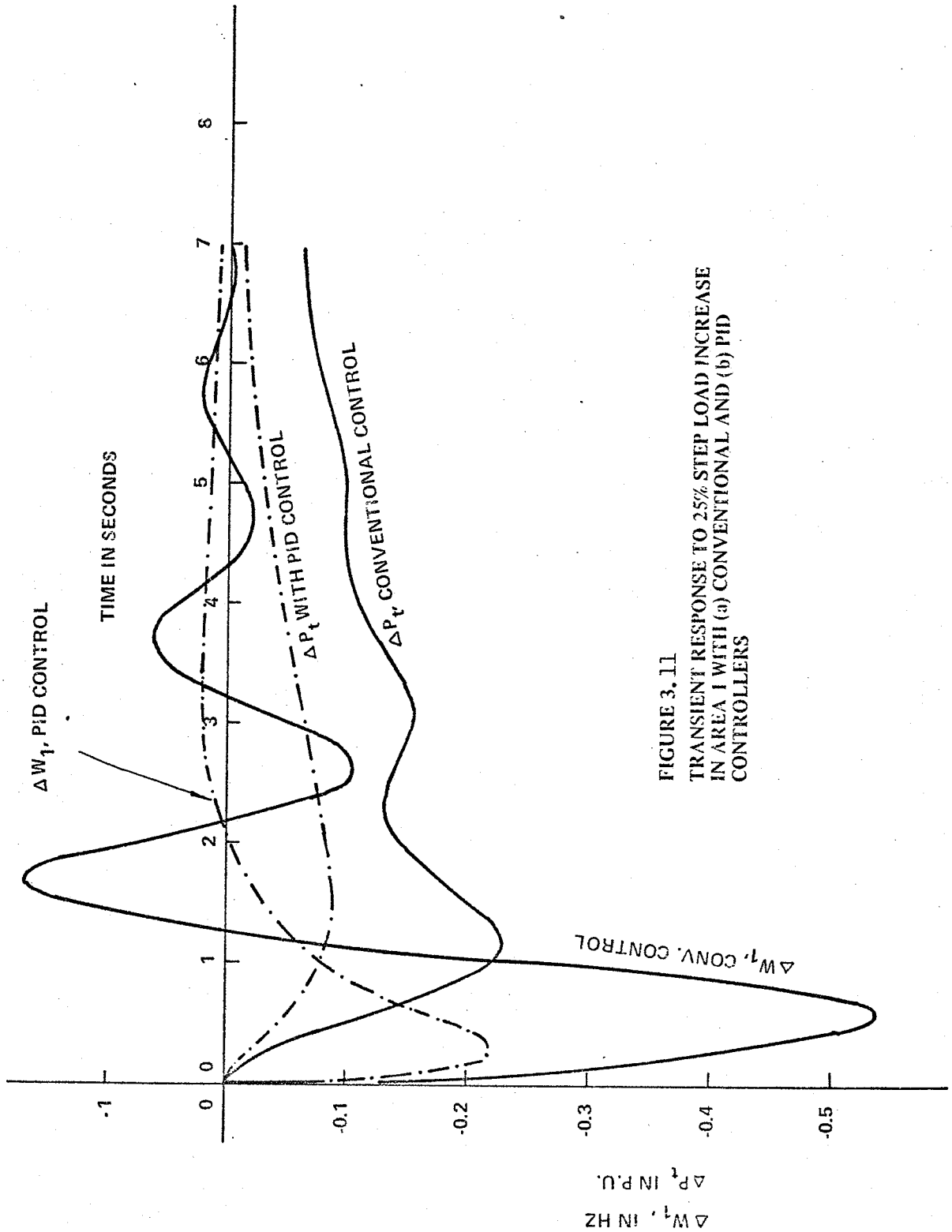

FIGURE 3.11
TRANSIENT RESPONSE TO 25% STEP LOAD INCREASE IN AREA 1 WITH (a) CONVENTIONAL AND (b) PID CONTROLLERS

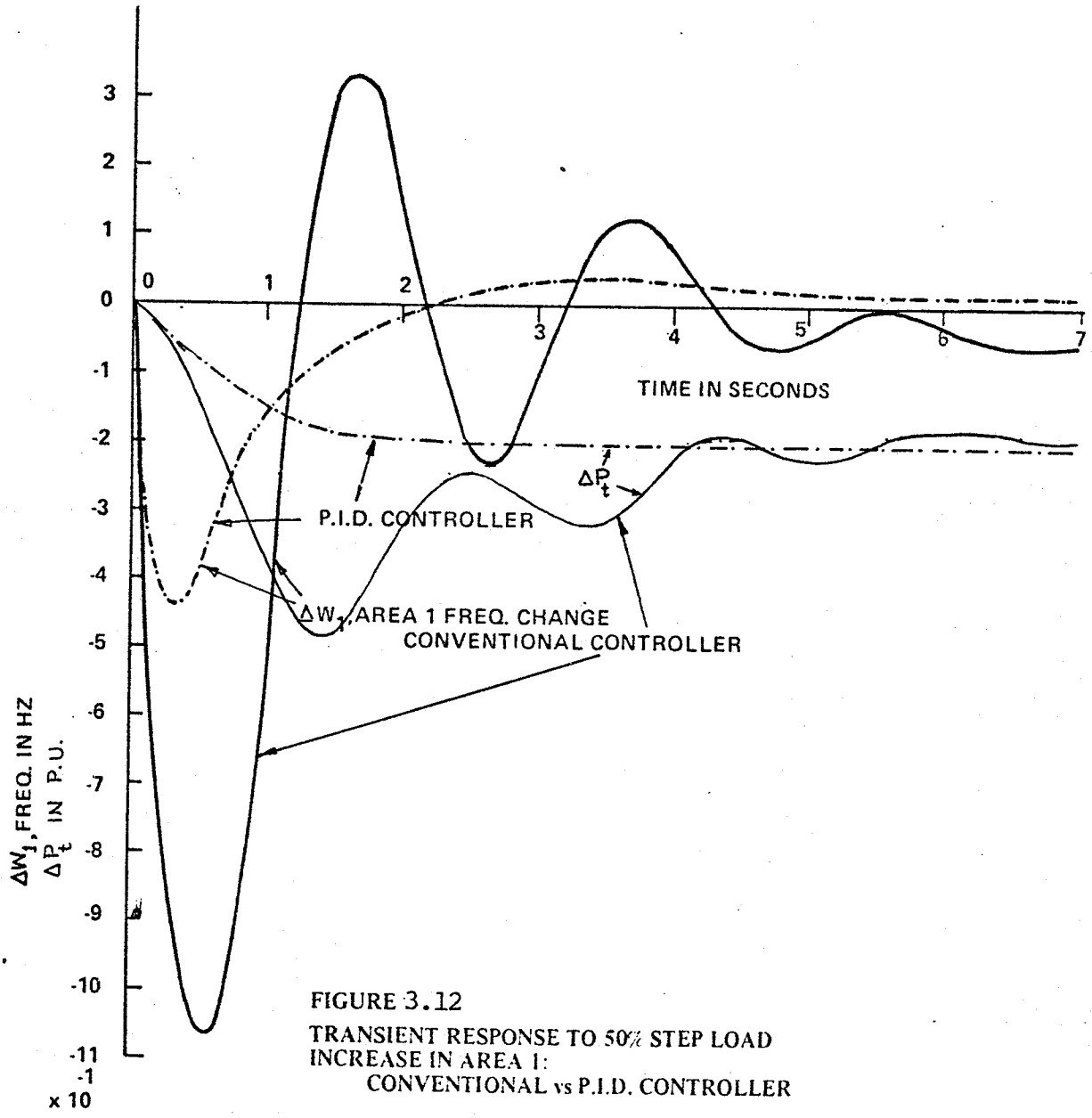

FIGURE 3.12

TRANSIENT RESPONSE TO 50% STEP LOAD INCREASE IN AREA 1:
CONVENTIONAL vs P.I.D. CONTROLLER

The interconnected system response in area 1 to 25 percent and 50 percent step load increases are shown in Figures 3.11 and 3.12 respectively. When the system is equipped with the PID controllers, the dynamic response is better for both 25 percent and 50 percent load increases. Behaviours of the conventional and PID controllers are similar in providing assistance to the troubled area (see Figure 3.12).

3.7 System Simplification, On-Line Indentification and Control

As discussed in section 3.4, an interconnected two-area power system generates a 10 th order system. The number of iterations and the amount of computer storage needed to design the controller is therefore small. But the order of the system dynamic equations increases geometrically as more areas are interconnected. Undue complexity, can be avoided, however, by using a simplified model for the areas external to the area under consideration.

Because the continued fraction approach developed by Chen and Shieh[48] and described in Appendix I provides a simplified model which retains the steady-state and dynamic characteristics of the original system, it is applied to simplify the external system. But this technique requires the external system model to be represented in the transfer-

function form. A conversion technique developed by Bollinger and Mathur[49] and described in Appendix I is therefore used to convert the state-space form of the external system dynamic equations into the transfer-function form.

To evaluate the simplication technique, an interconnected two-area system is again considered. If area 1 is assumed to be the local area and if area 2 and the tie-line are considered as the external system, then the transfer function of the external system is given by

$$G_e = \frac{2040.6 + 6189.9s + 3767.0\,s^2 + 518.6\,s^3 + 32.65\,s^4}{10.2 + 93.1\,s + 207.9\,s^2 + 115.8\,s^3 + 15.9\,s^4 + s^5}$$

and its simplified model is (see Appendix I)

$$G_e(s) = \frac{200.0}{1 + 6.09\,s}$$

The system responses based on both the detailed and simplified external system models are compared in Figure 3.13. In this comparison the detailed and simplified models provide a similar response. As shown in Figure 3.14, the dominant system eigenvalues are insensitive to the parameter changes in the external system. The controller for area 1 thus remains unchanged.

The above analysis justifies using simplified external model system to design a local PID load-frequency controller.

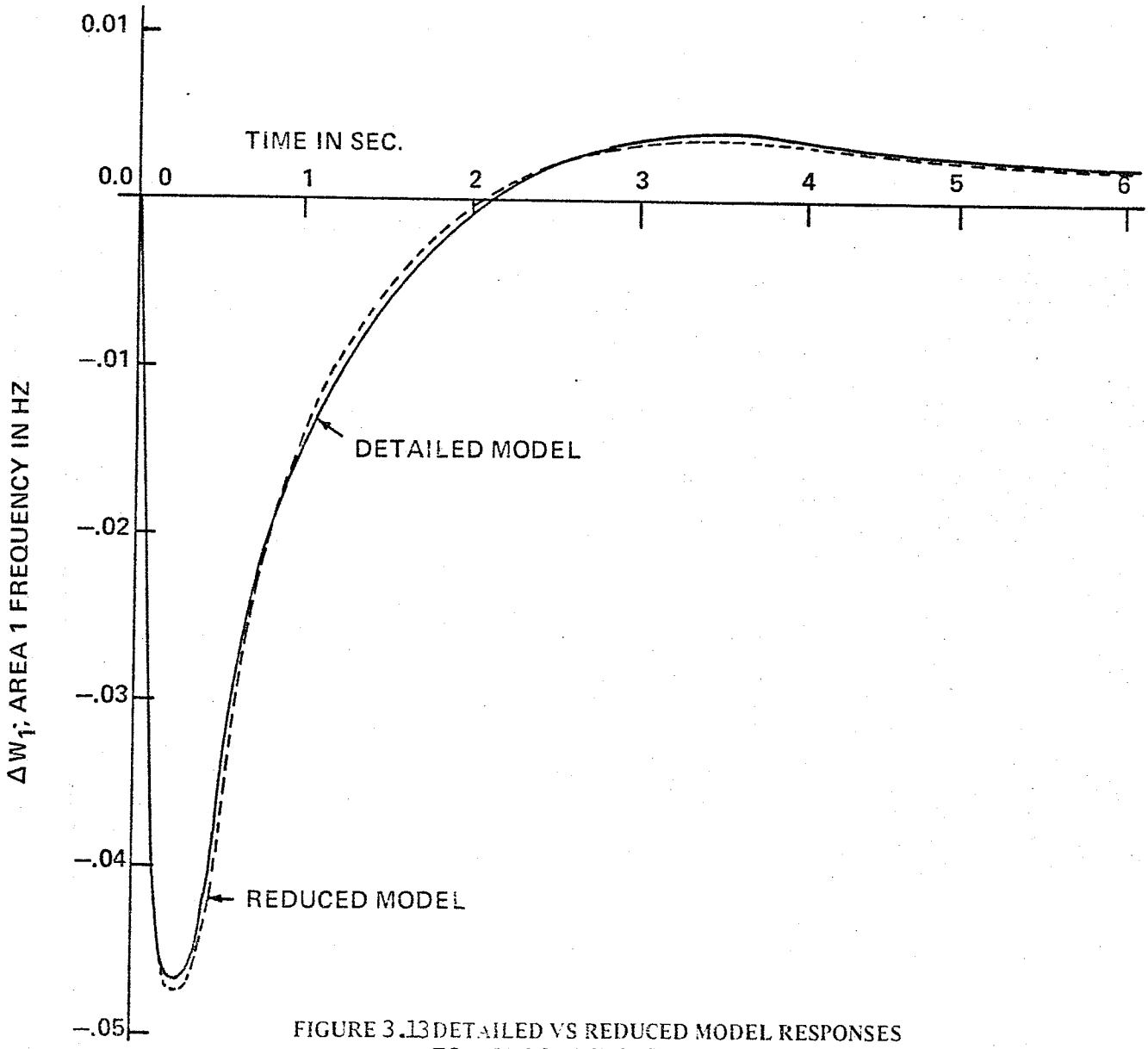

FIGURE 3.13 DETAILED VS REDUCED MODEL RESPONSES TO A 5% LOAD INCREASE IN AREA 1.

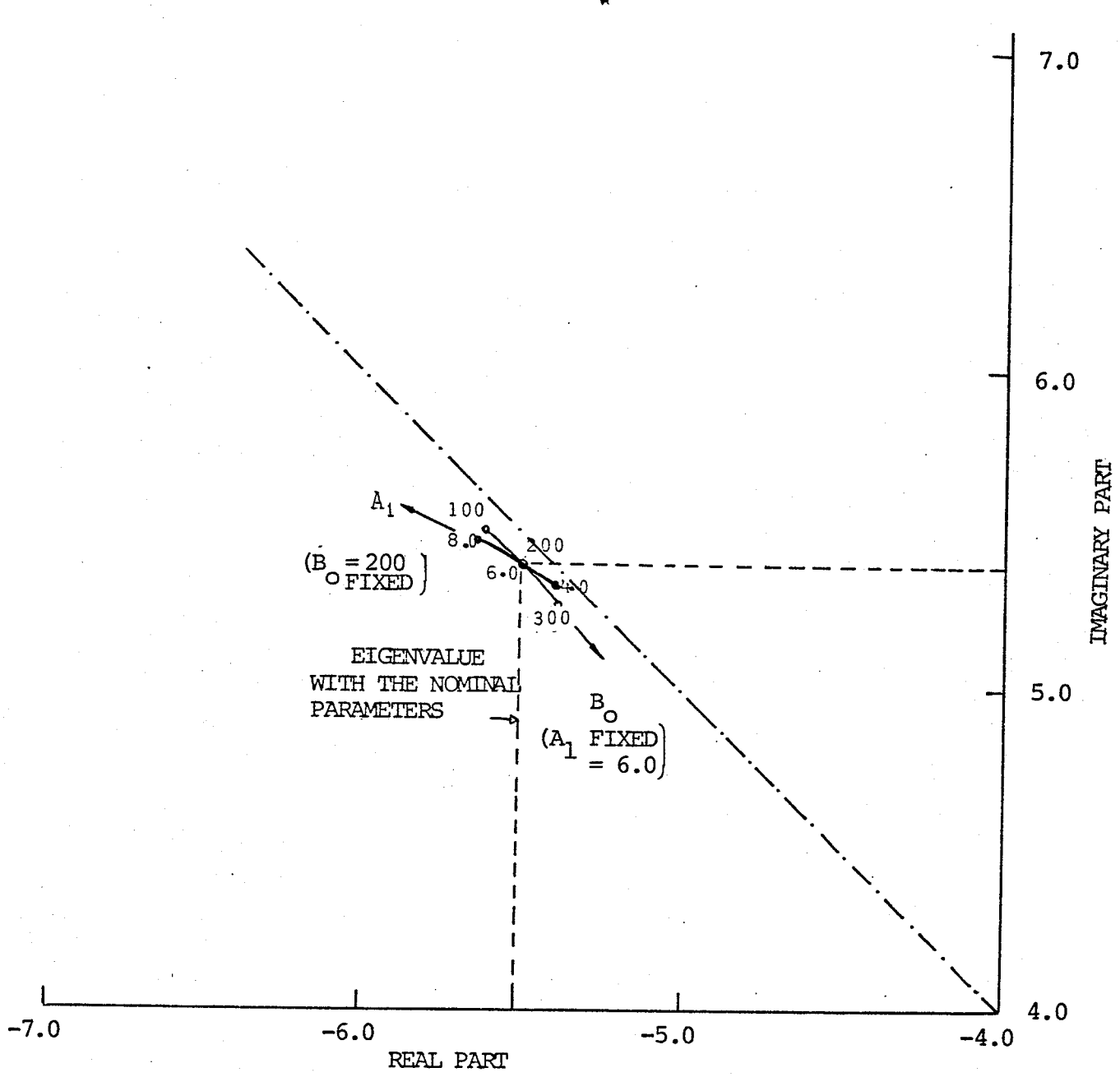

FIG. 3.14 Effect of changes in B_o and A_1 on the dominant eigenvalues

When the external system consists of a number of areas whose detailed dynamic model cannot be fully known, it becomes important 'to identify' the external system when designing a local area controller. Appendix II describes an on-line identification technique[50-51] for determining the parameters of the simplified external system model based only on the output signals recorded in the local area.

Simplification and on-line identification techniques suggested above thus provide a practical approach to the design of a load-frequency controller.

Conclusions

Based on local output signals only, a decentralized PID controller has been designed and has successfully been applied to an interconnected two-area power system. Moving the system eigenvalues to a specified sector in the s-plane has provided the desired degree of system stability. The designed PID controller has been shown superior to the conventional controller both for the small and large disturbance conditions.

Model simplification and on-line identification techniques have been described and applied to determine the model for a portion of the interconnected system external to a local area. It has been shown that the

simplified model of the external system is all that is necessary to design a local PID load-frequency controller.

In Chapter 4, the effects of signal sampling on the controller design will be evaluated.

CHAPTER 4

DIGITAL CONTROLLER FOR AN INTERCONNECTED POWER SYSTEM

4.1 Introduction

Using digital computers for controlling on-line operations has been widespread,[52-53] but using them for the dynamic control of a power system has been limited.[53-55] Nevertheless, a digital controller used in either situation has several advantages over an analog controller. An analog control device can only be ordered and installed near the conclusion of system studies when the system configuration has been rigidly identified. A digital control device, on the other hand, can be ordered and installed well in advance of the commissioning time. Also at any future time a digital controller can easily be modified to suit a changed system dynamics.

A digital computer for on-line control applications can be used in either of two modes:

(i) The Digital Directed Analog Control (DDAC) mode

(ii) The Direct Digital Control (DDC) mode.

In the DDAC mode, the digital computer generates a

proper switching function and directs changes in the controller gains or in the controller structure.

In the DDC mode, an algorithm of a particular control design resides inside the computer and uses the computer output directly for the control of the system. Because only the control algorithms need to be changed to suit different situations, the DDC mode is superior to the DDAC mode. Also the DDC has the advantage of using the same computer equipment for other off-line and on-line duties[53-55] in the period between the control signal generation and the next sampling operation.

The use of a digital computer in the DDC mode introduces sampling and makes the system a sampled data control system.[56-60] In this chapter the effects of implementing a decentralized load-frequency control algorithm by a digital computer in the DDC mode is described. Then this algorithm is applied to an interconnected two-area system. The state equations of an interconnected two-area system equipped (i) with the conventional and (ii) with the PID controllers are first converted to state transition equations by a digitally oriented calculation method proposed by Hoppe.[59] Then the effects of sampling and of the controller gains on the dominant system eigenvalues are examined in the complex z-plane. A zone in z-plane, which corresponds to a sector in s-plane, is used to specify the criterion of relative stability. A time domain solution is

used to examine the intersampling oscillation and the large disturbance behaviour of the system. The z-domain and time-domain analyses are carried out to examine the influence of sampling on the dynamic performance of the system when the conventional and PID control algorithms are implemented digitally.

4.2 Mathematical Formulation

As described in Chapter 3, the linear dynamic equations for an interconnected s-area system can be written as:

$$\dot{x} = Ax + Bu + Sv \qquad 4.1$$

$$y = Cx$$

where $u = (u_1, u_2 \ldots\ldots u_s)^T$

With the digital controller in the loop as shown in Figure 4.1, equation 4.1 can be written in the discrete digital form as:

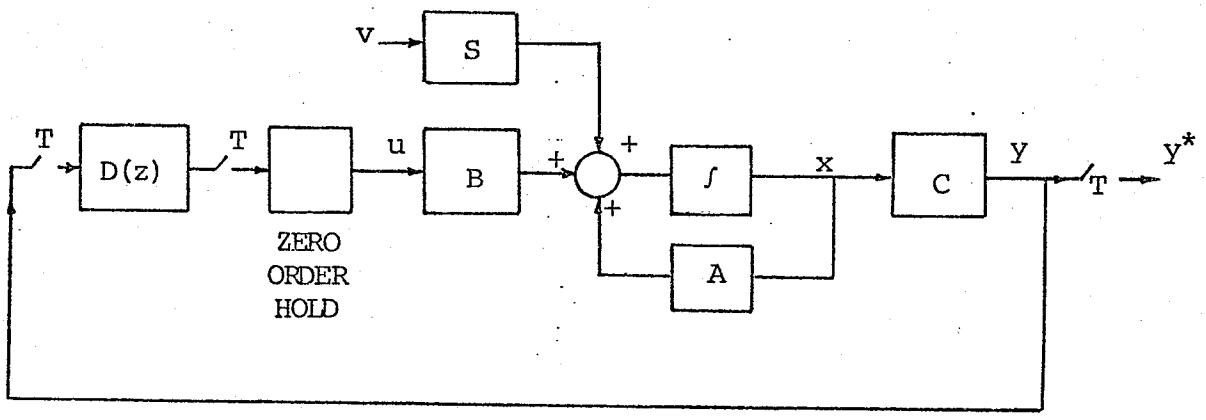

Figure 4.1 Closed Loop Computer Control System

$$x(k+1) = P\,x(k) + Q\,u(k) + R\,v(k)$$
$$y(k) = C\,x(k) \qquad 4.2$$

where

$$P = \text{the transition matrix} = e^{AT} \qquad 4.3$$

T = sampling period

$$Q = \int e^{A\tau} \cdot d\tau \cdot B$$
$$R = \int e^{A\tau} \cdot d\tau \cdot S \qquad 4.4$$

Equations for the digital controller can be written as:

$$z(k+1) = F\,z(k) + G\,y(k)$$
$$u(k) = H\,z(k) + K\,y(k) \qquad 4.5$$

Substituting the controller equations 4.5 into equations 4.2, we have:

$$x(k+1) = (P + QKC)\,x(k) + QH\,z(k) + R\,v(k) \qquad 4.6$$

The state transition equations for the complete system can therefore be written as:

$$\begin{bmatrix} x(k+1) \\ z(k+1) \end{bmatrix} = \begin{bmatrix} P + QKC & QH \\ GC & F \end{bmatrix} \begin{bmatrix} x(k) \\ z(k) \end{bmatrix} + \begin{bmatrix} R \\ o \end{bmatrix} [v(k)] \qquad 4.7$$

$$\text{or} \quad x_o(k+1) = P_o\,x_o(k) + R_o\,v(k) \qquad 4.8$$

where $z_o(k) = [x(k)\ z(k)]^T$

$$P_o = \begin{bmatrix} P + QKC & QH \\ GC & F \end{bmatrix}, \quad R_o = \begin{bmatrix} R \\ O \end{bmatrix}$$

The characteristic equation of the computer controlled system is therefore:

$$\left| Iz - P_o \right| = 0 \qquad 4.9$$

where I is the identity matrix

For stability, the roots of equation 4.9 must lie inside the unit circle in the z-plane.[56-60] For a specified relative stability, these roots must lie within a z-plane zone marked in Figure 4.2. A corresponding zone in the s-plane for a linear analysis is shown alongside.

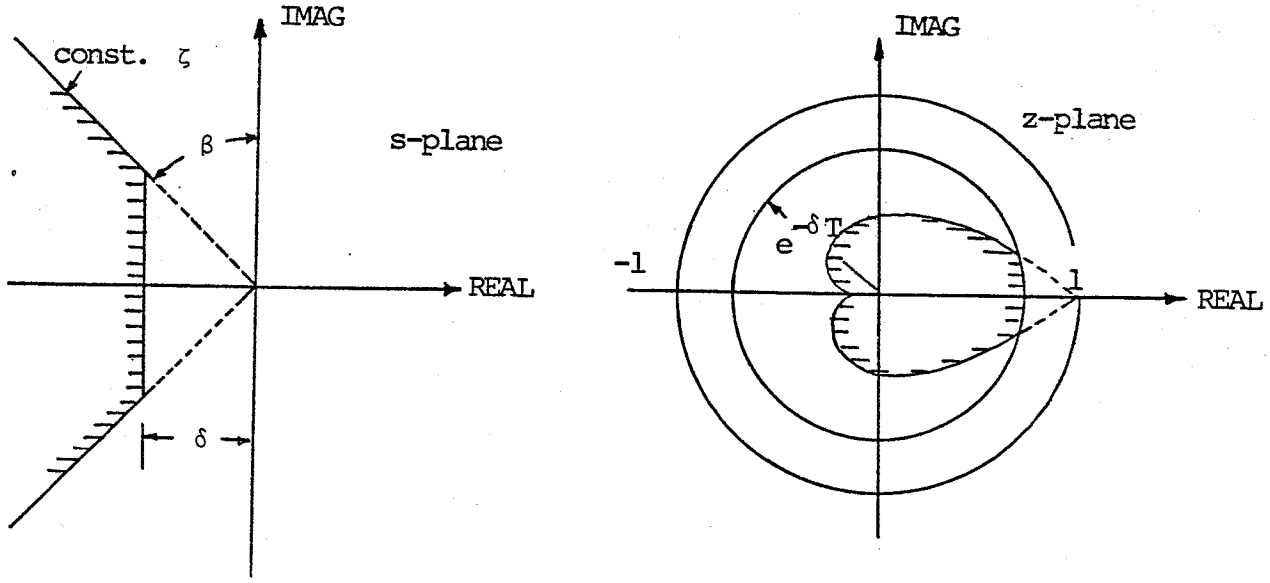

Figure 4.2 Desired zone for the closed loop poles in s and z planes.

In the s-plane, δ signifies settling time and ζ the damping ratio. A constant δ locus in s-plane becomes a circular locus with a radius $e^{-\delta T}$ in z-plane. A constant damping ratio, ζ locus in s-plane given by

$$s = - w \tan \beta + jw$$

becomes a logarithmic spiral given by

$$\begin{aligned} z &= e^{sT} \\ &= e^{(- w \tan \beta + jw)\, T} \\ &= e^{- 2 \pi w \tan \beta / W_s} \; \underline{|2\pi w / W_s} \end{aligned} \qquad 4.10$$

where $\beta = \sin^{-1} \zeta$

W_s = Sampling frequency

$= \frac{2\pi}{T}$

Note that a zone marked in the s-plane has been used in Chapter 3. A zone of similar type in the z-plane has been chosen to achieve a similar dynamic system performance.

4.3 Digital Representation of Controllers

Discrete equations for a general first order digital controller are derived from the z-domain transfer function represention by a direct programming approach.[57]

The general discrete equation is then used to derive the proportional, integral and derivative control laws used in the conventional and PID controllers (analog versions of these controllers have been described in Chapters 2 and 3).

A general first order digital controller can be described by a transfer function:

$$\frac{e_2(z)}{e_1(z)} = \frac{b_1 + b_o z}{a_1 + z} = \frac{b_o + b_1 z^{-1}}{1 + a_1 z^{-1}} \qquad 4.11$$

where e_1 and e_2 are input and output respectively,
b_o, b_1 and a_1 are constants,
and z is a complex operator.

In discrete form, equation 4.11 can be written as:

$$e_2(k) = b_o\, e_1(k) + b_1\, e_1(k-1) - a_1\, e_2(k-1) \qquad 4.12$$

By the direct programming method,[57] equation 4.12 can be transformed to the discrete state and output equations:

$$\begin{aligned} x(k+1) &= -a_1\, x(k) + e_1(k) \\ e_2(k) &= (b_1 - b_o\, a_1)\, x(k) + b_o\, e_1(k) \end{aligned} \qquad 4.13$$

where $x(k)$ = magnitude of vector x at k th sampling period.

$e_2(k)$ and $e_1(k)$ are the magnitudes of output and input at the k th sampling period.

Proportional, integral and derivative control laws are described first by the z-domain transfer function and then by the discrete state and output equations.

Proportional control:

$$\frac{e_2(z)}{e_1(z)} = 1$$

$$e_2(k) = e_1(k) \qquad 4.14$$

Integral control:

$$\frac{e_2(z)}{e_1(z)} = \frac{Tz}{z-1} = \frac{T}{1-z^{-1}}$$

$$x(k+1) = x(k) + e_1(k)$$

$$e_2(k) = T\,x(k) + T\,e_1(k) \qquad 4.15$$

Derivative control:

$$\frac{e_2(z)}{e_1(z)} = \frac{z-1}{Tz} = \frac{1}{T} - \frac{1}{T}z^{-1}$$

$$x(k+1) = e_1(k)$$

$$e_2(k) = -\frac{1}{T}x(k) + \frac{1}{T}e_1(k) \qquad 4.16$$

Equations 4.14, 4.15 and 4.16 are next used to derive the discrete equations for the conventional and PID controllers.

4.3.1 The Conventional Controller

Since the conventional controller uses an integral control law given by

$$u_i = \frac{K_{si}}{S} \Delta e_{ri} \qquad 4.17$$

where $\Delta e_{ri} = - (b_{si} \Delta w_i + \Delta p_{ti})$

equation 4.15 can be used to derive discrete equations for this controller. The discrete state and output equations for the i th area conventional controller can be written as:

$$z_i(k+1) = z_i(k) - b_{si} k_{si} \Delta w_i(k) - k_{si} \Delta p_{ti}(k) \qquad 4.18$$

$$u_i(k) = T z_i(k) - T b_{si} K_{si} \Delta w_i(k) - T k_{si} \Delta p_{ti}(k)$$

4.3.2 The PID Controller

Since the PID controller uses proportional, integral and derivative control laws given by

$$u_i = (B_{pi} + \frac{B_{ii}}{s} + B_{di}s) \Delta e_{ri} \qquad 4.19$$

where $\Delta e_{ri} = - (b_{si} \Delta w_i + \Delta p_{ti})$

equation 4.15 can be used to derive discrete equations for

this controller. The discrete state and output equations for the i th area PID controller can be written as:

Proportional control:

$$u_{pi}(k) = B_{pi}\ \Delta e_{ri}(k) \qquad 4.20$$

Integral control:

$$\begin{aligned} z_{ii}(k+1) &= z_{ii}(k) + B_{ii}\ \Delta e_{ri}(k) \\ u_{ii}(k) &= T\ z_{ii}(k) + T\ B_{ii}\ \Delta e_{ri}(k) \end{aligned} \qquad 4.21$$

Derivative control:

$$\begin{aligned} z_{di}(k+1) &= B_{di}\ \Delta e_{ri}(k) \\ u_{di}(k) &= \frac{-1}{T}\ z_{di}(k) + \frac{1}{T}\ B_{di}\ \Delta e_{ri}(k) \end{aligned} \qquad 4.22$$

For the PID controller, the output can be written as:

$$\begin{aligned} u_i(k) &= u_{pi}(k) + u_{ii}(k) + u_{di}(k) \\ &= (B_{pi} + T\ B_{ii} + \frac{1}{T}\ B_{di})\ \Delta e_{ri} + T\ z_{ii}(k) - \frac{1}{T}\ z_{di}(k) \end{aligned} \qquad 4.23$$

where the first subscripts p, i, d indicate the proportional, integral and derivative terms of the controller and the second subscript i indicates the area number.

4.4 System Analysis and Performance Evaluation

An interconnected two-area power system is used to study the effects of the digital form of conventional and PID controllers on the dynamic performance.

First, system equations for an interconnected two-area system (state equations 2.19 derived in chapter 2)

$$\dot{x} = Ax + Bu + Sv$$

are converted to the discrete digital form

$$x(k+1) = P\,x(k) + Q\,u(k) + R\,v(k)$$

by Hoppe's digitally oriented method.[59] A complete set of discrete equations for the interconnected system

$$x_o(k+1) = P_o\,x_o(k) + R_o\,v_o(k)$$

is derived by including the appropriate controller equations derived in section 4.3.

Elements of the matrix P_o change as the sampling period and controller gains change. For an interconnected two-area system equipped first with the conventional and then with the PID controllers, the effects of changes in the sampling period and in the controller gains on the z-domain eigenvalues are analysed and compared. The effects of intersampling oscillation and system nonlinearity are examined by the time-domain analysis.

4.4.1 Root-Locus Analysis in z-plane

4.4.1.1 The Conventional Controller

The locus of the dominant eigenvalues of an interconnected two-area system equipped with the digital form of the conventional load-frequency controller is shown in Figure 4.3. The desired region for the eigenvalues is marked on this diagram. Placing the eigenvalues in this region will ensure a maximum settling period ($\delta \leq -0.4$) and a minimum damping ratio ($\zeta \geq 0.707$).

The effect of varying the sampling period on the dominant eigenvalue is next considered. As shown in Figure 4.3 this eigenvalue remains inside the unit circle for a wide range of sampling periods, but it never enters the specified region marked on this diagram. An increase in the sampling period decreases the settling time without any significant change in the damping. The conventional controller can thus provide stable operation with poor damping for a wide range of sampling periods.

Also shown in Figure 4.3 are the changes in the eigenvalue due to changes in the integral gain of the conventional controller. For a fixed sampling period of 0.1 second, the damping is reduced and the settling time is increased as the integral gain is increased. System instability is ex-

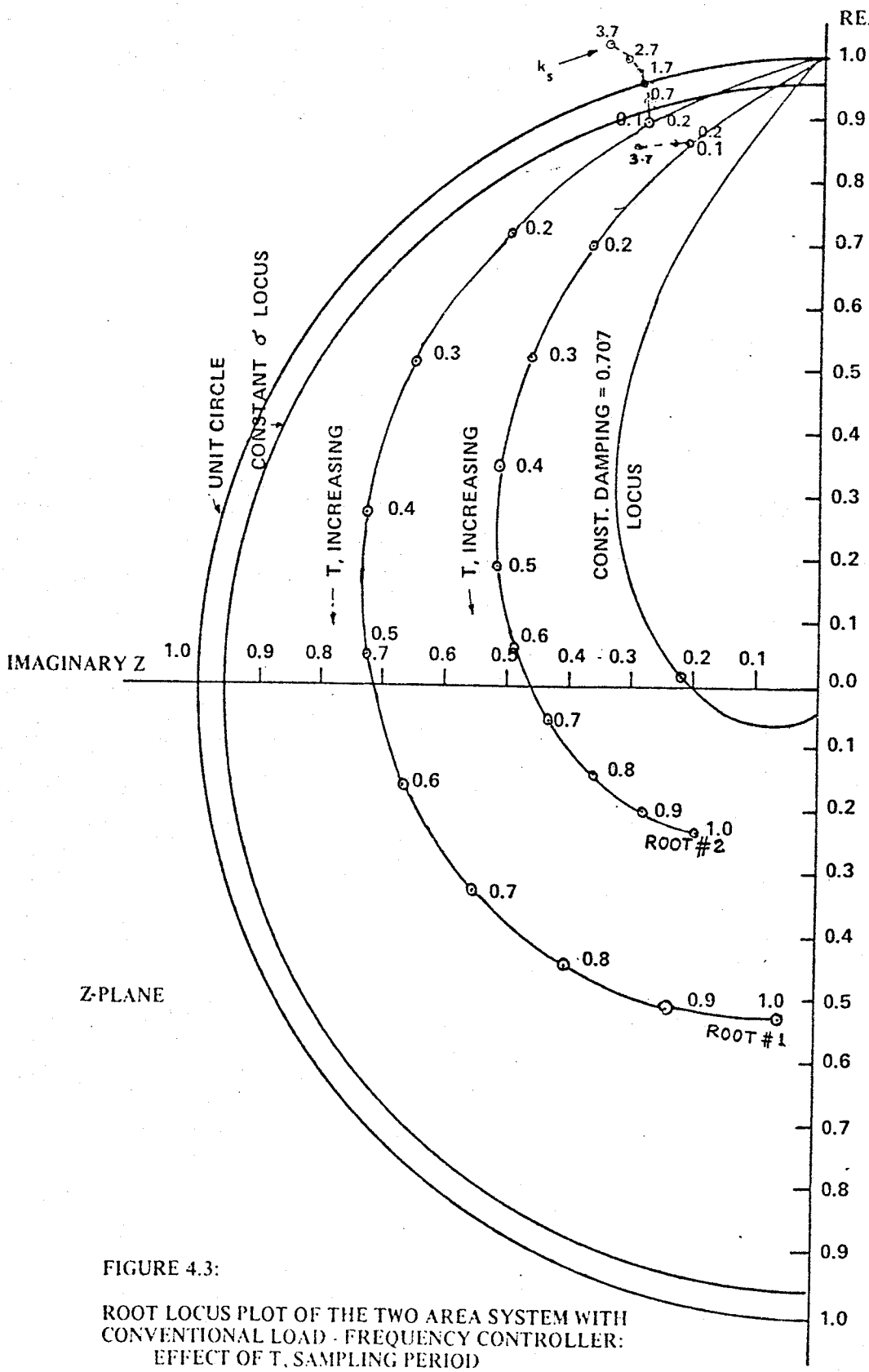

FIGURE 4.3:

ROOT LOCUS PLOT OF THE TWO AREA SYSTEM WITH CONVENTIONAL LOAD - FREQUENCY CONTROLLER:
EFFECT OF T, SAMPLING PERIOD
AND k_s, INTEGRAL GAIN

perienced for an integral gain higher than 1.7 pu at a sampling period of 0.1 second.

From the above analysis, it is concluded that the system remains stable for a wide range of sampling periods when the integral gain of the conventional controller is small. However as recorded in Figure 4.3, no combination of the integral gain and settling time can provide the specified degree of relative stability. Also the movement of eigenvalue in z-plane indicates that the dominant eigenvalue is more sensitive to the sampling period than to the integral gain.

4.4.1.2 The PID Controller

The effects of changes in the sampling period and the proportional, integral and derivative gains of the PID controller on the dominant eigenvalue of an interconnected two-area system are shown in Figure 4.4. Again a desired relative stability region is marked on this diagram.

When the effects of sampling period are examined, the gains of the PID controller are fixed at the following optimum values (as derived from the linear analysis given in Chapter 3):

B_p , proportional gain = 0.8

B_i , integral gain = 0.6

B_d , derivative gain = 0.7

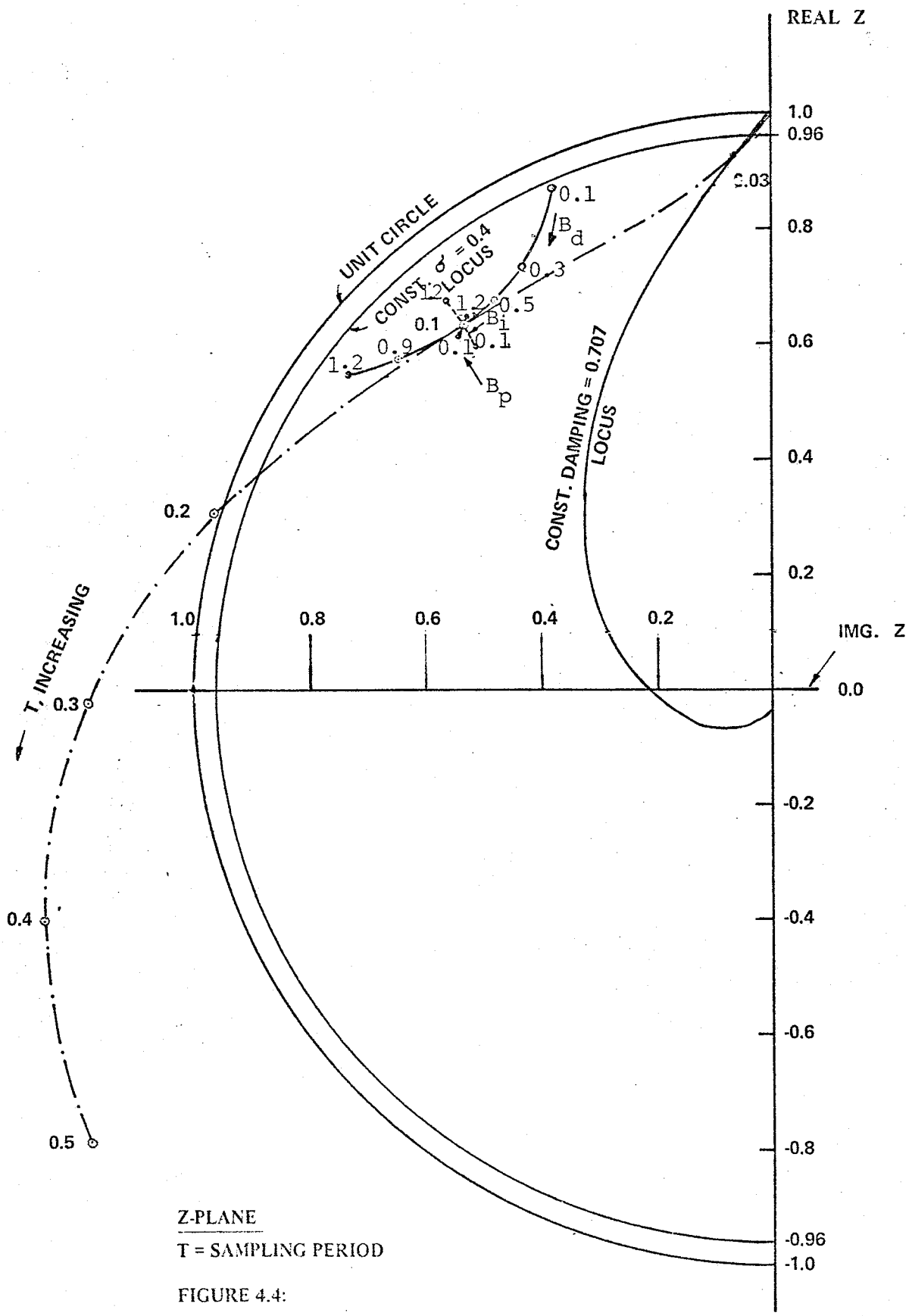

Z-PLANE

T = SAMPLING PERIOD

FIGURE 4.4:

ROOT LOCUS PLOT:
TWO AREA SYSTEM WITH PID CONTROLLERS

EFFECT OF T, B_p, B_i, B_d

As shown in Figure 4.4 the system remains stable (eigenvalues within the unit circle) for a sampling period less than 0.2 second; it becomes unstable for values greater than or equal to 0.2 second. As the sampling period is increased, the settling time is increased and the damping is reduced. Only a small sampling period (close to 0.03 second) provides the desired degree of relative stability.

The effect of varying the gains of the controller are next examined for a fixed sampling period of 0.1 second. As shown in Figure 4.4, the dominant eigenvalue is most sensitive to the derivative gain and least sensitive to the proportional gain. But as in the conventional controller, no combination of the PID gains can bring the eigenvalues to the specified sector in z-plane. Consequently, changes in the controller gains provide only marginal changes in the dynamic performance.

4.4.1.3 Comparison: Conventional vs. PID controllers

The effects of the type of controller and the period of sampling on the dominant eigenvalue of an interconnected two-area power system are shown in Figure 4.5.

The system with the conventional controller remains stable for a wide range of sampling periods (0 - 1.0 second), whereas the system with the PID controller becomes unstable

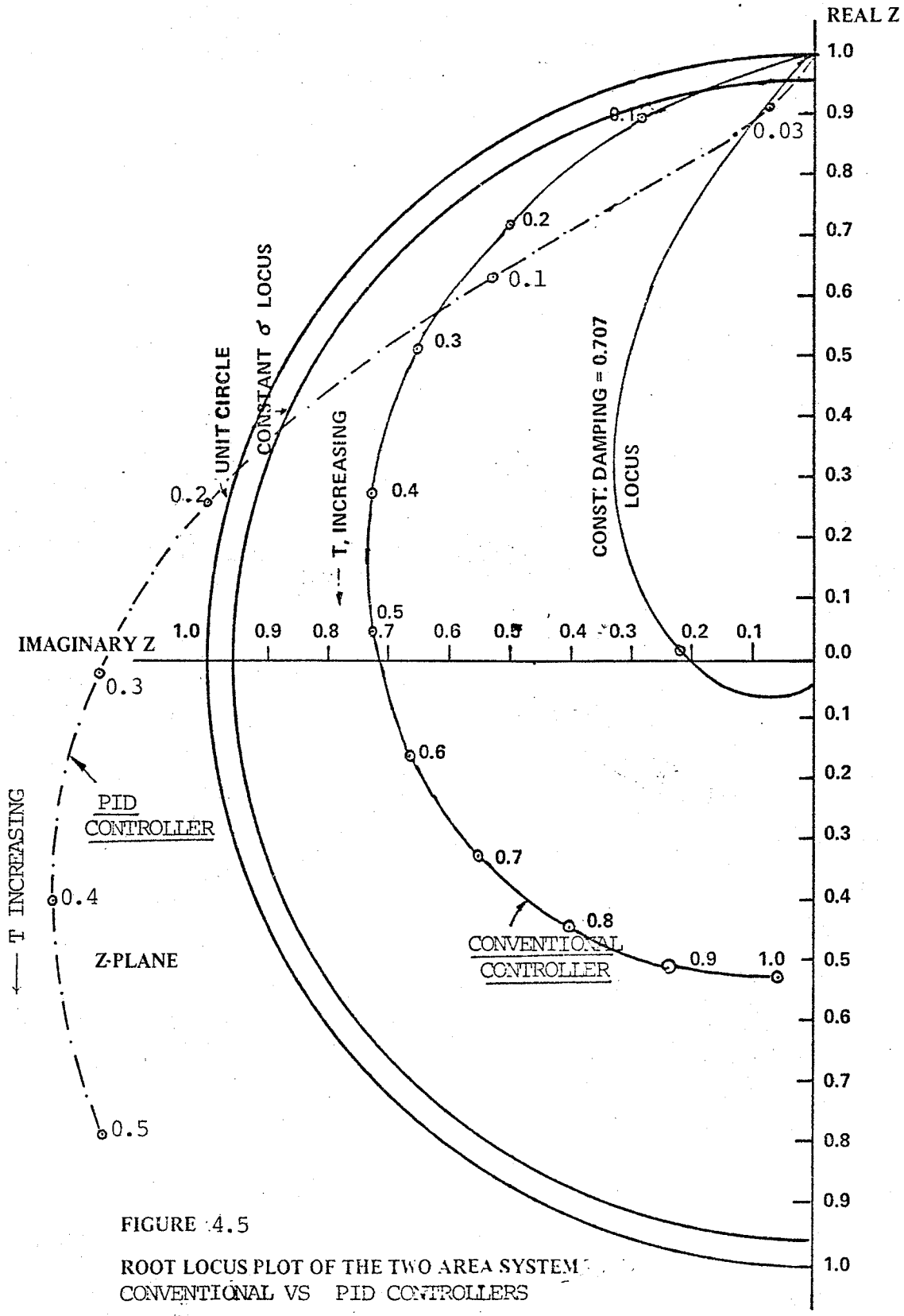

FIGURE 4.5

ROOT LOCUS PLOT OF THE TWO AREA SYSTEM
CONVENTIONAL VS PID CONTROLLERS

for a sampling period greater than or equal to 0.2 second. For samping periods greater than 0.12 second, the conventional controller provides better damping and settling time than the PID controller. For sampling periods less than 0.12 second, a PID controller provides a better dynamic performance than a conventional controller. At a sampling period of 0.03 second, the PID controller provides the specified degree of relative stability. Table 4.1 compares the dynamic performances achieved by the digital form of both the conventional and the PID controllers.

TABLE 4.1 Comparison of dynamic performances: Conventional vs. PID controllers

Controller type	Stability	Damping (= 0.707)
Conventional	Always stable	Not possible
PID	Stable: $T < 0.2$ second	Possible if $T \leq 0.03$ second.

4.4.2 Time-domain Analysis

The z-domain analysis performed in section 4.4.1 is valid only when the disturbance is small; for when the dis-

turbance is large, the nonlinearity of the system can invalidate the conclusions of linear analysis. Moreover, even for a small disturbance, the z-plane analysis indicates the degree of stability only at sampling instants. Therefore the time-domain solution of the discrete nonlinear system dynamic equations are carried out using CSMP for both small and large disturbances.

4.4.2.1 Small Disturbance Behaviour

Sampling periods of 0.03 second and 0.2 second are used to examine the effect of the sampling period on the stability of an interconnected two-area system equipped first with the conventional controllers and then with the PID controllers. The dynamic responses of the system for a 5 percent load increase in area 1 are shown in Figures 4.6 and 4.7. As predicted by the z-domain analysis, the PID controller provides a better damping and settling time than the conventional controller when the sampling period is 0.03 second (see Figure 4.6). The system with the PID controller becomes unstable when the sampling period is 0.2 second. The system with the conventional controller, however, remains stable at this sampling period (see Figure 4.7). In all cases the intersampling oscillations are absent.

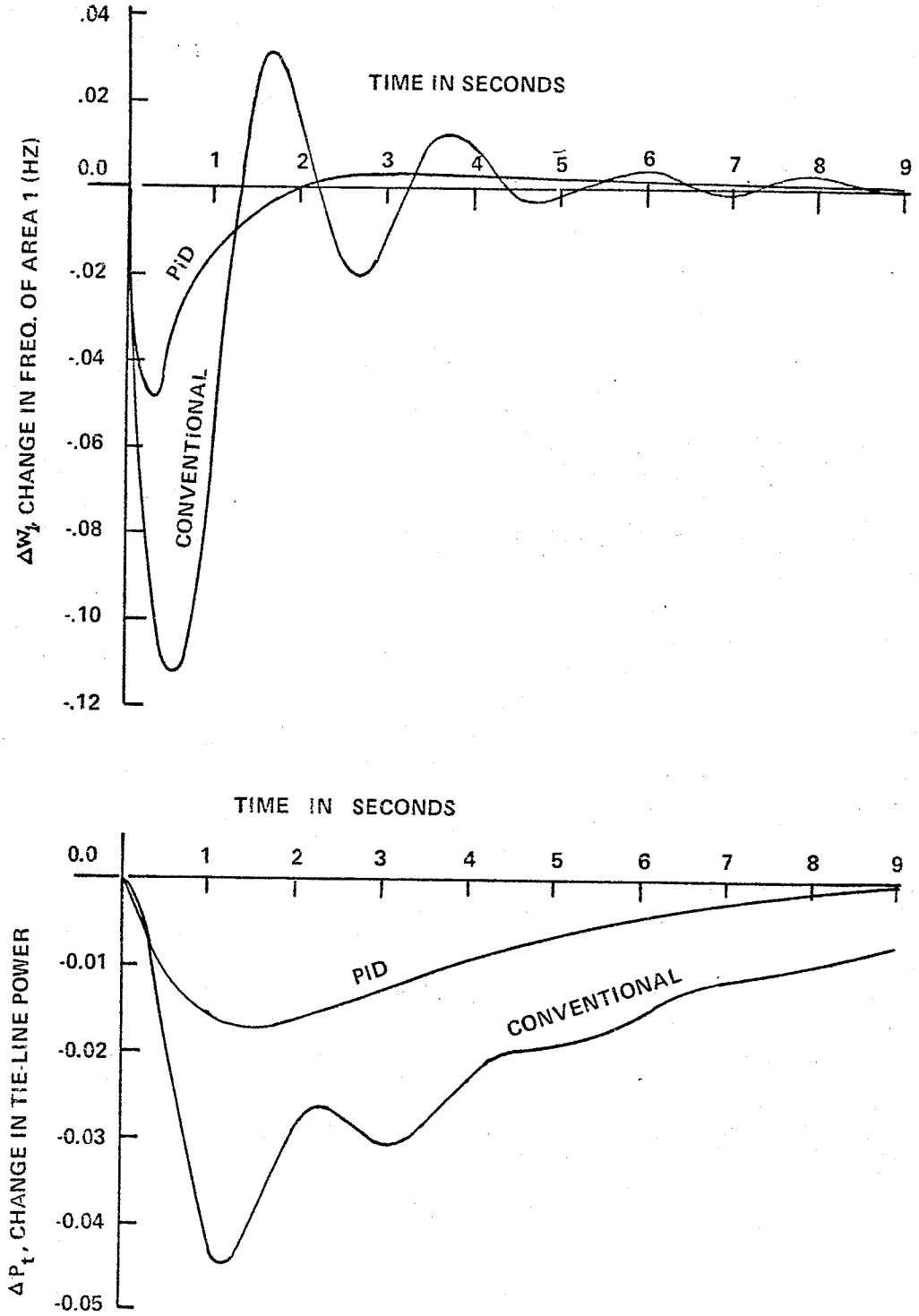

FIGURE 4.6:
TRANSIENT RESPONSE TO 5% LOAD INCREASE IN AREA 1:
SAMPLING PERIOD 0.03 SEC.

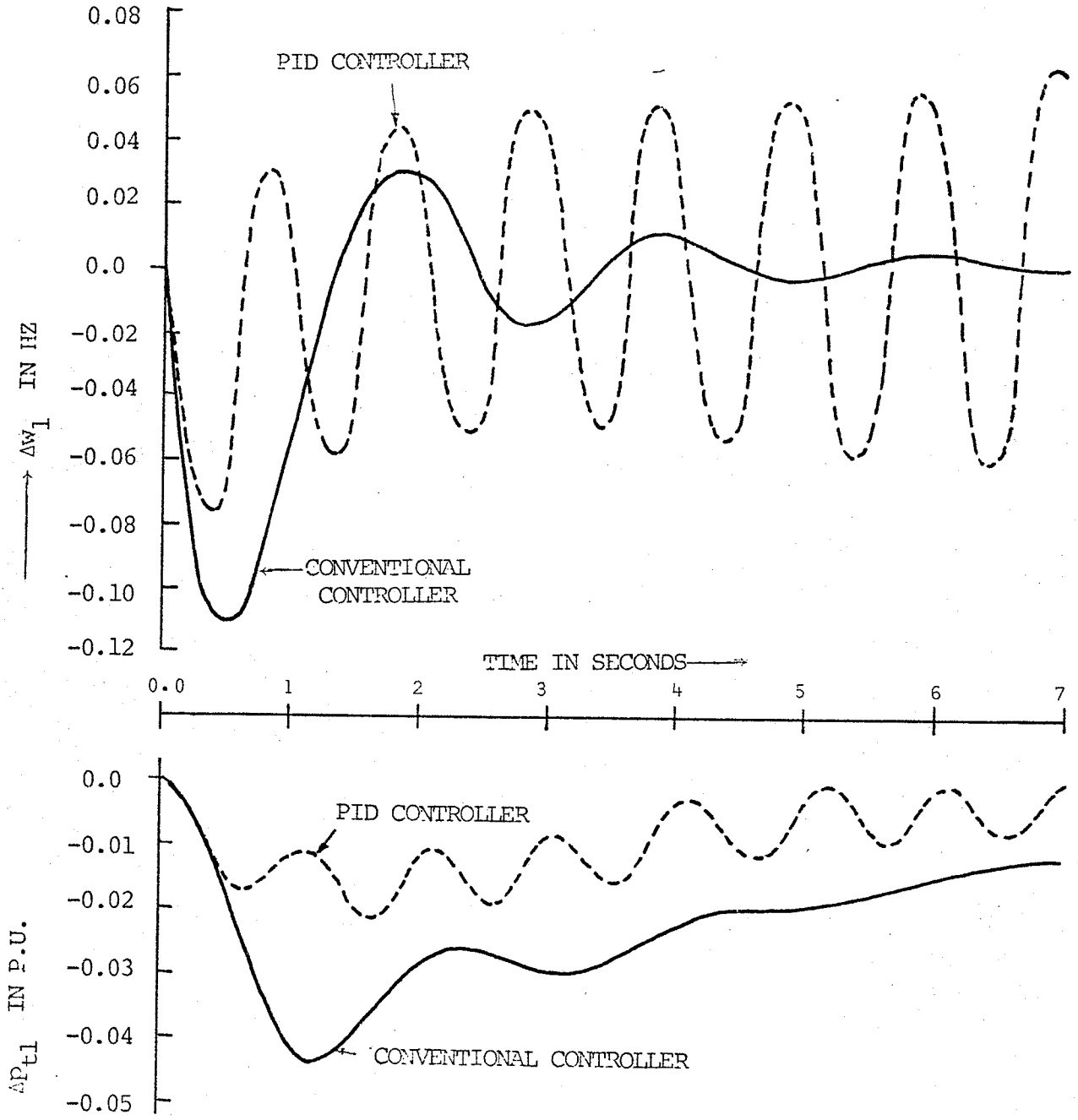

FIG. 4.7 Transient response to a 5% step load increase in Area 1

Sampling period = 0.2 second

4.4.2.2 Large Disturbance Behaviour

Since the system is normally subjected to both small and large disturbances, the controller should provide optimum responses for both circumstances.

The effect of tie-line nonlinearity on the dynamic performance of the interconnected system is evaluated by a large step load increase of 25 percent in area 1. Sampling periods of 0.03 second and 0.2 second are again chosen. When the sampling period is 0.03 second (see Figure 4.8), the system dynamic behaviour is more stable with the PID controller than with the conventional controller. Again when the sampling period is greater than or equal to 0.2 second, the system with the PID controller becomes unstable. In these situations the conventional controller provides a stable response, but the damping and settling time are poor. Thus even for large disturbance conditions, the conclusions of the z-domain analysis are still valid.

4.5 Conclusion

The z-domain technique, especially suited for analysing a discrete large-order dynamic system, has been programmed to examine the effects of the sampling period and the controller gains for two types of controllers for an interconnected two-area power system.

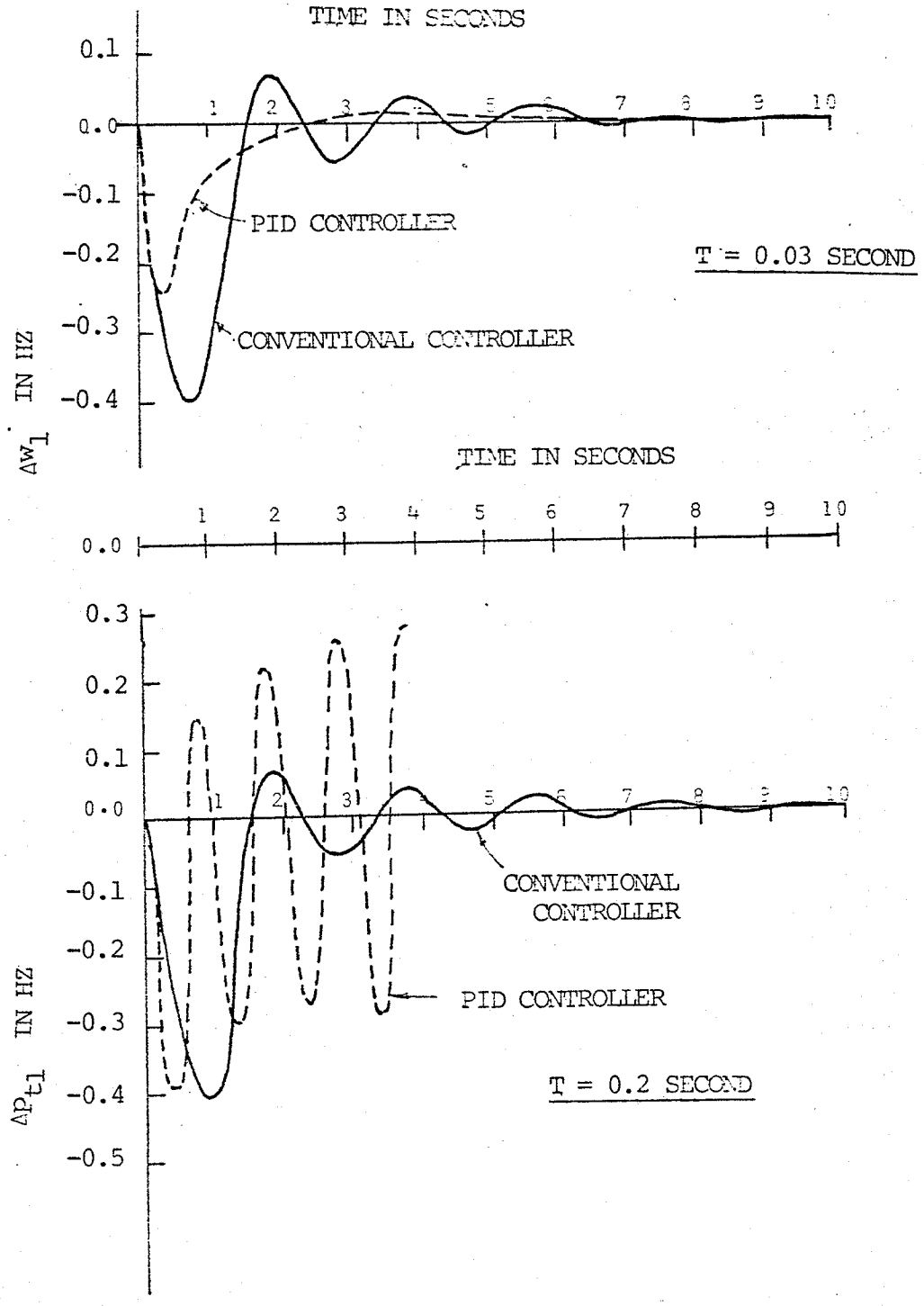

FIG. 4.8: Transient response to a 25% step load increase in Area 1

T = 0.03, 0.2 Seconds

It has been shown that the sampling period has the dominant effect on the location of eigenvalues in z-plane and thus on the stability of an interconnected power system. A specified degree of stability is provided by the digital PID controller only when the sampling period is small. With the PID controller the system becomes unstable when the sampling period is increased above 0.2 second, whereas, with the conventional controller the system remains stable for a wide range of sampling periods even though the damping and the settling time are poor.

Controller gains determined from either the continuous system analysis in s-plane or the discrete system analysis in z-plane are found to be identical. The conventional controller cannot provide an optimum damping of 0.707 with any combination of integral gain and sampling period. The PID controller can achieve an optimum damping of 0.707 only when the sampling period is small. When the sampling period is higher than 0.03 second and limited by other factors, analog control is superior to direct digital control.

CHAPTER 5

THE EFFECTS OF A DC LINK ON THE LOAD-FREQUENCY CONTROLLER DESIGN

5.1 Introduction

Over the past decade HVDC transmission has become an important element of many power systems. Two modes are considered here:

(i) An asynchronous d.c. link within one of two areas.

(ii) An asynchronous d.c. link between two areas.

When a d.c. link forms part of an area, it can be used separately or in conjunction with the governing system (governor-turbine) for the area load-frequency control. Structure requires the co-ordination of control efforts provided both by the slow mode element (governor-turbine) and by the fast mode element (d.c. link). This chapter examines the effects of participation by these parallel acting slow and fast elements on the dynamic load-frequency controller design.

A second factor influencing the design is that a d.c. link as an interconnecting tie prevents dynamic interaction

between areas. But since this condition violates the purpose of an interconnection to provide assistance to an area which cannot meet its load demand, a d.c. link between areas needs to be modified to function like an a.c. link. This chapter therefore examines this factor as well.

5.2 Asynchronous D.C. Link within One of Two Areas

Both rectifier and inverter stations of a two terminal d.c. link reside in one of the areas of an interconnected power system. It is assumed that the load-frequency controller of the area modulates the turbine and d.c. link powers to meet its area requirements.

5.2.1 System Representation

The system under consideration is comprised of two areas of unequal MW capacities; these areas are interconnected by an a.c. tie. A two-terminal d.c. link resides in area 1. This representative example is diagrammed in Figure 5.1. Because the d.c. link response is much faster than the governing system response, a first-order lag model for the d.c. link (developed in Appendix III) is shown in Figure 5.1.

As seen in Figure 5.1, each area is provided with a PID controller with the area control requirement as its input. The output of this controller in area 1 changes the set point

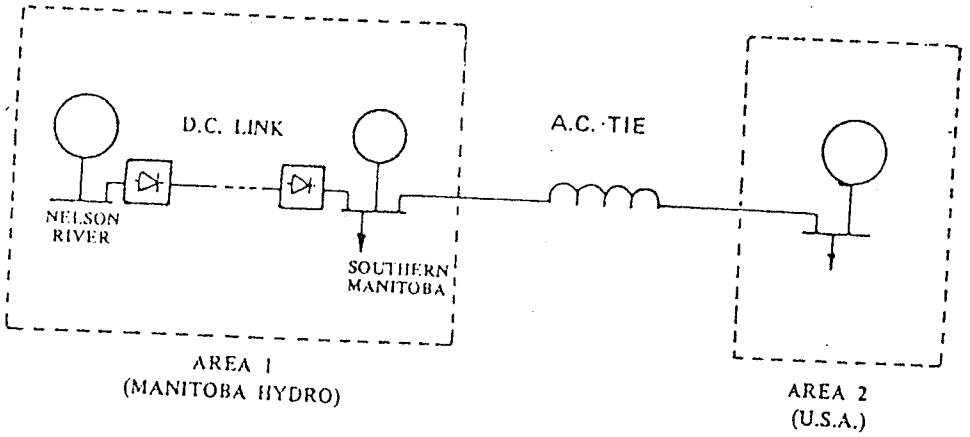

FIGURE 5.1a: AN INTERCONNECTED TWO-AREA SYSTEM WITH AN ASYNCHRONOUS D.C. LINK IN AREA 1.

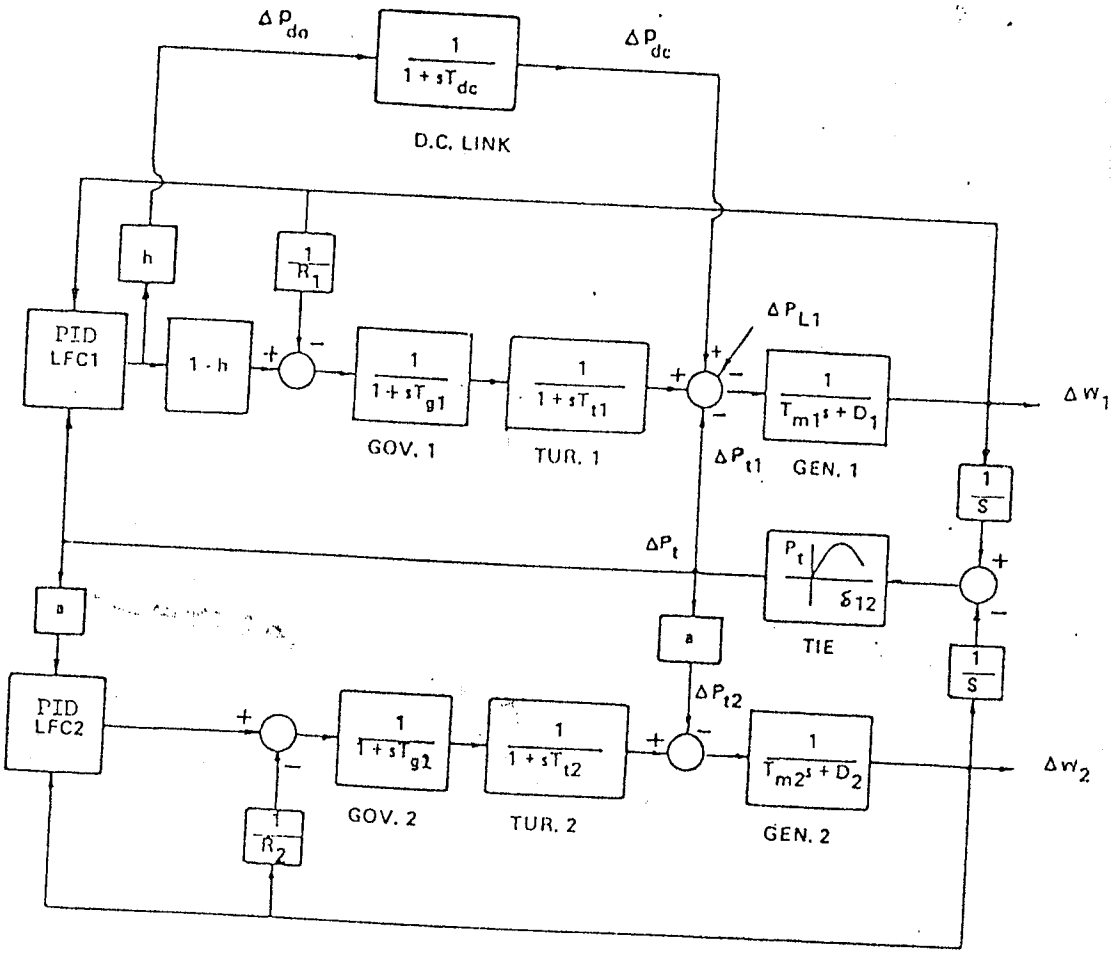

FIGURE 5.1b:

BLOCK DIAGRAM OF THE LOAD-FREQUENCY CONTROL WITH AN ASYNCHRONOUS D.C. LINK IN AREA 1 AND AN A.C. TIE BETWEEN AREA 1 AND AREA 2.

of the power order of the d.c. link and the set point of the governor. The division of the controller output between the d.c. link and the governing system depends on the participation factor h.

The state-space equations for the system (shown in Figure 5.1) are

$$\Delta\dot{w}_1 = -\frac{D_1}{T_{m1}}\Delta w_1 + \frac{1}{T_{m1}}\Delta p_{m1} - \frac{1}{T_{m1}}\Delta p_t + \frac{1}{T_{m1}}\Delta p_{dc} - \frac{1}{T_{m1}}\Delta p_{L1}$$

$$\Delta\dot{z}_1 = \left(-\frac{1}{R_1 T_{g1}} + a_{I1}\right)\Delta w_1 - \frac{1}{T_{g1}}\Delta z_1 + a_{23}\Delta p_{m1} + a_{24}\Delta w_2 + a_{27}\Delta p_t + \frac{(1.0-h)}{T_{g1}}\Delta u_{I1} + a_{210}\Delta p_{dc}$$

$$\Delta\dot{p}_{m1} = \frac{1}{T_{t1}}\Delta z_1 - \frac{1}{T_{t1}}\Delta p_{m1}$$

$$\Delta\dot{w}_2 = -\frac{D_2}{T_{m2}}\Delta w_2 + \frac{1}{T_{m2}}\Delta p_{m2} - \frac{a}{T_{m2}}\Delta p_t - \frac{1}{T_{m2}}\Delta p_{L2}$$

$$\Delta\dot{z}_2 = a_{51}\Delta w_1 + \left(a_{54} - \frac{1}{R_2 T_{g2}}\right)\Delta w_2 - \frac{1}{T_{g2}}\Delta z_2 + a_{56}\Delta p_{m2} + a_{57}\Delta p_t + \frac{1}{T_{g2}}\Delta u_{I2}$$

$$\Delta\dot{p}_{m2} = \frac{1}{T_{t2}} z_2 - \frac{1}{T_{t2}}\Delta p_{m2}$$

$$\Delta\dot{p}_t = T_{k12}\Delta w_1 - T_{k12}\Delta w_2$$

$$\Delta\dot{u}_{I1} = -b_{s1} B_{i1}\Delta w_1 - B_{i1}\Delta p_t$$

$$\Delta\dot{u}_{I2} = -b_{s2} B_{i2}\Delta w_2 - aB_{i2}\Delta p_t$$

$$\Delta\dot{p}_{dc} = a_{101}\Delta w_1 + a_{103}\Delta p_{m1} + a_{104}\,\Delta w_2 + a_{107}\,\Delta p_t + \frac{h}{T_{dc}}\,\Delta u_{I1}$$

$$+ \left[a_{1010} - \frac{1}{T_{dc}}\right]\Delta p_{dc}$$

where $a_{11} = \frac{(1-h)}{T_{g1}}\left[-B_{p1}b_{s1} + \frac{B_{d1}b_{s1}D_1}{T_{m1}} - B_{d1}\bar{T}_{k12}\right]$

$$a_{23} = -\frac{B_{d1}b_{s1}(1-h)}{T_{m1}\,T_{g1}}$$

$$a_{24} = \frac{(1-h)}{T_{g1}}\,B_{d1}T_{k12}$$

$$a_{27} = \frac{(1-h)}{T_{g1}}\left[\frac{B_{d1}b_{s1}}{T_{m1}} - B_{p1}\right]$$

$$a_{210} = -\frac{(1-h)}{T_{g1}}\,\frac{B_{d1}b_{s1}}{T_{m1}}$$

$$a_{54} = \frac{1}{T_{g1}}\left[-B_{p2}b_{s2} + \frac{B_{d2}\,b_{s2}\,D_2}{T_{m2}} + a\,B_{d2}T_{k12}\right]$$

$$a_{51} = -\frac{a\,B_{d2}\,T_{k12}}{T_{g2}}$$

$$a_{56} = -\frac{B_{d2}\,b_{s2}}{T_{m2}\,T_{g2}}$$

$$a_{57} = \frac{1}{T_{g2}} \left(\frac{B_{d2}\, b_{s2}\, a}{T_{m2}} - a\, B_{p2} \right)$$

$$a_{101} = \frac{h}{T_{dc}} \left(- B_{p1}\, b_{s1} + \frac{B_{d1}\, b_{s1}\, D_1}{T_{m1}} - B_{d1}\, T_{k2} \right)$$

$$a_{103} = \frac{-h}{T_{dc}} \quad \frac{B_{d1}\, b_{s1}}{T_{m1}}$$

$$a_{104} = \frac{B_{d1}\, T_{k12}\, h}{T_{dc}}$$

$$a_{107} = \frac{h}{T_{dc}} \left(\frac{B_{d1}\, b_{s1}}{T_{m1}} - B_{p1} \right)$$

$$a_{1010} = - \frac{B_{d1}\, b_{s1}\, h}{T_{m1}\, T_{dc}}$$

The above set of equations can be written in the matrix form:

$$\dot{x}_o = A_o x_o + D_o v_o \qquad 5.1$$

where A_o is (10 x 10) state coefficient matrix

D_o is (10 x 2) disturbance coefficient matrix

x_o is the state vector

and v_o is the disturbance vector

$$x_o = [\Delta w_1\ \Delta z_1\ \Delta p_{m1}\ \Delta w_2\ \Delta z_2\ \Delta p_{m2}\ \Delta p_t\ \Delta u_{I1}\ \Delta u_{I2}\ \Delta p_{dc}]^T$$

$$v_o = [\Delta p_{L1}\ \Delta p_{L2}]^T$$

Matrix A_o includes the PID controller dynamics.

5.2.2 System Analysis

The iterative pole-placement technique described in Chapter 3 is applied to the linearised set of system equations 5.1 to determine the parameters of PID controller in area 1. The parameters of the area 2 controller are kept constant and are the same as those derived in Chapter 3. A sector in s-plane given by

$$\delta \leq -0.4$$

$$\text{and } \zeta \geq 0.707$$

is used to apply the iterative pole-placement technique. Values of the system constants used in this study are given in Table 5.1.

Parameters of the area 1 and area 2 PID controllers which fulfill the specified sector criterion of stability are:

$$B_{p1} = 2.0 \qquad B_{p2} = 0.8$$
$$B_{i1} = 1.7 \qquad B_{i2} = 0.6$$
$$B_{d1} = 1.0 \qquad B_{d2} = 0.7$$

with the eigenvalues

$$\lambda_{1,2} = -6.7681 \pm j\ 6.1011$$
$$\lambda_{3,4} = -1.9403 \pm j\ 1.8823$$
$$\lambda_{5,6} = -0.8875 \pm j\ 0.0443$$
$$\lambda_{7} = -1.7394$$
$$\lambda_{8} = -0.4434$$
$$\lambda_{9} = -12.7421$$
$$\lambda_{10} = -172.6479$$

TABLE 5.1

SYSTEM PARAMETERS

Governor time constants, $T_{g1} = T_{g2} = 0.08$ sec

Turbine time constants, $T_{t1} = T_{t2} = 0.3$ sec

Area regulation constants, $R_1 = R_2 = 0.04$ pu

Inertia constants, $T_{m1} = T_{m2} = 10.0$ sec

D.c. link time constant, $T_{dc} = 0.02$ sec

System voltages, $V_1 = V_2 = 1.0$ pu

Tie line impedance $x_{12} = 10.0$ pu

Initial operating angle, $\sigma_{12} = 30^{o}$

Area 1 capacity, $P_{R1} = 2000$ MW

Area 2 capacity, $P_{R2} = 16000$ MW

Area control frequency biases, $b_{s1} = b_{s2} = 25.0$ pu

The effects on dominant eigenvalues (λ_3, λ_4) of the tie-line loading constant T_{k12} and of the d.c. link participation factor h are shown in Table 5.2 and Figure 5.2. For up to 10 percent d.c. link participation (h = 1.0 → 0.1), the system eigenvalues never leave the specified sector for a wide range of tie-line loading conditions (T_{k12} = 32.65 → 5.0).

Since the controller parameters are derived from a linearised set of system equation, the dynamic behaviour predicted from the above analysis is valid only for the small disturbances. The time-domain analysis is therefore carried out to examine the effect of tie-line nonlinearity for a step load increase of 25 percent in area 1. As shown in Figure 5.3, the designed controller provides a damped system response even for the large disturbance.

The effect of d.c. link participation in the load-frequency control is next examined. Figure 5.4 provides a comparison of the dynamic responses to a 5 percent step load increase in area 1 with and without d.c. link participation. Reduced overshoot and increased damping are achieved when the d.c. link participates in the load-frequency control.

5.3 Asynchronous D.C. Link between Two Areas

When a d.c. link acts as an interconnection between areas, the rectifier and inverter stations must belong to

TABLE 5.2

Effect of Tie line loading, T_{k12} and the d.c. link Participation, h on Eigenvalues

CASE I

T_{k12} = 32.648 (30^{o})

Full participation h = 1	10% participation h = 0.1
- 172.0	- 61.4893
- 12.7420	- 5.7062 ±j 5.6469
- 6.7681 ±j 6.1011	- 6.9012 ±j 6.1806
- 1.9403±j 1.8823	- 3.6225
- 0.8874 ±j 0.0445	- 0.9125 ±j 0.2420
- 1.7394	- 1.6698
- 0.4434	- 0.4434

CASE II

T_{k12} = 5.0

h = 1.0	h = 0.1
- 173.4578	- 61.7065
- 12.7278	- 6.7941 ±j 6.0784
- 6.8781 ±j 6.1714	- 6.9009 ±j 6.1790
- 1.8920 ±j 1.4281	- 1.9753
- 0.7112	- 0.2263
- 0.2264	- 1.6587
- 1.6615	- 0.8688
- 0.4393	- 0.4393

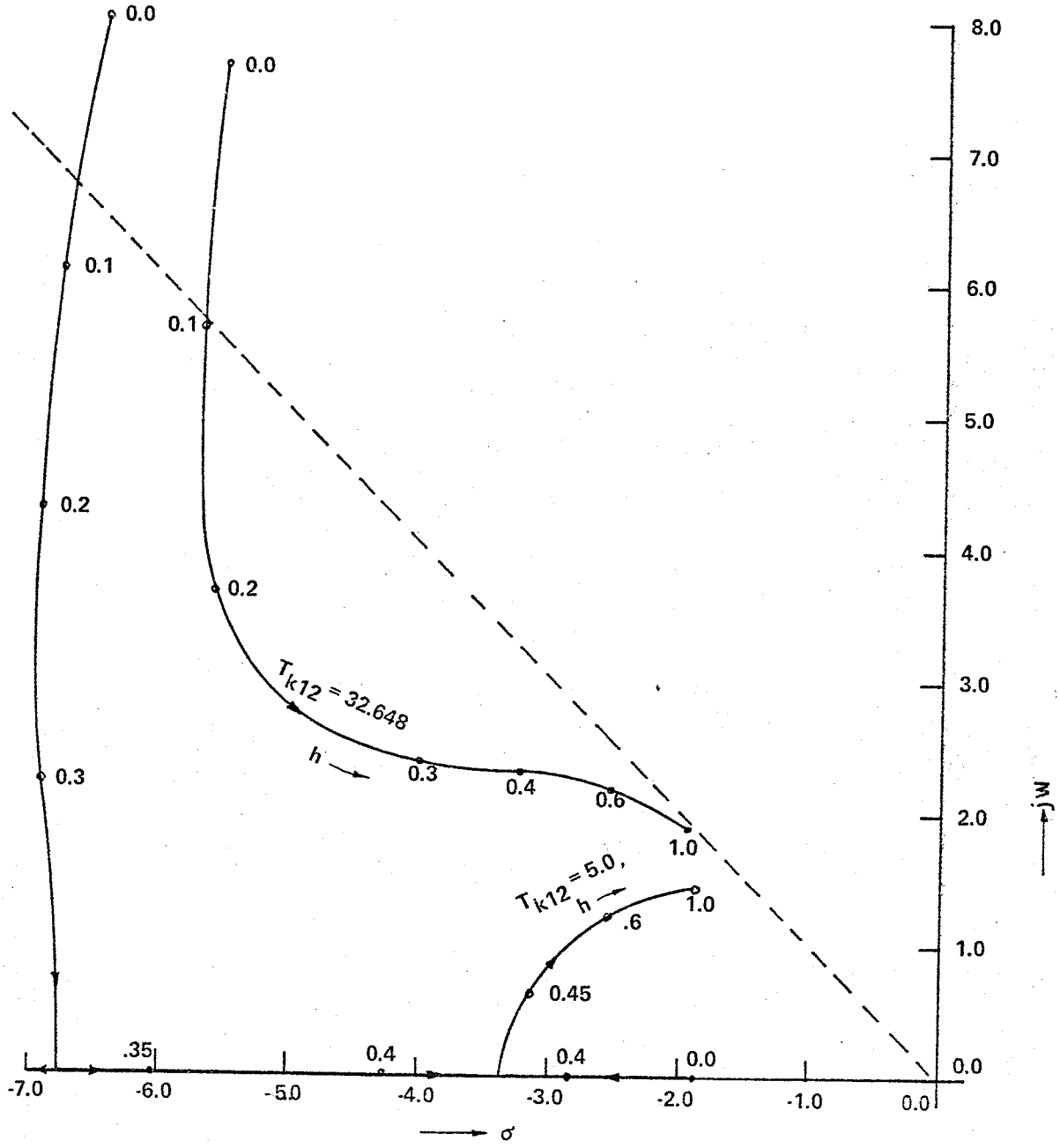

FIGURE 5.2:
EFFECT OF D.C. LINK PARTICIPATION, h
AND TIE-LINE LOADING ON THE DOMINANT EIGENVALUE

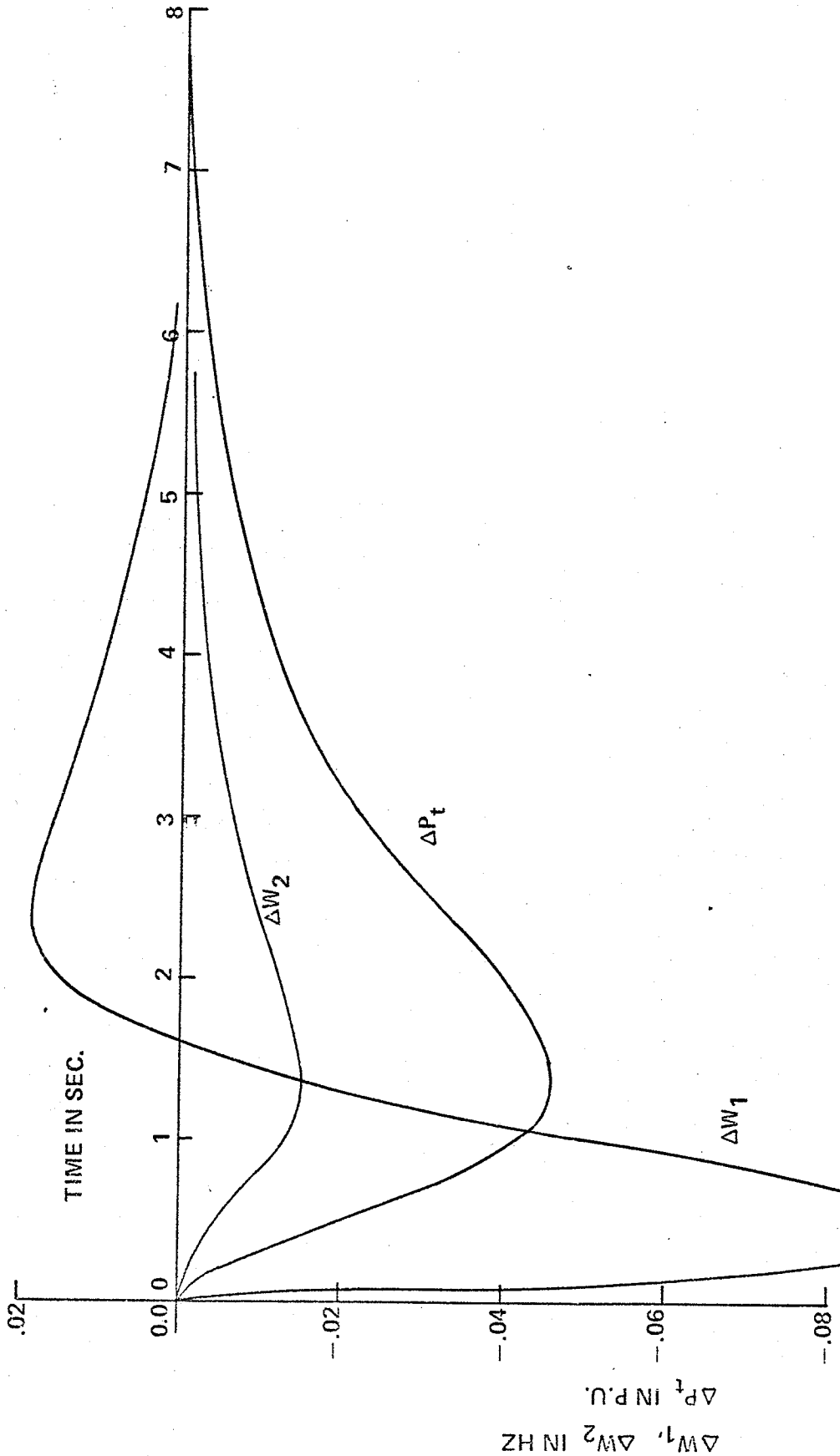

FIGURE 5.3 TRANSIENT RESPONSE TO 0.25 P.U. LOAD INCREASE IN AREA 1: FULL PARTICIPATION BY D.C. LINK

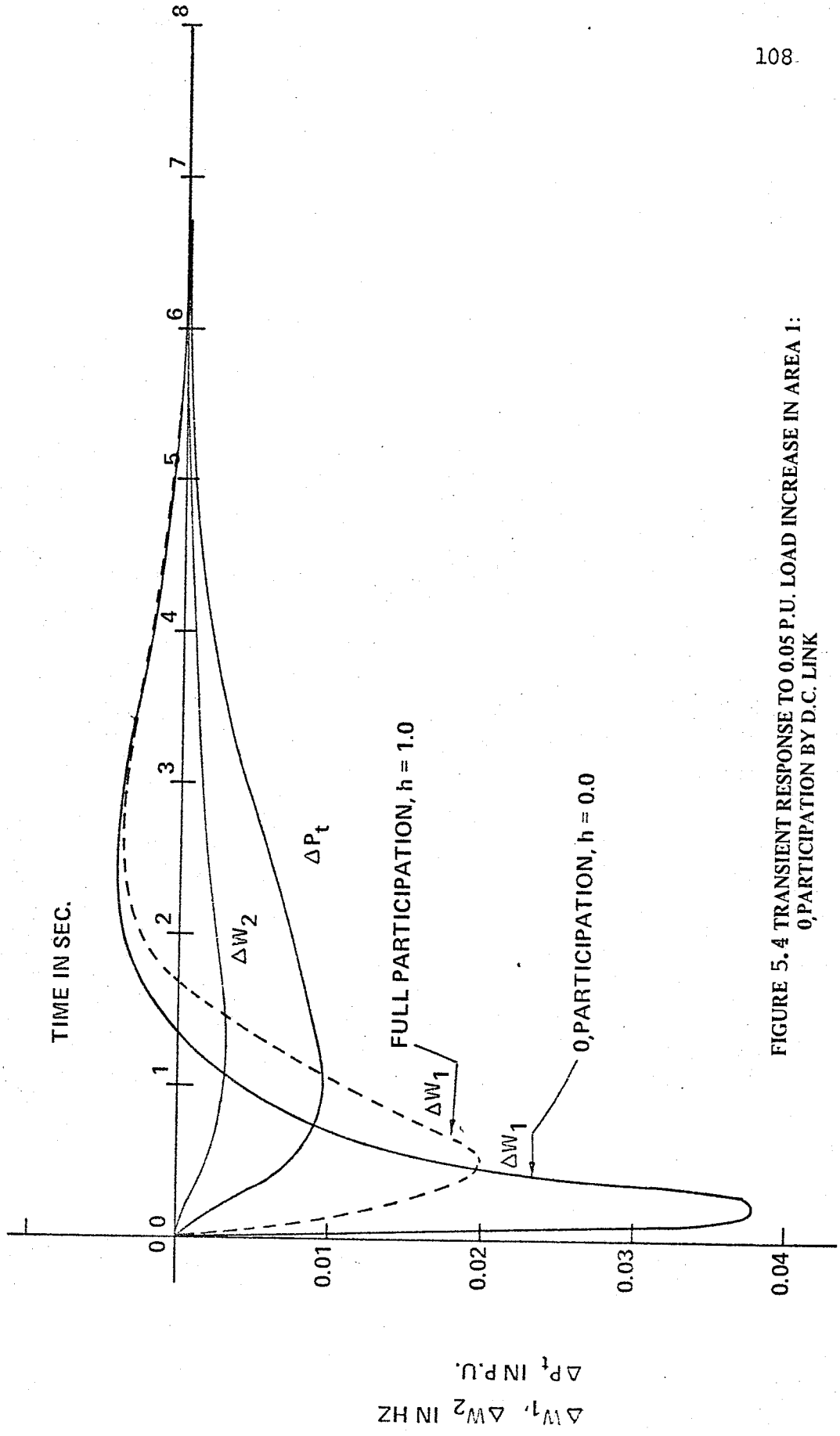

FIGURE 5.4 TRANSIENT RESPONSE TO 0.05 P.U. LOAD INCREASE IN AREA 1: 0, PARTICIPATION BY D.C. LINK

separate areas. This kind of d.c. link can transmit scheduled power only. Load changes in one area cannot affect the tie-line schedule, and therefore the other area will be unaffected. The load-frequency controller in each area will mainly control its own area frequency. With this arrangement, the adjoining areas can operate at different frequencies without affecting tie-line flows. The dynamic problems of each area will remain separate and will be regulated independently by each area controller.

In contrast, an a.c. interconnection always creates interactions between areas. In this situation reduction of the area control error in one area is not possible unless the dynamics of the other area are also taken into account. But the disadvantage of an asynchronous d.c. link is that it cannot provide assistance to another area which cannot meet its load demand. This disadvantage will cause collapse of the area deficient in generation. If this disadvantage is to be eliminated from the proposed controller design, the d.c. link power needs to be modulated to make it function like an a.c. tie.

5.3.1 System Analysis without Power Modulation on the D.C. Link

In this mode of operation, tie-line power does not deviate from its scheduled value. The area controller regulates the area frequency. Thus a knowledge of the internal dynamics

of an individual area is all that is necessary for designing the controller for that area.

The dynamic equations of an area equipped with a PID controller are:

$$\Delta\dot{w}_i = -\frac{D_i}{T_{mi}}\Delta w_i + \frac{1}{T_{mi}}\Delta p_{mi} - \frac{1}{T_{mi}}\Delta p_{Li}$$

$$\Delta\dot{z}_i = \left[-\frac{1}{R_i}\frac{1}{T_{gi}} + a_{21}\right]\Delta w_i - \frac{1}{T_{gi}}\Delta z_i + a_{23}\Delta p_{mi} + \frac{1}{T_{gi}}\Delta u_{ii}$$

$$\Delta\dot{p}_{mi} = \frac{1}{T_{ti}}\Delta z_i - \frac{1}{T_{ti}}\Delta p_{mi} \qquad 5.2$$

$$\Delta\dot{u}_{ii} = -b_{si}\,B_{ii}\,\Delta w_i$$

where $$a_{21} = \frac{1}{T_{gi}}\left[-B_{pi}\,b_{si} + \frac{B_{di}\,b_{si}\,D_i}{T_{mi}}\right]$$

$$a_{23} = -\frac{B_{di}\,b_{si}}{T_{mi}\,T_{gi}}$$

The PID gains of the area controller needed to bring the eigenvalues of an isolated area to an specified sector

$$\sigma \leq -0.4$$

$$\zeta \geq 0.707$$

are

$$B_{pi} = 0.5$$

$$B_{ii} = 0.6$$

$$B_{di} = 0.7$$

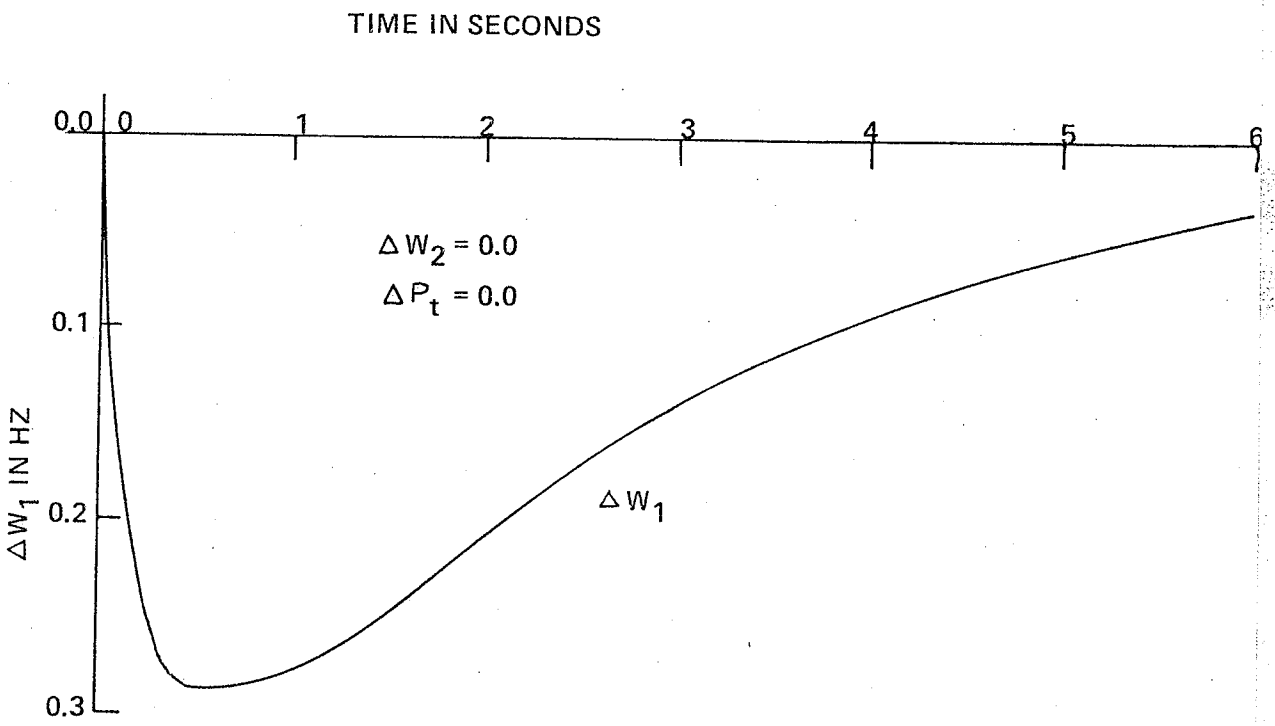

FIGURE 5.5 TRANSIENT RESPONSE TO 25% LOAD INCREASE IN AREA 1:
ASYNCRONOUS D.C. LINK
AREA 1 CAPABILITY > LOAD DEMAND

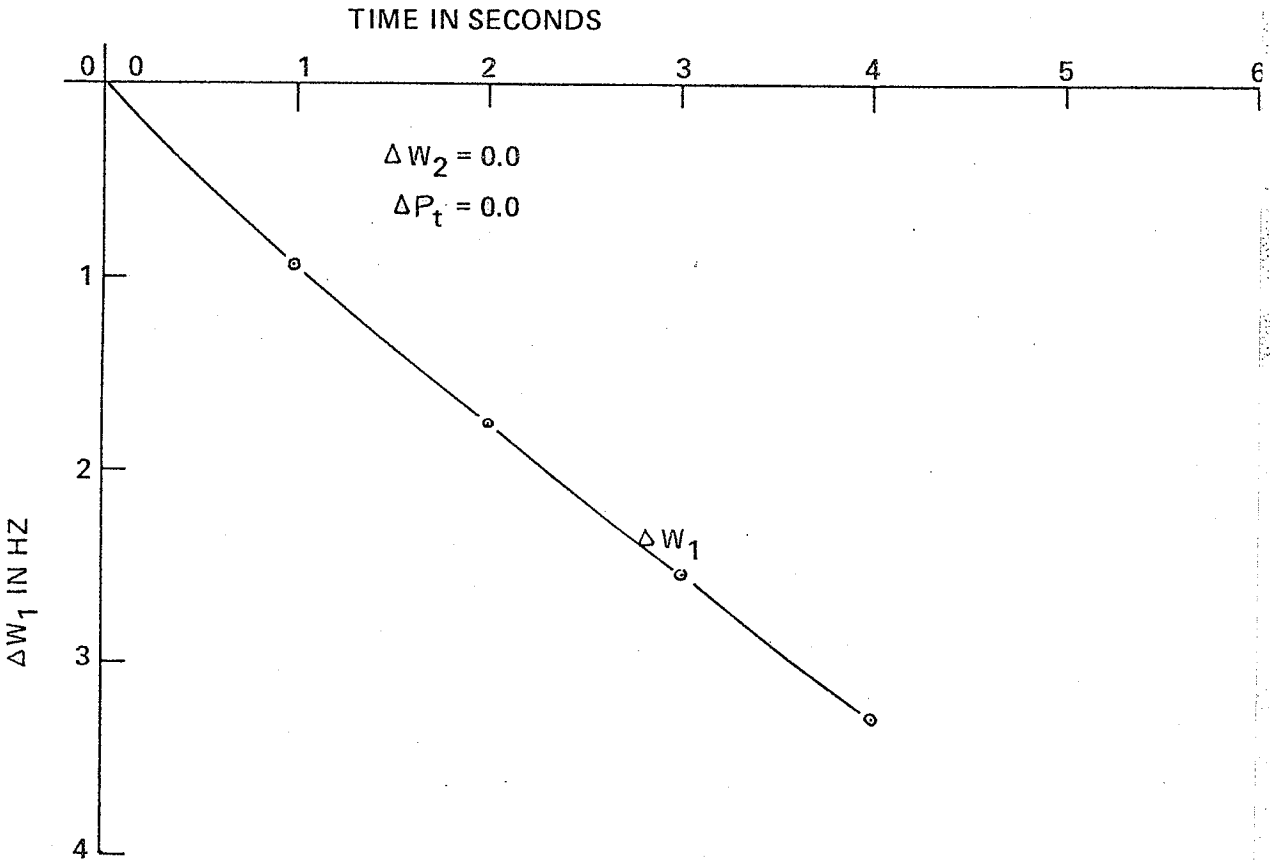

FIGURE 5. 6 TRANSIENT RESPONSE TO 25% LOAD INCREASE IN AREA 1:
ASYN. D.C. LINK
AREA 1 CAPABILITY < LOAD DEMAND

An area frequency response to a 25 percent step load increase is shown in Figure 5.5. It is assumed that the generation in this area is sufficient to meet this load demand. The frequency response of the same area for a similar disturbance when the generation is insufficient is shown in Figure 5.6. This graph indicates the tendency of a system to collapse. When this extreme condition occurs, the d.c. link will cease transmission and thus will affect both areas adversely.

5.3.2 System Analysis with Power Modulation on the D.C. Link

A d.c. link can be given desirable characteristics similar to an a.c. link by modulating its power according to the equation

$$\Delta p_{do} = \frac{B}{S} (\Delta w_1 - \Delta w_2)$$

where Δw_1 and Δw_2 are the area frequencies and B is a constant.

An interconnected two-area system with the above modification is diagrammed in Figure 5.7.

Unlike an a.c. tie, the d.c. tie has no stability limits on power transfer capability between areas. The magnitude of the synchronising torque coefficient B (= T_{k12}) is therefore unaffected by the scheduled tie-line loading. The system behaviour is therefore the same for small and large disturbances. For the constants given in Table 5.1 and B = 32.5, the PID

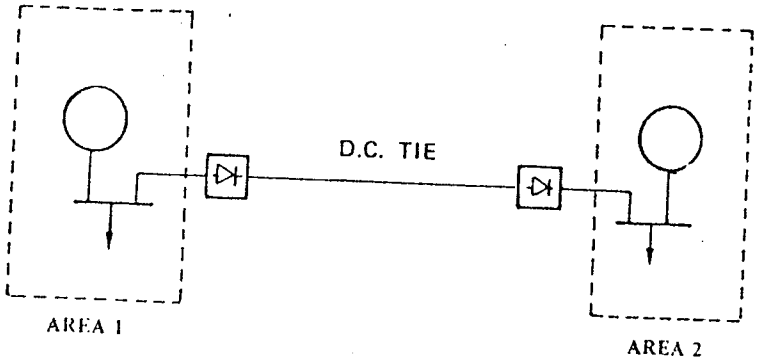

FIGURE 5.7a: AN INTERCONNECTED TWO-AREA SYSTEM WITH AN ASYNCHRONOUS D.C. TIE.

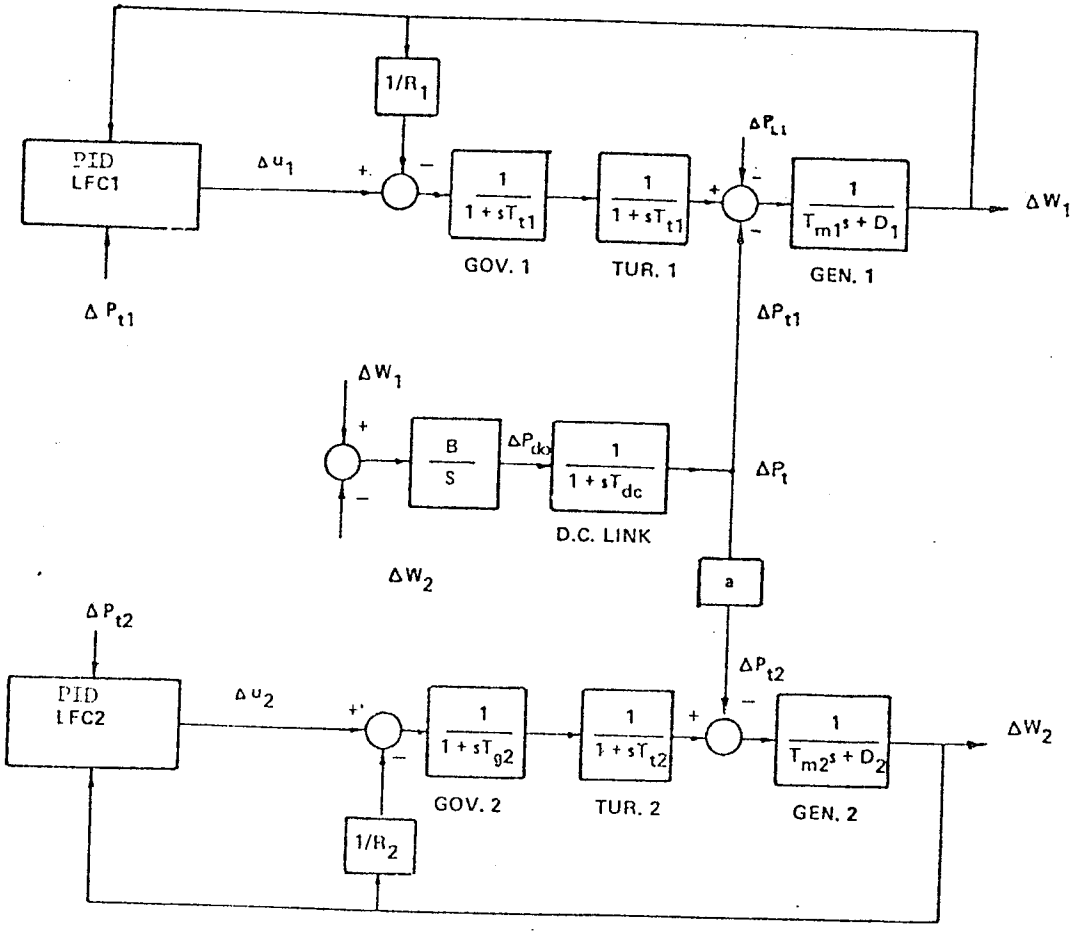

FIGURE 5.7b:

BLOCK DIAGRAM OF THE LOAD-FREQUENCY CONTROL : ASYNCHRONOUS D.C. LINK AS A TIE BETWEEN AREA 1 AND AREA 2.

controller gains are;

$$B_{p1} = B_{p2} = 0.8$$
$$B_{i1} = B_{i2} = 0.6$$
$$B_{d1} = B_{d2} = 0.7$$

They are the same gains as found in Chapter 3. The d.c. link dynamics thus has little influence on the controller gains.

The dynamic behaviour of the interconnected two-area system to a 25 percent load increase in area 1 is shown in Figure 5.8. In this example area 1 has received assistance from area 2 through the d.c. link even though area 1 is capable of supplying 10% of the extra load by itself. Thus the behaviour of this modulated d.c. asynchronous system is similar to the a.c. interconnected system considered in Chapter 3.

5.4 Conclusion

The dynamic performance of an interconnected system is improved when a d.c. link in an area participates in the load-frequency control. The PID gains of an area controller with the d.c. link are increased to satisfy the sector criterion of relative stability.

Even though an asynchronous d.c. link does not cause interaction between the dynamics of the adjoining areas, it

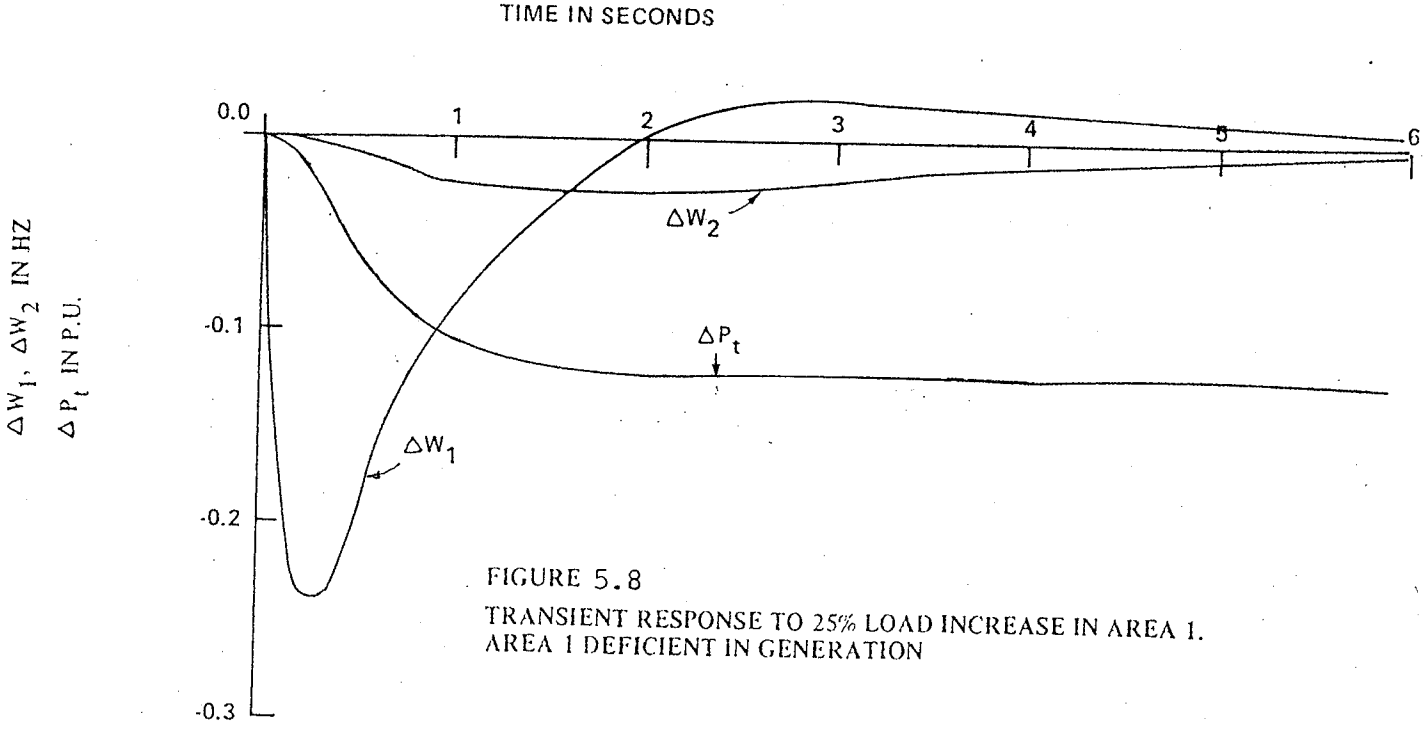

FIGURE 5.8

TRANSIENT RESPONSE TO 25% LOAD INCREASE IN AREA 1.
AREA 1 DEFICIENT IN GENERATION

can lead to system collapse when an area fails to meet its load demand. But if an asynchronous d.c. link is given the desired characteristics of the system assistance found in an a.c. link, then system stability can be maintained. Unlike an a.c. tie, a d.c. link has no stability load limit or nonlinearity. The system performance is optimal for all tie-line loadings and disturbances. Thus the performance of the entire interconnected system can be improved when a d.c. link participates in the load-frequency control.

CHAPTER 6

CONCLUSIONS

Strictly speaking the following conclusions apply only to the system studied in this thesis.

1. A PID controller can be used to provide load-frequency control superior to the present commonly used "conventional" control.

   Reasons for selecting the PID controller rather than the optimal controller are:

   (i) It permits placement of the eigenvalues in the desired sector even though it is relatively low-order controller.

   (ii) It is easily constructed (either an analog or digital version) and commonly used in the industry.

   (iii) It requires measurements of local signals only whereas additional measurements are needed for an optimal controller.

   (iv) It helps an area deficient in generation in receiving assistance from adjoining areas. An optimal controller denies such assistance.

2. An iterative pole-placement technique can be used to determine the gains for the PID controller such that all the eigenvalues of the system are in a specified region in the s-plane.

   Placement of eigenvalues in a specified region ensures a desired degree of dynamic stability with a minimum damping and a maximum settling time.

3. It is sufficient to represent the "external system" as a simple first-order system for controller design purposes, and an appropriate system identification and reduction method is described.

4. For a digital PID controller, the system eigenvalues are sensitive to the sampling period but not so sensitive to the controller gains.

5. The system with a digital PID controller becomes unstable above a certain sampling period, whereas the system with a conventional controller remains stable for a wide range of sampling periods.

6. When a d.c. link within an area participates in the control function, the system response to a disturbance

has decreased overshoot and increased damping.

7. A d.c. link may be controlled such that it behaves like an a.c. link and thus is able to provide load-frequency control action.

REFERENCES

1. 'IEEE Standard Definitions of terms for Automatic Generation Control on Electric Power Systems' IEEE Trans. on PAS, July/Aug. 1970, pp. 1356-1364.

2. Kirchmayer, L.K.: 'Economic Control of Interconnected Systems', Wiley, New York, 1959.

3. Cohn, N.: 'Control of Generation and Power on Interconnected Systems', John Willey and Sons, Inc., New York, 1966.

4. Concordia, C. and Kirchmayer, L.K.: 'Tie-Line Power and Frequency Control of Electric Power Systems', AIEE Trans., vol. 72, June 1953, pp. 562-572.

5. Concordia, C. and Kirchmayer, L.K.: 'Tie-Line Power and Frequency Control of Electric Power Systems - Part II', AIEE Trans., vol. 72, April 1954, pp. 133-146.

6. Concordia, C., Kirchmayer, L.K. and Szymanski, E.A.: Effect of Speed-Governor Dead-Band on Tie-Line Power and Frequency Control Performance', AIEE Trans., Aug. 1957, pp. 429-435.

7. Elgerd, O.I. and Fosha, C.E.: 'Optimum Megawatt-Frequency Control of Multiarea Electric Energy Systems', IEEE Trans. on PAS, vol. PAS-89, April 1970, pp. 556-563.

8. Fosha, C.E. and Elgerd, O.I.: 'The Megawatt-Frequency Control Problem: A New Approach Via Optimal Control Theory', IEEE Trans. on PAS, vol. PAS-89, April 1970, pp. 563-577.

9. Cavin III, R.K., Budge Jr., M.C. and Rasmussen, P.: 'An Optimal Linear Systems Approach to Load-Frequency Control', IEEE Trans. on PAS, vol. PAS-90, Nov./Dec. 1971, pp. 2472-2482.

10. Miniesy, S.M. and Bohn, E.V.: 'Two-Level Control of Interconnected Power Plants', IEEE Trans. on PAS, vol. PAS-90, Nov./Dec. 1971, pp. 2742-2748.

11. Bohn, E.V. and Miniesy, S.M.: 'Optimum Load-Frequency Sampled-Data Control with Randomly Varying System Disturbances', IEEE Trans. on PAS, vol. PAS-91, Sept./Oct. 1972, pp. 1916-1923.

12. Miniesy, S.M. and Bohn, E.V.: 'Optimum Load-Frequency Continuous Control with Unknown Deterministic Power Demand', IEEE Trans. on PAS, vol. PAS-91, Sept./Oct. 1972, pp. 1910-1915.

13. Glover, J.D. and Schweppe, F.C.: 'Advanced Load-Frequency Control', IEEE Trans. on PAS, vol. PAS-96, Sept./Oct. 1972, pp. 2095-2103.

14. Calovic, Milan: 'Linear Regulator Design for a Load and Frequency Control', IEEE Trans. on PAS, vol. PAS-91, Nov./Dec. 1972, pp. 2271-2285.

15. Machida, T., Yoshida, Y. and Nakamura, H.: 'A Method of Automatic Frequency Ratio Control by a D.C. System', IEEE Trans. on PAS, vol. PAS-86, March 1967, pp. 263-267.

16. Cahen, F.M., Perna, A.D. and Gavrilovic, A: 'The Sardinia - Italian Mainland HVDC Transmission Scheme - Frequency Control of the Sardinian System', IEE Conf. on HVDC Transmission, Part I Sept. 1966, p. 50-55.

17. Uhlmann, E.: 'AC Network Stabilization by D.C. Links', CIGRE, Paper No. 32-01, 1970 Session.

18. Patterson, W.A., Dalzell, J.N. and Desilets, G.: 'More Effective Damping on AC Systems Through the Addition of External Control Signals to a HVDC Link', - The Eel River Case, CEA, March 1972.

19. Haywood, R.W. and Ralls, K.J.: 'Use of HVDC For Improving AC System Stability and Speed Control', Proceedings, Manitoba Power Conf. EHV-DC, Winnipeg, Canada, 1971, pp. 780-803.

20. Iliceto, F.: 'D.C. Link and A.C. Network Combined Power Control Requirements', Direct Current, vol. 9, May 1964, pp. 37-39, 60.

21. Haywood, R.W. and Chand, J.: 'Auxiliary power controls on the Nelson River HVDC scheme to enhance A.C. system Performance - A report on recent development', CIGRE meeting, Scandanavia, Aug. 1979.

22. Astrom, K.J.: 'Modelling and Identification of Power System Components', Real-Time Control of Electric Power Systems - Proceedings of Brown, Boveri & Company, 1971 - Edited by E. Handschin, Elsevier Publ. Comp., New York, 1972.

23. Rosenbrock, H.H. and McMorran, P.D.: 'Good, Bad or Optimal?', IEEE Trans. Automat. Contr., vol. AC-16, Dec. 1971, pp. 552-554.

24. Horowitz, I.C. and Shaked, U.: 'Superiority of Transfer Function Over State-Variable Methods in Linear Time-Invariant Feedback System Design', IEEE Trans. Automat. Contr., vol. AC-20, Feb. 1975, pp. 84-97.

25. Siljak, D.D. and Sundareshan, M.K.: 'A Multilevel Optimization of Large-Scale Dynamic Systems', IEEE Trans. Automat. Contr., vol. AC-21, Feb. 1976, pp. 79-84.

26. Wang, S.H. and Davison, E.J.: 'On the Stabilization of Decentralized Control Systems', IEEE Trans. Automat. Contr., vol. AC-18, Oct. 1973, pp. 473-478.

27. Mesarovic, M.D., Macko, D. and Takahara, Y.: 'Theory of Heirarchical Multilevel Systems', Academic Press, New York, 1970.

28. Davison, E.J.: 'The Robust Decentralized Control of a General Servomechanism Problem', IEEE Trans. Automat. Contr., vol. AC-21, Feb. 1976, pp. 14-24.

29. Wonham, W.M.: 'On Pole Assignment in Multi-Input Controllable Linear Systems', IEEE Trans. on Automatic Control, vol. AC-12, No. 6, Dec. 1967, pp. 660-665.

30. Simon, J.D. and Mitter, S.K.: 'A Theory of Modal Control', Inform. Contr. vol. 13, Oct. 1968, pp. 316-353.

31. Levine, W.S. and Athans, M.: 'On the Determination of the Optimal Constant Output Feedback Gains for Linear Multivariable Systems', IEEE Trans., on A.C., vol. AC-15, No. 1, Feb. 1970, pp. 44-48.

32. Brasch, F.M. Jr. and Pearson, J.B.: 'Pole Placement Using Dynamic Compensations', IEEE Trans. on Automatic Control, vol. AC-15, No. 1, Feb. 1970, pp. 34-43.

33. Ding, C.Y., Brasch, Jr., F.M. and Pearson, J.B.: 'On Multivariable Linear Systems', IEEE Trans. on A.C., vol. AC-15, No. 1, pp. 96-97.

34. Johnson, T.L. and Athans, M.: 'On the Design of Optimal Constrained Dynamic Compensators for Linear Constant Systems', IEEE Trans. on A.C., vol. AC-15, No. 6, Dec. 1970, pp. 658-660.

35. Chen, C.T. and Hsu, C.H.: 'Design of Dynamic Compensators for Multivariable Systems', Proc. 1971 Joint Automatic Control Conference, pp. 893-900.

36. Chen, C.T.: 'Analysis and Synthesis of Linear Control Systems', New York: Holt, Rinehart & Winston, Inc., 1975.

37. Koschmann, J.E.: 'Compensator Design for Linear Multivariable Systems', IEEE Trans. on A.C., vol. AC-20, Nov. 1, Feb. 1975, pp. 113-120.

38. Seraji, H.: 'Restrictions on Attainable Poles and Methods for Pole Assignment with Output Feedback', Proc. IEE, vol. 3, No. 3, March 1974, pp. 205-212.

39. McBrinn, D.E. and Roy, R.J.: 'Stabilization of Linear Multivariable Systems by Output Feedback', IEEE Trans. Automatic Contr., vol. AC-17, April 1972, pp. 243-245.

40. Sirisena, H.R. and Choi, S.S.: 'Pole Placement in Prescribed Regions of the Complex Plane Using Output Feedback', IEEE Trans. Automatic Control, vol. AC-20, No. 6, Dec. 1975, pp. 810-812.

41. Fadeev, D.K. and Fadeeva, V.N.: 'Computational Methods of Linear Algebra', San Francisco, Calif.: Freeman, 1963.

42. Athans, M. and Falb, P.: 'Optimal Controls', McGraw-Hill, New York, 1966.

43. Athans, M.: On the Design of P.I.D. Controllers Using Optimal Linear Regulator Theory, Automatica, vol. 7, pp. 643-647.

44. Merriam III, C.W.: 'Optimization Theory and the Design of Feedback Control Systems', McGraw Hill Book Company, N.Y., 1964.

45. Chen, Chi-Tsong: 'Analysis and Synthesis of Linear Control Systems', Holt, Rinehart and Winston, Inc., New York, 1975.

46. Rolnik, J.A. and Horowitz, I.M.: 'Feedback Control System synthesis for plants with large parameter variations', IEEE Trans. Automat. Contr., Dec. 1969, pp. 714-718.

47. Belanger, P.R. and Chung, R.: 'Design of low order compensator by gain matching', IEEE Trans. Automat. Contr., Aug. 1976, pp. 627-629.

48. Chen, C.F. and Shieh, L.S.: 'A Novel Approach to Linear Model Simplification', Int. J. Control, vol. 8, No. 6, pp. 561-570.

49. Bollinger, K.E. and Mathur, J.C.: 'To compute the zeros of large systems', IEEE Trans. Automat. Contr., vol. AC-17, April 1972, pp. 261.

50. Young, P.C.: 'Applying parameter estimation to Dynamic Systems, Parts I and II, Control Eng'g. 16, 119-125 (1969) No. 10; No. 11, pp. 118-124.

51. Graupe, Daniel: 'Identification of Systems', Van Nostrand Reinhold Company, New York, 1972.

52. Coury, E.F.: 'A Practical Guide to Minicomputer Applications', IEEE Press, 1972.

53. Fiedler, H.J. and Kirchmayer, L.K.: 'Digital Computer Control of System Operation', The American Power Conference, Chicago, March 1963.

54. Russell, J.C. and Rades, W.: 'The Wisconsin Electric Power Company Energy Control System', PICA Conf. 1973, pp. 135-141.

55. Dyliacco, T.E. and Rosa, D.L.: 'Designing an Effective Man. Machine Interface for Power System Control', PICA Conf. 1975, pp.262-266.

56. Tou, J.T.: 'Digital and Sampled Data Control Systems', McGraw Hill Book Company, Inc., New York, 1959.

57. Kuo, B.C.: 'Analysis and synthesis of Sampled Data Control Systems', Prentice-Hall, Inc., Englewood Cliffs, N.J., 1963.

58. Dorf, R.C.: 'Time-Domain Analysis and Design of Control Systems', Addition-Wesley Publishing Company, Inc., N.Y., 1970.

59. Cadzow, J.A. and Martens, J.R.: 'Discrete-Time and Computer Control Systems', Prentice-Hall, Inc., Englewood Cliffs, N.J., 1970.

60. Imad, F.P. and Van Ness, J.E.: 'Finding the Stability and the Sensitivity of Large Sampled Systems', IEEE Trans. Automat. Contr., Aug. 1967.

APPENDIX I

MODEL SIMPLIFICATION

There are two main approaches to the model order reduction[48]:

(i) The dominant eigenvalue approach

(ii) The continued fraction approach

The first approach has the advantage of retaining only the dominant eigenvalue in the reduced models, the approach also has the following disadvantages:

(i) It is limited to the systems which have dominant eigenvalues.

(ii) The steady-state behaviour of the reduced system is unknown.

In the continued fraction approach the reduced model is obtained by expanding the system transfer function and then ignoring the lower quotients of the fraction. The continued fraction approach used by Chen and Shieh[48] has the advantage that it retains exactly the steady-state chracteristic of the original system and that it provides dynamic characteristics depending on the number of continued fraction terms retained. This approach ensures that the reduced and unreduced system

model time responses are sufficiently close for a minimum number of quotients in the continued fraction.

For the load-frequency control, the steady-state and the dynamic characteristics are equally important. The continued fraction approach proposed by Chen and Shieh[48] is therefore used here to simplify the detailed external system model.

I.1 Simplifying a transfer function

If the detailed model of the system is given by a transfer function

$$G(s) = \frac{b_1 s^{n-1} + b_2 s^{n-2} + \text{---} + b_n}{s_n + a_1 s^{n-1} + \text{-----} + a_n}$$

The polynomials are then re-written in the ascending order as

$$G(s) = \frac{b_n + b_{n-1}\, s + \text{----} + b_2 s^{n-1} + b_1 s^{n-1}}{a_n + a_{n-1}\, x + \text{----} + a_2 s^{n-2} + a_1 s^{n-1} + s^n} \qquad \text{I.2}$$

Equation I.2 is next expanded into a continued fraction:

$$G(s) = \cfrac{1}{H_1 + \cfrac{1}{\cfrac{H_2}{s} + \cfrac{1}{H_3 + \cfrac{1}{\cfrac{H_4}{s} + \cfrac{1}{\ddots}}}}} \qquad \text{I.3}$$

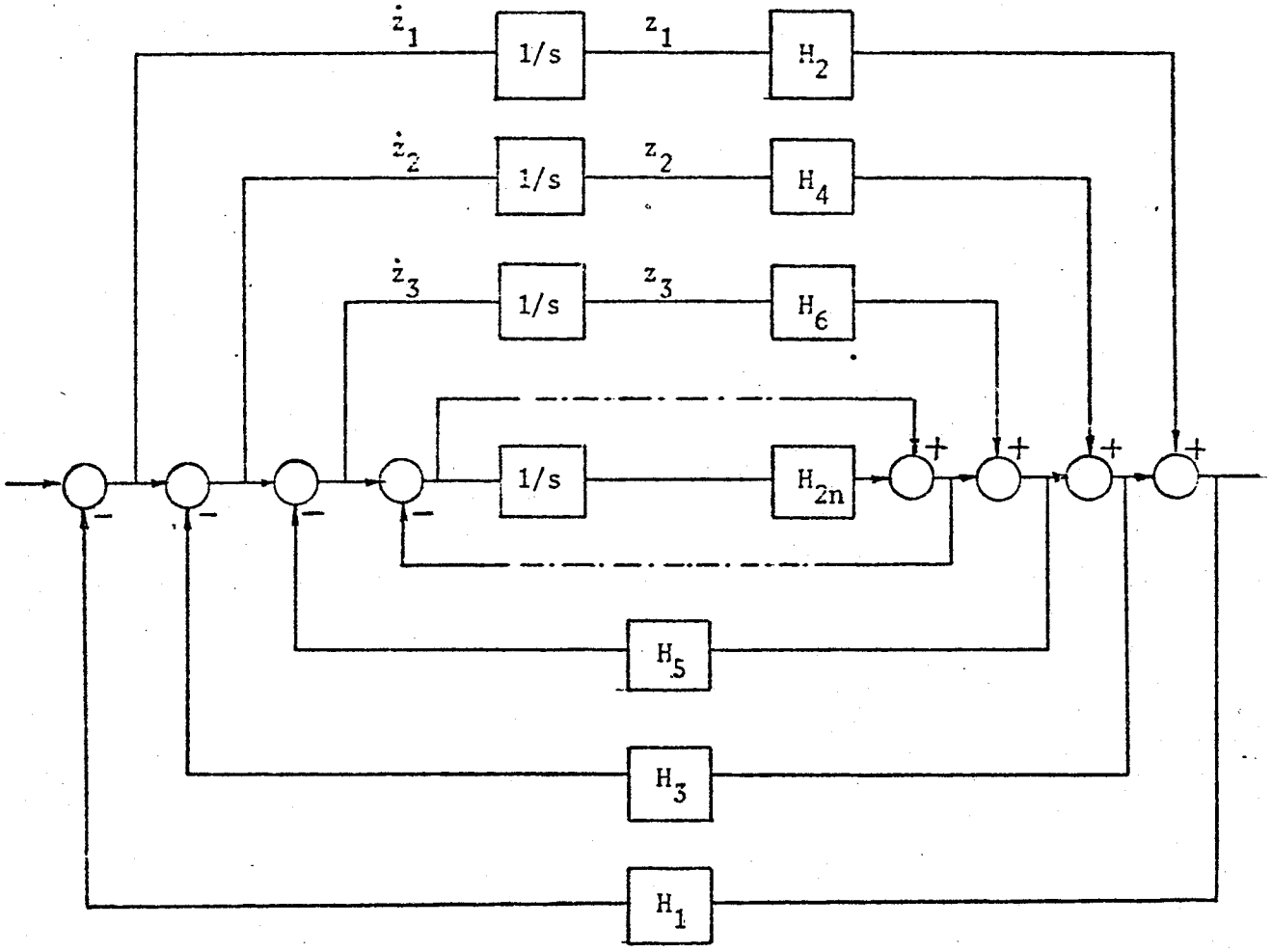

FIGURE I.1 : BLOCK DIAGRAM CORRESPONDING TO THE CONTINUED FRACTION EXPANSION.

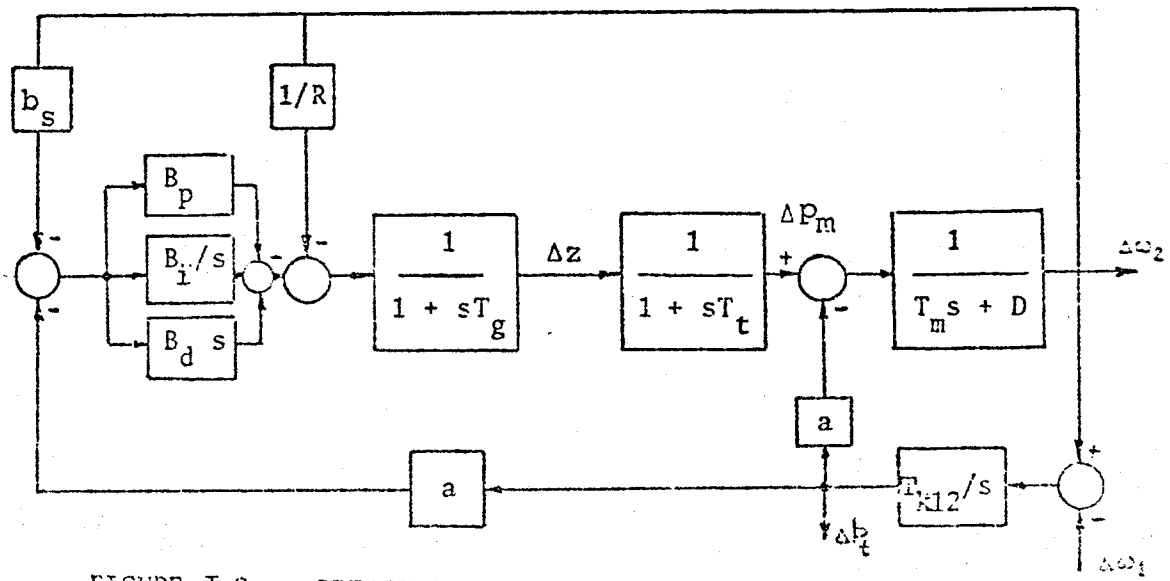

FIGURE I.2 : DETAILED MODEL OF THE EXTERNAL SYSTEM

This expansion corresponds to a combination of many feedback and feedforward blocks as shown in Figure I.1. H_2 is the dominant term; H_2/s the next dominant term. Accordingly, as the quotients are extended their influence on the performance of the system decreases.

If an m^{th} order simplied model is desired, only 2m quotients are kept in I.3.

I.2 Simplifying State Equations

State-equations given by

$$\dot{x} = Ax + Bu, \qquad \text{I.4}$$

where x and u are the state and control vectors respectively, can be simplified by first determining the transfer function between the desired input-output pair.

Equation I.4 in Laplace domain can be written as

$$[sI - A]\ x(s) = [B]\ U(s) \qquad \text{I.5}$$

Equation I.5 is the standard form of system representation from which the various transfer functions can be determined. Applying Cramer's rule, the transfer function relating an output variable X_p, of the state vector x, to the independent vector U_q, of the control vector u can be written as

$$\frac{X_p(s)}{U_q(s)} = \frac{|sI - A|^1}{|sI - A|} \qquad I.6$$

where $|sI-A|^1$ is the determinant of [sI-A] with column 'p' replaced by column 'q' of matrix [B].

$|sI-A|^1$ can be expanded to the form

$$|sI-A|^1 = s\,|sI-A_{pp}| - |sI-A^1| \qquad I.7$$

where A^1 is the matrix formed by replacing the column 'p' in [A] by 'q' column of [B]. A_{pp} is the (n-1) th order matrix obtained by eliminating the 'p'th column and the 'p' th row from matrix A.

The method of Danilevsky[49] for computing the coefficients of the characteristic polynomial of a matrix is applied to generate the characteristic polynomials of A_{pp}, A^1 and A. The numerator and denominator terms of the transfer function given by equations I.6 are thus obtained in the form of equation I.2. Then the continued fraction expansion is used to simplify this transfer function.

A flow chart of the program developed to simplify the system dynamics from the state-space equations is given in appendix IV.

I.3 Simplified Model of the External System

The detailed model of the external system is shown in Figure I.2. It includes the area controller and the interconnecting tie-line. The system state equations are given by:

$$\Delta\dot{w}_2 = -\frac{D}{T_m}\Delta w_2 + \frac{1}{T_m}\Delta p_m - \frac{a}{T_m}\Delta p_t$$

$$\Delta\dot{z} = -\frac{1}{RT_g}\Delta w_2 - \frac{1}{T_g}\Delta z + \frac{1}{T_g}\Delta u$$

$$\Delta\dot{p}_m = \frac{1}{T_t}\Delta z - \frac{1}{T_t}\Delta p_m$$

$$\Delta\dot{p}_t = T_{k12}\Delta w_1 - T_{k12}\Delta w_2$$

$$\Delta\dot{u}_I = -b_s B_i \Delta w_2 - a B_i \Delta p_t \qquad \text{I.8}$$

$$\Delta\dot{u} = (-b_s B_p + \frac{b_s B_d D}{T_m} + a B_d T_{k12})\Delta w_2 - \frac{b_s B_d}{T_m}\Delta p_m$$

$$+ (\frac{a b_s B_d}{T_m} - a B_p)\Delta p_t + \Delta u_I - a B_d T_{k12}\Delta w_1$$

The set of equations given by I.8 are of the form

$$\dot{x} = A x + B u$$

where

$$A = \begin{bmatrix} -\frac{D}{T_m} & 0 & \frac{1}{T_m} & -\frac{a}{T_m} & 0 \\ -\frac{1}{RT_g} + \frac{C_1}{T_g} & -\frac{1}{T_g} & -\frac{b_s B_d}{T_g T_m} & \frac{C_2}{T_g} & \frac{1}{T_g} \\ 0 & \frac{1}{T_g} & -\frac{1}{T_t} & 0 & 0 \\ -T_{k12} & 0 & 0 & 0 & 0 \\ -b_s B_i & 0 & 0 & -a B_i & 0 \end{bmatrix}$$

$$C_1 = -b_s B_p + \frac{b_s B_d D}{T_m} + a B_d T_{k12}$$

$$C_2 = \frac{a b_s B_d}{T_m} - a B_p$$

$$B = \begin{bmatrix} 0 & -\frac{aB_d T_{k12}}{T_g} & 0 & T_{k12} & 0 \end{bmatrix}^T$$

$$x = \begin{bmatrix} \Delta w_2 & \Delta z & \Delta p_m & \Delta p_t & \Delta u_I \end{bmatrix}^T$$

$$u = [\Delta w_1]$$

The tie line power Δp_t and the frequency of local area Δw_1 are readily available in the control centres. The transfer function of the external system can, therefore, be written as

$$G_e(s) = \frac{\Delta p_t\ (s)}{\Delta w_1\ (s)}$$

$$= \frac{s|sI-A_{pp}|-|sI-A^1|}{|sI-A|}$$

$$A_{pp} = \begin{bmatrix} -\frac{D}{T_m} & 0 & \frac{1}{T_m} & 0 \\ -\frac{1}{RT_g}+\frac{C_1}{T_g} & -\frac{1}{T_g} & -\frac{b_s B_d}{T_g T_m} & \frac{1}{T_g} \\ 0 & \frac{1}{T_t} & -\frac{1}{T_t} & 0 \\ -b_s B_i & 0 & 0 & 0 \end{bmatrix}$$

$$A^1 = \begin{bmatrix} -\frac{D}{T_m} & 0 & \frac{1}{T_m} & 0 & 0 \\ -\frac{1}{RT_g}+\frac{C_1}{T_g} & -\frac{1}{T_g} & -\frac{b_s B_d}{T_g T_m} & -\frac{aB_d T_{k12}}{T_g} & \frac{1}{T_g} \\ 0 & \frac{1}{T_t} & -\frac{1}{T_t} & 0 & 0 \\ -T_{k12} & 0 & 0 & T_{k12} & 0 \\ -b_s B_i & 0 & 0 & 0 & 0 \end{bmatrix}$$

For the constants given in table I.1

$$G_e(s) = \frac{2040.6 + 6189.9s + 3767.0s^2 + 518.6s^3 + 32.65s^4}{10.2 + 93.1s + 207.9s^2 + 115.8s^3 + 15.9s^4 + s^5}$$

The continued fraction expansion of this transfer function is

$$G_e(s) = \cfrac{1}{.005 + \cfrac{1}{\cfrac{32.829}{s} + \cfrac{1}{\ddots}}}$$

The reduced first order model of the external system is:

$$G_{e1}(s) = \frac{200.0}{1 + 6.09s}$$

The accuracy of the simplified model can be checked by comparing its reponse to a 5% load increase to that of a detailed model for the same load increase. In the above case both responses are closely matched (see Figure I.3)

The external system can therefore be represented by the simplified first order model

$$G_{el} = \frac{\Delta p_t}{\Delta w_1} = \frac{b_o}{1+a_1 s}$$

where b_o and a_1 are the parameters of the external system.

TABLE I.1

CONSTANTS FOR THE EXTERNAL SYSTEM

$D = 0.5$

$T_m = 10.0$

$a = -0.125$

$T_g = 0.08$

$R = 0.04$

$T_t = 0.3$

$T_{k12} = 32.648$

$b_s = 25.0$

$B_i = 0.6$

$B_p = 0.8$

$B_d = 0.7$

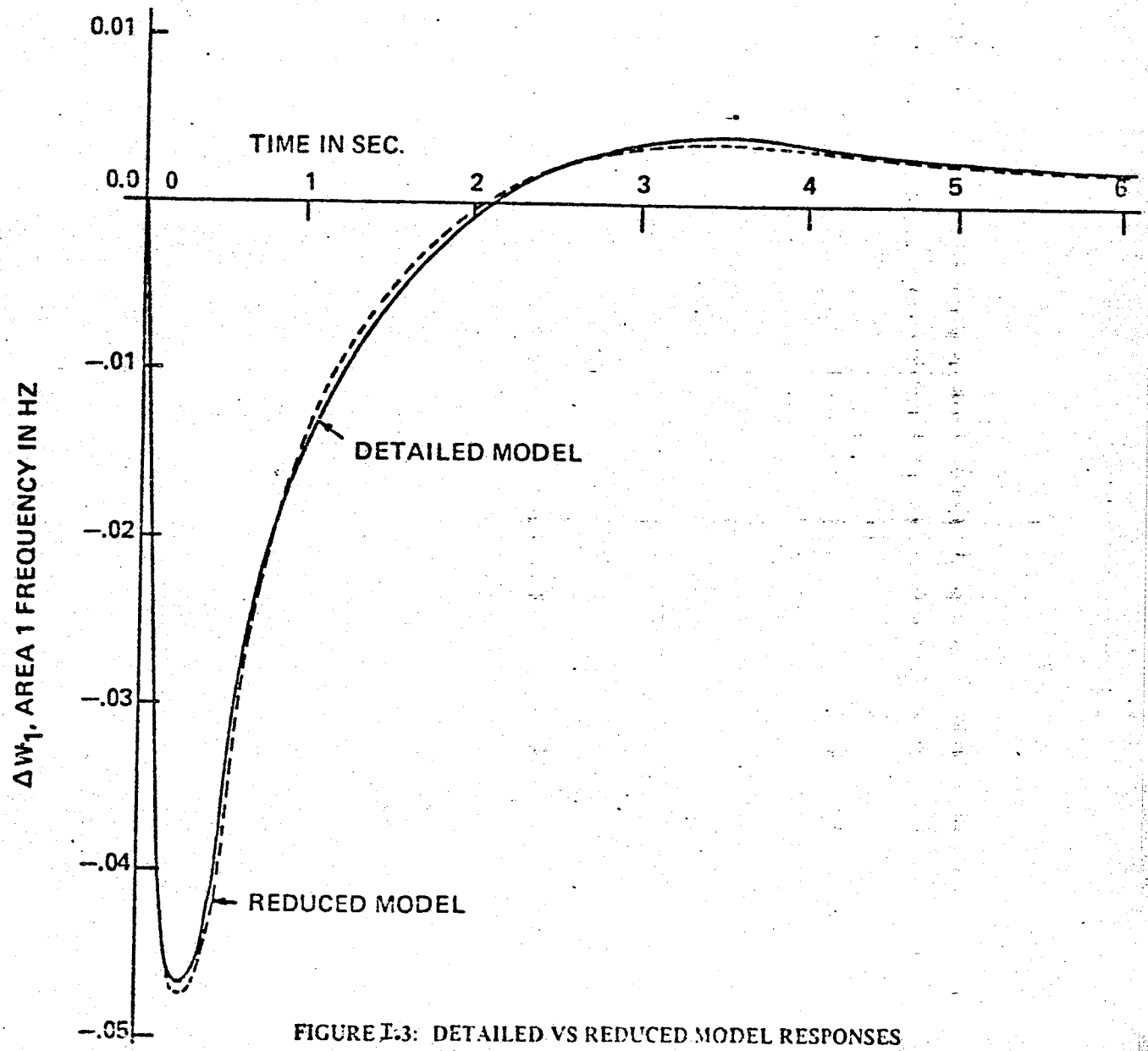

FIGURE I.3: DETAILED VS REDUCED MODEL RESPONSES TO A 5% LOAD INCREASE IN AREA 1.

APPENDIX II

On-Line Parameter Identification

II.1 Method of Identification

This section describes the linear filtering method used for estimating on-line the parameters of the reduced order model of the external system. Since this method uses recursive least-square-estimation alogrithms, it is ideally suited for on-line parameter identification. The identification is almost continuously updated and the maximum input-output data storage is directly proportional to the number of parameters to be identified.

The process for estimating the parameters on-line is outlined in the block diagram of Figure II.1. The input u and the output y are each passed through a linear filter $G_f(s)$.

If the transfer function to be identified is given by

$$\frac{y}{u} = G(z) = \frac{b_o + b_1 z + \text{-----} + b_m z^m}{1 + a_o z + \text{-----} + a_n z^n} \qquad \text{II.1}$$

where $n \geq m$,

then the filtered output can be written as

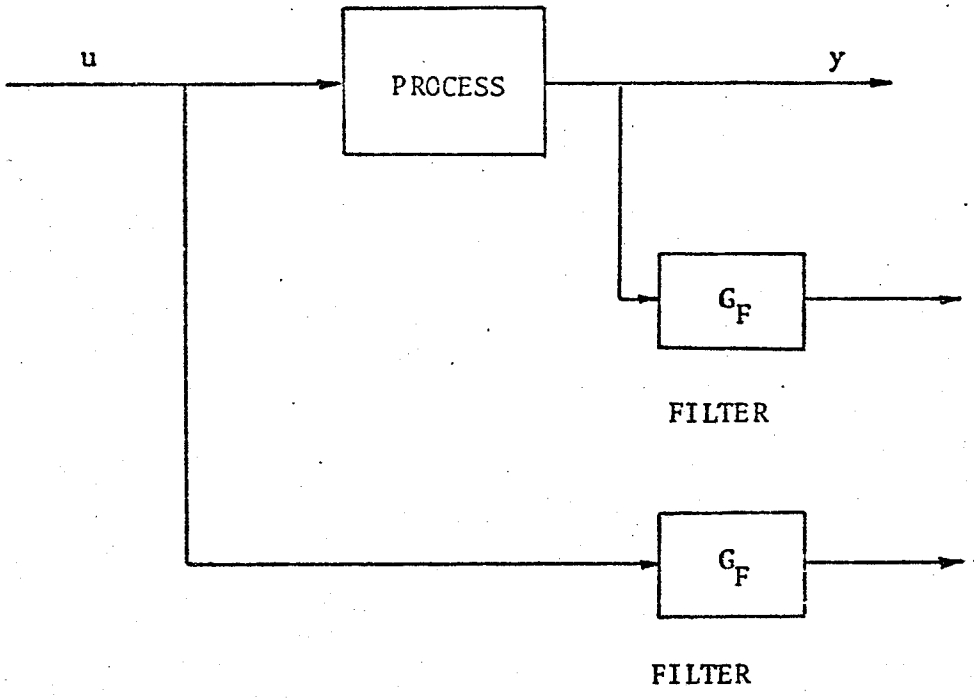

FIGURE II.1 : ON-LINE IDENTIFICATION OF PARAMETERS

$$y(k) = m^T(k)\, p(k) \qquad \text{II.2}$$

Where $m^T(k) = [-y(k-1), -y(k-2), ---, u(k), u(k-1), ---]$

$$p(k) = [a_1, a_2, ----, a_m, b_o, b_1, ----, b_m]^T$$

Finally, parameters of the assumed model can be identified by solving the following set of equations recursively:[50-51]

$$p(k) = p(k-1) + K(k)\,[y(k) - m^T(k)p(k-1)]$$

$$p(k) = \frac{1}{\lambda}\,[P(k-1) - K(k)\, m^T(k)\, P(k-1)] \qquad \text{II.3}$$

$$K(k) = P(k-1)\, m(k)\, [1 + m^T(k)\, P(k-1) m(k)]^{-1}$$

A large initial value of $P(o)$ and an initial guess $p(o) = o$ can be used to start the solution.

II.2 Solution for the external system

The reduced first order model for the external system developed in Appendix I is given by

$$G_{el}(s) = \frac{\Delta p_t}{\Delta w_1} = \frac{b_o}{1 + a_1 s}$$

For an on-line identification, this equation is changed into the discrete form

$$\frac{\Delta p_t}{\Delta w_1} = \frac{b_o^1}{1+a_1^1 z} \qquad \text{II.4}$$

where $b_o^1 = \frac{b_o T}{T+a_1}$

$$a_1^1 = \frac{a_o}{T+a_1}$$

and T is the sampling period.

At the k^{th} sampling period, the vectors p and m are

$$p(k) = (a_1^1, b_o^1)^T$$

$$m(k) = [-\Delta p_t(k-1), \Delta w_1(k)]^T$$

Storage of only the most recent value for the tie-line power is required for the identification.

Validity of this identification procedure is next checked against the known model of the external system by applying a 5% step load increase in area 1 (the local area). The tie line power Δp_t and the area 1 frequency Δw_1 are sampled every 0.2 second to solve the set of equations II.3.

The parameter vector p is initially assumed to be:

$$p(0) = (0.0, 0.0)^T$$

Figure II.2 shows the convergence of parameters a_1^1 and b_o^1 (to true values) at each sampling and iteration cycle. Fast convergence of parameters to true values indicates the accuracy of the alogrithm for on-line identification of the external area dynamics.

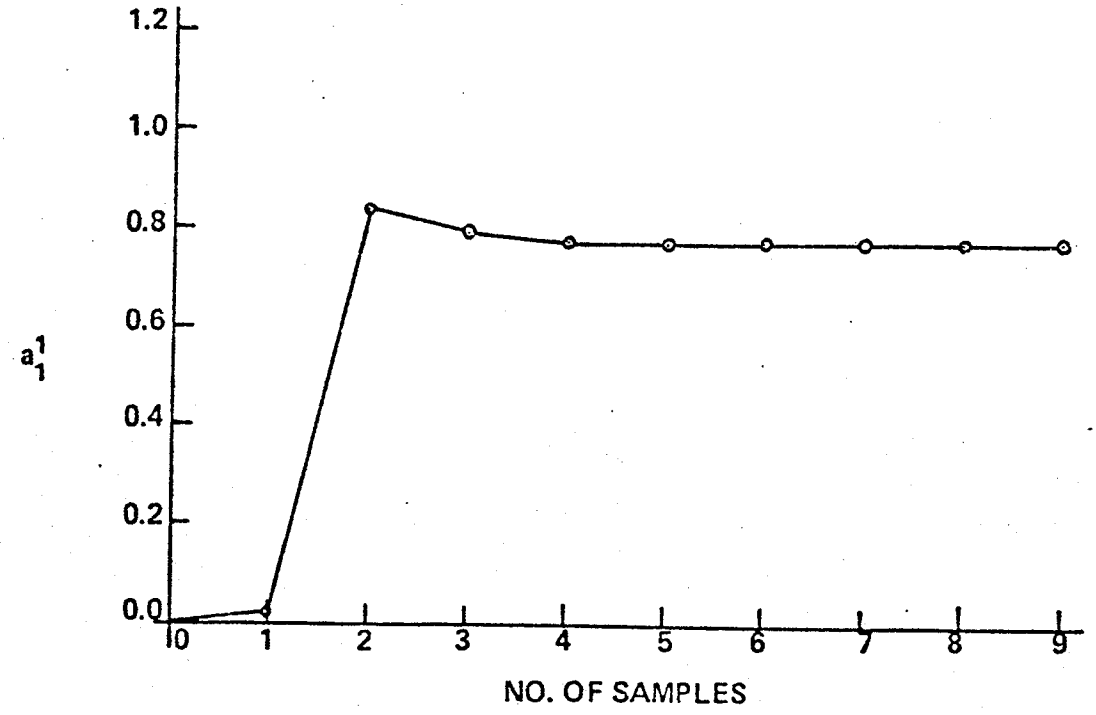

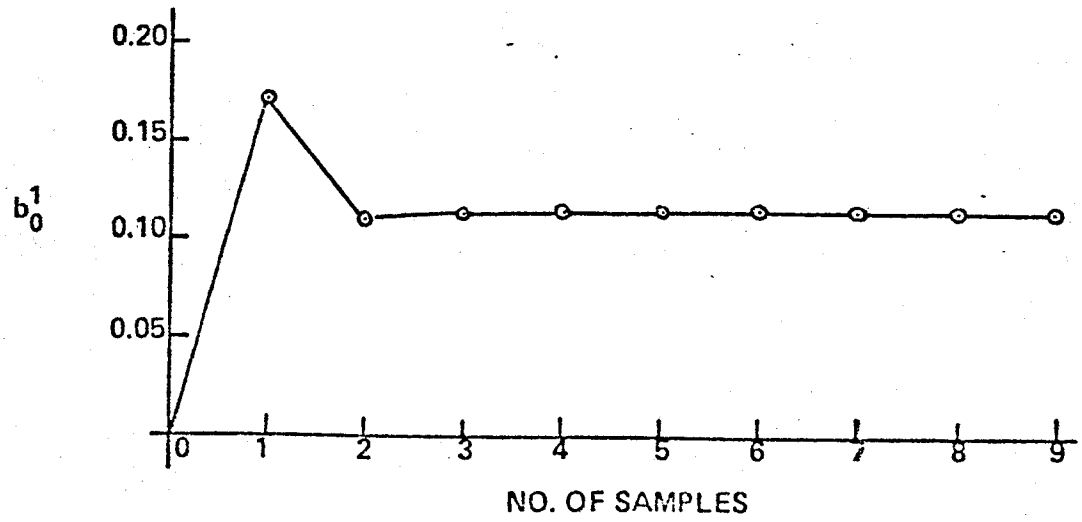

FIGURE II.2 CONVERGENCE OF a_1^1 AND b_0^1

APPENDIX III

Mathematical Model of a D.C. Link for the Load-Frequency Control

A typical d.c. link consists of two converting stations and a transmission line as shown in Figure III.1. The rectifier station normally controls current and the inverter maintains a constant extinction angle. The recent d.c. links also use a phase-locked oscillator for providing equidistant firing pulses to the converter bridges. A detailed discrete mathematical model of such a d.c. link is derived first and then a simplified linear model for the load-frequency control is developed.

Rectifier and Inverter Voltage Equation:

(i) Rectifier

$$e_r = \frac{3\sqrt{2}}{\pi} E_r \cos\alpha_n$$

$$\therefore \quad \Delta e_r = -\frac{3\sqrt{2}}{\pi} E_r \sin\alpha_o \Delta\alpha_n \qquad \text{III.1}$$

where E_r = sending end a.c. voltage

α_n = normal firing angle

Δ = denotes change

(ii) Inverter

$$e_i = \frac{3\sqrt{2}}{\pi} E_i \cos\delta_c$$

$$\therefore \quad \Delta e_i = 0.0 \qquad \text{III.2}$$

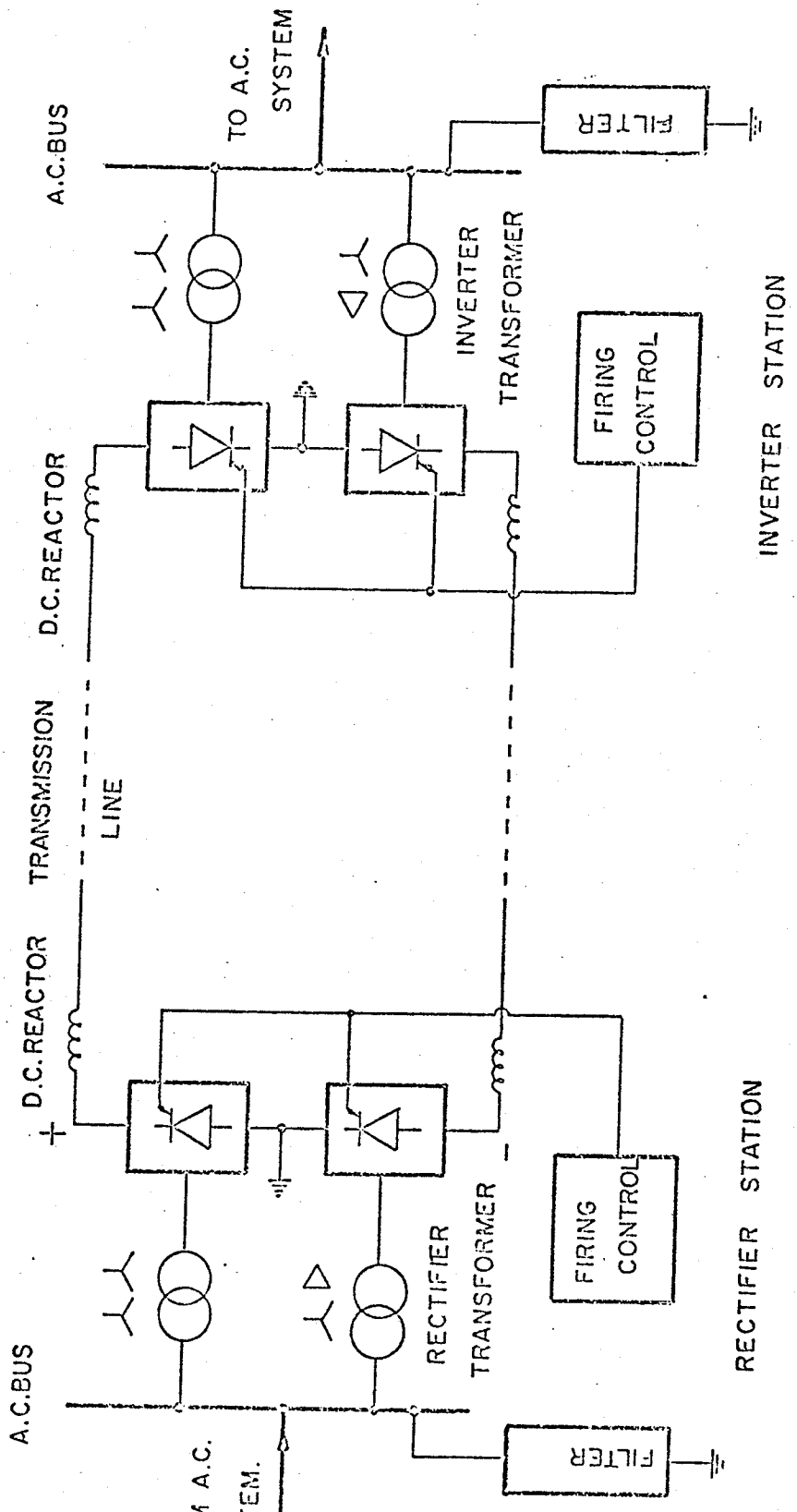

Figure III.1 General layout of a h.v.d.c. scheme interconnecting two a.c. systems.

where E_i = receiving end a.c. voltage

δ_c = constant extinction angle.

D.C. Line

A simple R.L. circuit can be assumed. Hence the d.c. line current can be written as

$$\Delta I_d = \frac{\Delta e_r - \Delta e_i}{(R + sL)}$$

$$= \frac{\Delta e_r}{(R + sL)} \qquad \text{III.3}$$

where I_d = d.c. current

s = Laplace operator.

D.C. Control

An analog device generates a control signal V_c given by

$$V_c = \frac{K_1 (s + a_1)}{s (s + b)} (\Delta I_{do} - \Delta I_d) \qquad \text{III.4}$$

where I_{do} = current order

K_1 = controller gain

a_1 and b are controller parameters.

The control signal V_c is used by the phase-locked oscillator to generate the firing pulses according to the equation

$$e_o = A \sin (12\pi ft + 6 \alpha_o - KV_c(t) \qquad \text{III.5}$$

where A is the amplitude of the oscillator output

f is the system frequency

$V_c(t)$ is the control signal.

Firing signals are generated when e_o in equation III.5 is zero. Thus

$$12\pi ft_n + 6 \alpha_o - K V_c(t) = 2 n \pi \qquad \text{III.6}$$

Considering $t_n = \frac{n\pi}{3w} + \tau_n$ where n is the integer.

$$= \frac{n\pi}{3w} + \frac{\Delta \alpha_n}{w}$$

Equation III.6 can be written as

$$6\Delta \alpha_n = K \Delta V_c(t_n) \qquad \text{III.7}$$

Now $$\Delta V_c(t_n) = \Delta V_c\left(\frac{n\pi}{3w} + \frac{\Delta \alpha_n}{w}\right)$$

From Taylor series expansion

$$\Delta V_c(t_n) = \Delta V_c(n) + \frac{\Delta \alpha_n}{w} \Delta \dot{V}_c(n) + \ldots$$

Neglecting derivative terms,

$$\Delta V_c(t_n) = \Delta V_c(n) \qquad \text{III.8}$$

From equations III.7 and III.8,

$$\Delta \alpha_n = \frac{K}{6} \Delta V_c(n) \qquad \text{III.9}$$

The detailed model of the d.c. link is next derived from equations III.2, III.3, III.4 and III.9, as shown in Figure III.2.

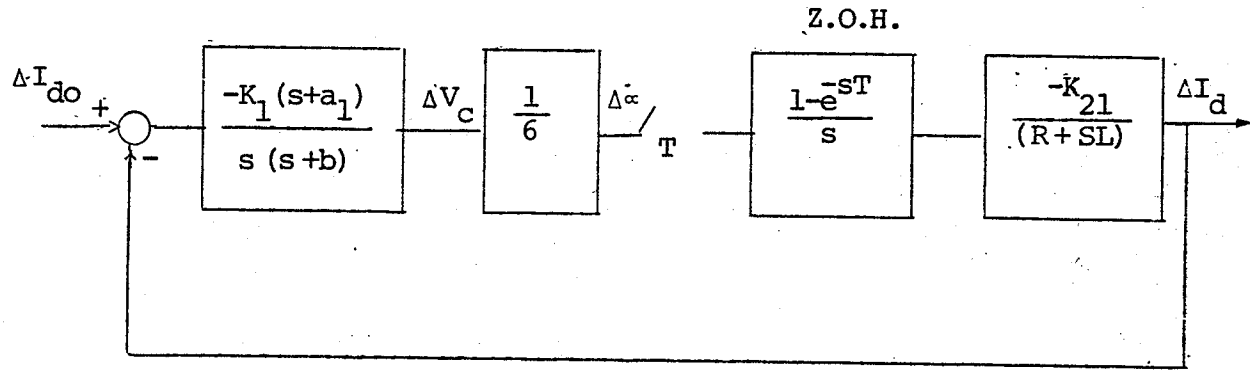

Figure III.2 A detailed discrete model of the d.c. link.

Because of the fast sampling rate of the d.c. link, a simple model can be assumed for the load-frequency control (see Figure III.3). This model is derived using the linear simplification technique described in Appendix I.

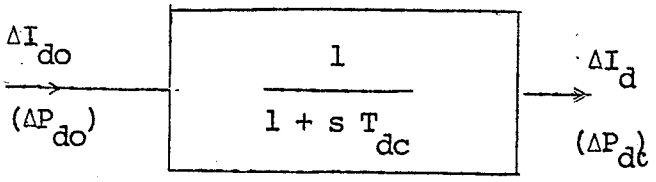

Figure III.3 A simplified linear model of the d.c. link.

APPENDIX IV

PROGRAM FLOW CHARTS AND LISTINGS

IV.1 PID Controller Design

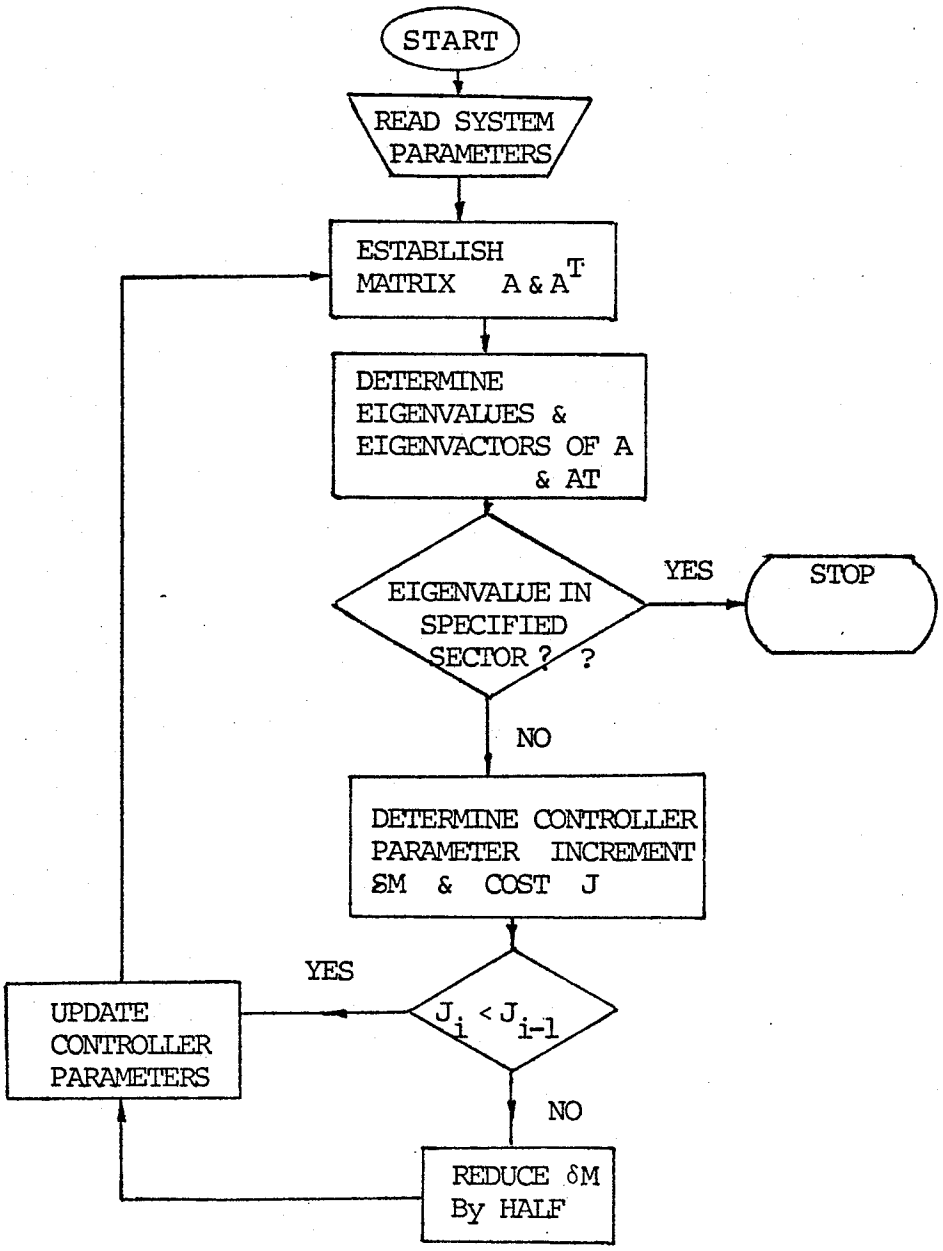

FLOW CHART OF ANALOG PID CONTROLLER DESIGN.

IV.2 DIGITAL PID Controller Design

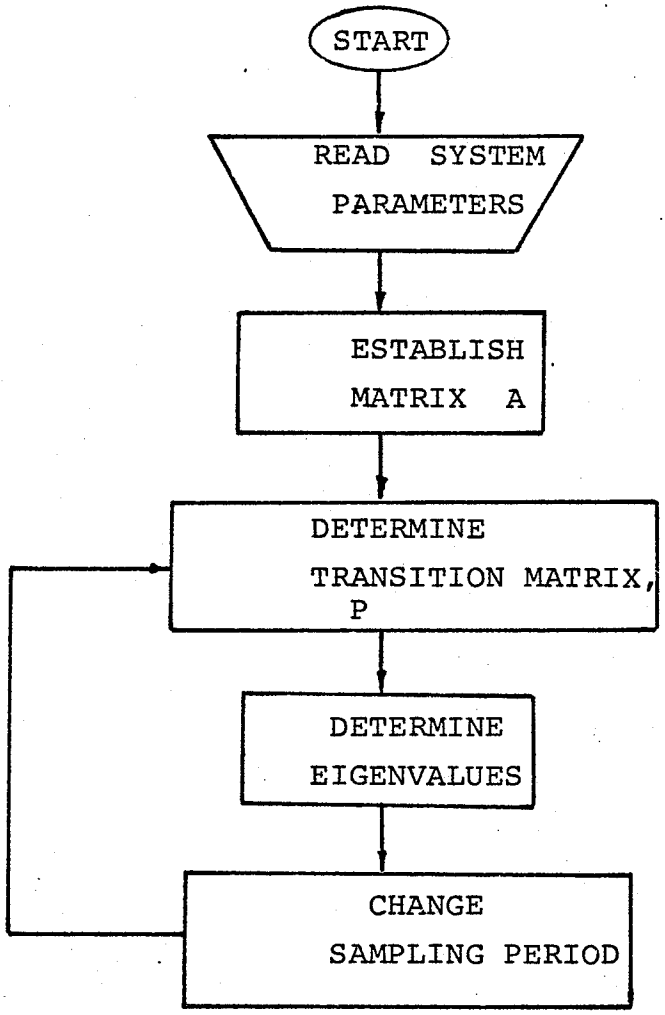

IV.3 Model Simplification

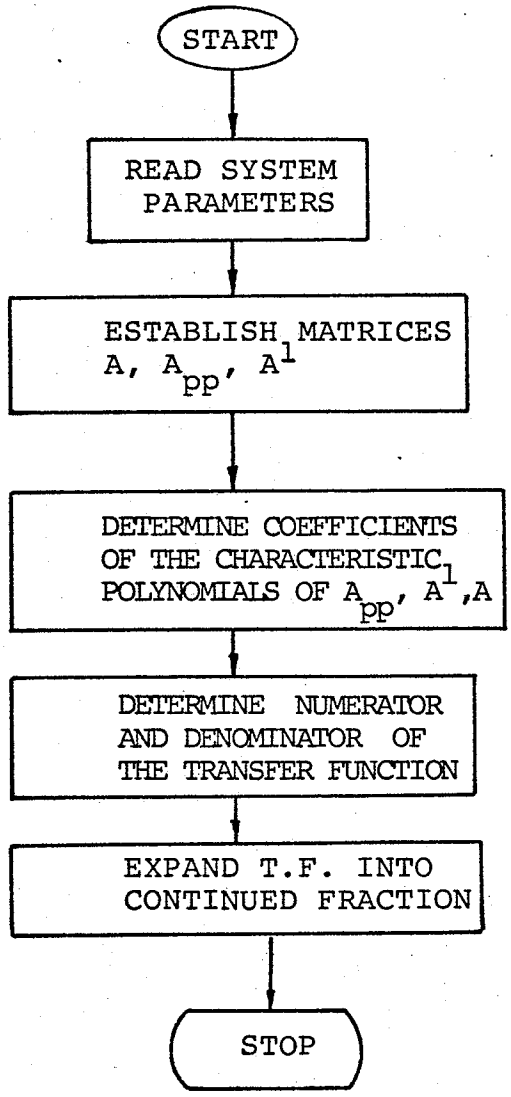

IV.4 On-line Parameter Identification

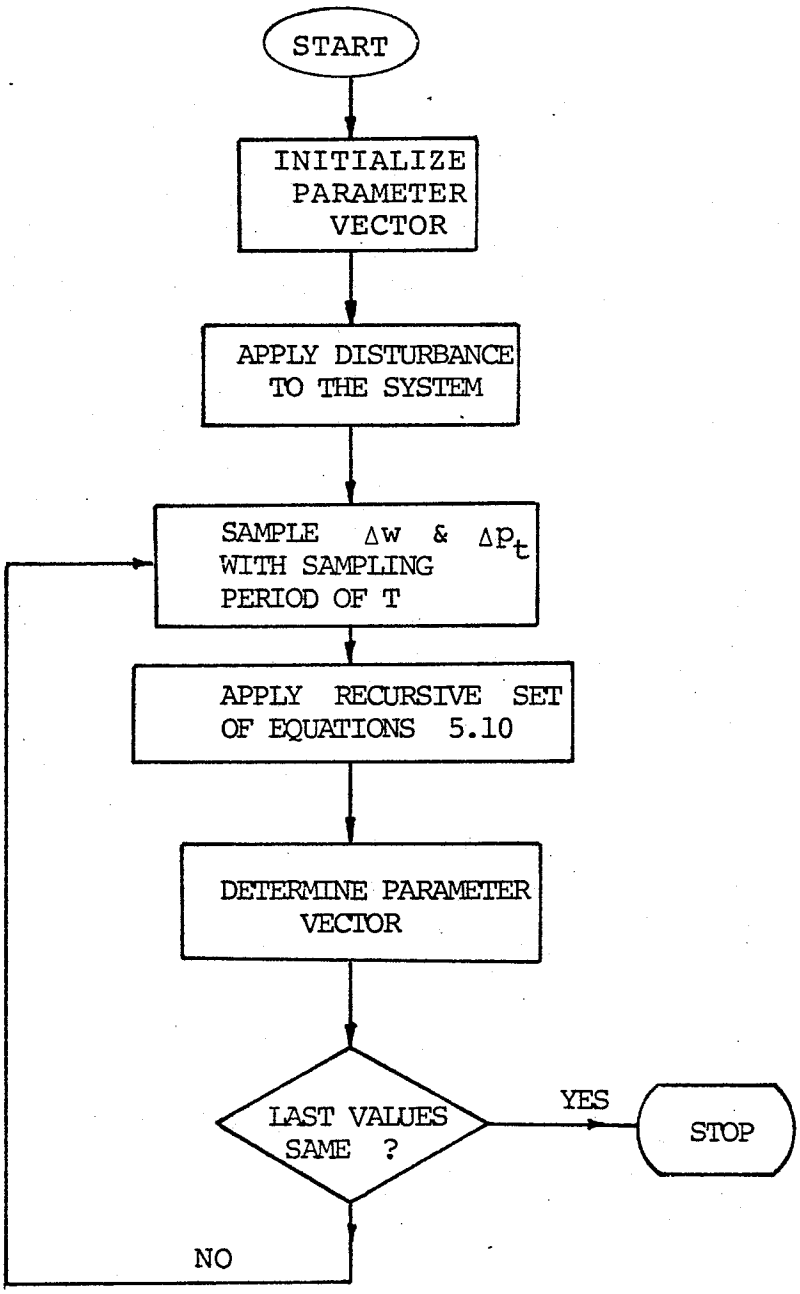

APPENDIX V

LIST OF SYMBOLS

Governor:

R	regulation constant, pu
T_g	governor time constant in sec.
z	gate position in pu
w_r	reference speed setting in pu

Turbine:

T_t	turbine time constant in sec.
p_m	mechanical power output in pu

Generator:

T_m	inertia time constant in sec.
D	damping constant in pu
w	speed (frequency) in pu

Tie-line:

p_t	tie-line power in pu
T_{k12}	tie-line coupling coefficient in pu
a	ratio of MW capacity of Area 1 over area 2 with negative sign

v system voltage, pu

x_{12} tie-line impedance in pu

σ_{120} initial operating angle in degrees

p_R area capacity in MW

D.c. Link:

p_{do} d.c. power order, pu

I_{do} d.c. current order, pu

p_{dc} actual d.c. power, pu

I_{dc} actual d.c. current, pu

T_{dc} d.c. line time constant in sec.

h d.c. link participation, pu

B d.c. link regulation constant, pu

Load:

p_L electrical load demand, pu

Load-Frequency Controller:

u controller out-put in pu

b_s area frequency bias

k_s integral gain of the conventional controller

B_p, B_i, B_d proportional, integral and derivative gains of PID controller in pu

Miscellaneous symbols:

Δ	prefix used to indicate small deviations of a variable
i	subscript denoting area i (i = 1, 2)
s	laplace operator
$\cdot$	differentiation, $\frac{d}{dt}$